Geochemistry

By Gary A. Nowlan and Ted G. Theodore

This section of the report includes two parts. In the first part, the Rock Analysis Storage System (RASS), the geochemical data base of the United States (PLUTO), and National Uranium Resource Evaluation (NURE) computerized data bases of the U.S. Geological Survey are examined, largely on the basis of regional geochemistry. In addition, descriptions of a number of mineral occurrences obtained during our investigation are included. Table 10 lists sources of data that have been released, and tables 11 and 12, respectively, list geochemical data and sample descriptions from selected rocks collected from a small number of mineralized systems in the East Mojave National Scenic Area (EMNSA). In the second part, the implications of data obtained from analyses of 1,050 rocks by the U.S. Bureau of Mines (1990a) from various sites within the EMNSA are examined; these samples are mostly mineralized or altered samples from mines and prospects.

RASS, PLUTO, and NURE Data Bases

The objective of the examination of RASS, PLUTO, and NURE data is to recognize geochemical patterns that might be related to mineralization. Application of the principles of mineral-deposit models (Cox and Singer, 1986) includes the recognition of characteristic geochemical signatures for each model. The regional geochemistry addresses geochemical signatures in terms of possible mineral deposits without regard to the size or grade of the deposits. The discussion of the geochemistry of each area includes some descriptions of known mineral occurrences and classifies them in terms of mineral-deposit models.

Analytical data for the EMNSA that are stored in the RASS, PLUTO, and NURE data bases were retrieved and examined using the Statistical Package (STATPAC) system (VanTrump and Miesch, 1977) of the U.S. Geological Survey. The RASS and PLUTO data bases contain data for rock, stream-sediment, heavy-mineral-concentrate, and soil samples, as well as other types of geologic samples collected by the U.S. Geological Survey and other sample types such as water and vegetation. The NURE data base contains data for samples collected during the National Uranium Resource Evaluation Program of the U.S. Department of Energy (Cook and Fay, 1982).

The RASS and PLUTO data bases were designed and managed by the Branches of Exploration Geochemistry and Analytical Laboratories, respectively, of the U.S. Geological Survey before their merger into the Branch of Geochemistry in 1987. The two data bases are similar in content and characteristics, but major differences in their operation have hindered their merger into a single data base; in addition, the logistical problem of merging two large data bases is a major obstacle during a time of limited budgets. Since merger of the two branches into the Branch of Geochemistry in 1987, most new data have gone into the PLUTO data base; however, most data for the EMNSA were obtained before 1987 and, therefore, are resident in both RASS and PLUTO data bases. Before the merger of the branches, RASS data tended to be from large mineral-resource evaluations of public lands or other large projects, whereas the PLUTO data base tended to receive data from more specialized projects and from a wider variety of types of projects.

The data for selected elements useful in mineral-resource evaluations were studied and, from them, map plots were produced. The data in the RASS, PLUTO, and NURE data bases are available to the public, but most data have not been released as either published or open-file reports; table 9 lists sources of data that have been released.

Sample Types

Sieved stream-sediment samples, heavy-mineral-concentrate samples (in most cases, panned from stream sediments), and rock samples from the RASS and PLUTO data bases were considered because they were the most widely sampled media in the study area and also are the standard sample media for mineral-resource evaluations by the U.S. Geological Survey. The PLUTO data base contained some samples that have very approximate coordinates (rounded to one-half minute or more of latitude or longitude); these samples were not considered in this study.

Standard coding in the RASS and PLUTO data bases does not always specify the size fraction analyzed for the stream-sediment samples. Examination of the original requests for analysis or consultation with the original investigators confirmed that the minus–80-mesh (<0.177 mm) fraction of each stream-sediment sample was the fraction analyzed.

Heavy-mineral-concentrate samples from the RASS data base are the nonmagnetic heavy fraction of stream sediments, except for 15 samples from the west side of the Ivanpah Mountains that were panned from mine-dump material. The RASS concentrate samples were prepared by subjecting panned samples to a series of magnetic and heavy-liquid separations, resulting in samples consisting of nonmagnetic ore minerals and accessory heavy minerals such as sphene and zircon. The PLUTO heavy-mineral-concentrate samples were all derived from stream sediments; after panning, the highly magnetic minerals (mostly magnetite) were removed with a hand magnet, and the less-magnetic fraction was ground and analyzed (Jean Juilland, oral commun., 1991). Because of the major difference in the processing of RASS and PLUTO heavy-mineral-concentrate samples, they were treated as different sample media in the data analysis; drastic differences in concentrations of common elements such as Fe, Ca, and Mn confirmed that the RASS and PLUTO concentrate samples should be treated as different sample media.

Of the 944 RASS and PLUTO rock samples, about 700 are specified by coding or by notes to be samples of mineralized or altered rocks or from faults. These 700 samples may be thought of as samples of the channels where mineralizing fluids passed. Coding for about 140 of the 944 samples does not indicate whether they are of economic significance; for most elements in these approximately 140 samples, the range of concentrations varies from 1 to 2 orders of magnitude, and the maximum concentrations indicate that some samples may be mineralized. In any case, concentrations significantly above expected regional background are of interest, especially if several elements have anomalously high concentrations in the same samples or same areas. For mineralized rocks, the geochemical signature is more important than absolute concentrations because, typically, no way exists to determine the exact nature of the sample or the intent of the sampler. For example, the sample may be from a highly mineralized vein, may be a composite of dump samples, or may be a sample of altered but not obviously mineralized rock. For this mineral-resource evaluation, data from all 944 rock samples were combined for data analysis and considered to be mineralized.

The NURE data consist of analyses of the 35– to 18–mesh (0.5–1.0 mm) fraction of stream sediments from the Kingman 1:250,000–scale quadrangle and of the minus–100-mesh (<0.149 mm) fraction of stream sediments and soils from the Needles, San Bernardino, and Trona 1:250,000–scale quadrangles. The data also contain 13 playa-sediment samples. Comparison of the minus–100-mesh stream-sediment and soil data showed that the two media could be combined into one data set, and so this was done. Comparison of data from the Kingman quadrangle (35–18 mesh) with data from the Needles-San Bernardino-Trona quadrangles (minus–100 mesh) showed biases in the means of the concentrations of as much as two to one for the nine elements (Ce, Dy, Eu, La, Lu, Sm, Th, U, and Yb) included in this report. However, the bias was high for Ce, Dy, Eu, and Lu in Kingman samples and high for La, Sm, Th, U, and Yb in Needles-San Bernardino-Trona samples; therefore, the biases in the means are difficult to attribute to differences in sample grain size and may represent either geologic differences or analytical biases.

Evaluation of Data

The standard method of analysis for RASS and PLUTO samples was semiquantitative, direct-current arc-emission spectrography (Myers and others, 1961; Grimes and Marranzino, 1968); RASS samples were usually analyzed for 31 elements by this method, while PLUTO samples were analyzed for those 31 elements plus about 15 more, mostly rare earth elements (REE). RASS and PLUTO samples from specific areas in the EMNSA were analyzed by atomic absorption and other methods; these additional analyses were examined but their usefulness is limited because of poor areal coverage.

Concentrations of elements determined by the emission-spectrographic method are usually reported as one of six steps per order of magnitude; the steps represent intervals of some power of 10 times 1.2 to 1.8, 1.8 to 2.6, 2.6 to 3.8, 3.8 to 5.6, 5.6 to 8.3, and 8.3 to 12 (Motooka and Grimes, 1976). For most samples in this report, those intervals are represented by the values (steps) 1.5, 2, 3, 5, 7, and 10, respectively (or powers of 10 of these numbers). For some samples, the reported values are somewhat different but still represent approximately the same intervals. Upper and lower limits of determination (table 13) varied somewhat with method and with time during the approximately 6–year period when the samples were analyzed. This is reflected in table 13 by variations in lower determination limits and by some maximum concentrations greater than the customary upper determination limits listed. The precision of the emission-spectrographic method is approximately plus or minus one reporting interval at the 83 percent confidence level and plus or minus two reporting intervals at the 96 percent confidence level (Motooka and Grimes, 1976).

In the NURE program, stream-sediment and soil samples were routinely analyzed by neutron-activation analysis for approximately 17 elements (Cook and Fay, 1982). These routine procedures did not include most of the elements that are generally of interest in mineral-resource evaluations. The NURE program made extensive use of a supplemental package of analyses that includes most elements of interest in the search for hydrothermal ore deposits, but those supplemental analyses were performed only on samples from the Kingman quadrangle. In addition, certain ambiguities exist between the digital NURE data base and the published reports. For example, it is not clear whether a reported value of zero means that an analysis was not performed or that an analysis was performed but the concentration was less than the lower limit of determination. Therefore, the NURE data base is of limited usefulness for evaluations of elements that might be indicative of hydrothermal processes, but it is useful for evaluating the presence of U, Th, and rare earth elements (REE). Coefficients of variation for three NURE stream-sediment or soil samples that were each analyzed from 16 to 297 times by neutron-activation analysis for various elements ranged from 5.0 to 47.8 percent (Cook and Fay, 1982, table 2).

The RASS and PLUTO 31–element emission-spectrographic data for stream-sediment samples appeared to be compatible, and so the two data bases were merged into one data set for statistical evaluation and map plotting. The RASS and PLUTO 31–element emission-spectrographic data for rocks also appeared to be compatible, and they were also merged into a single data set. The additional elements, mostly REE, analyzed by emission spectrography for PLUTO stream-sediment samples and rock were treated as separate data sets. Data for RASS and PLUTO concentrate samples were treated as separate data sets because differences in sample preparation led to incompatible geochemical results.

Data Coverage

Figure 49 shows geographic areas covered by the geochemical data sets in and along the border of the EMNSA. This map is used as a base map for other figures in this section of the report. Sampling localities for the various sample media are shown in figures 50 to 53. Stream-sediment samples (fig. 50) were collected in almost all areas outlined on figure 49; sampling density is quite sparse except in areas in the Clark Mountain Range, the Ivanpah Mountains, and the Providence Mountains. PLUTO concentrate samples (fig. 51) are quite evenly but sparsely distributed throughout the area. RASS concentrate samples (fig. 51) are limited to several areas, and sampling density is fairly adequate for geochemically characterizing those areas; the Providence Mountains were heavily sampled, allowing an excellent geochemical characterization of that area. Distribution of sampling sites of rocks (fig. 52) is spotty, dominated by heavy sampling in the Providence Mountains. NURE samples (fig. 53) are distributed fairly uniformly, although somewhat sparsely.

Geochemical Evaluation

Symbol plots of selected elements in the various sample media were prepared in order to show geochemical trends in the EMNSA and adjacent areas. The selected elements were the possibly ore-related elements Ag, As, Au, B, Ba, Be, Bi, Co, Cu, Mn, Mo, Nb, Pb, Sb, Sn, Th, U, W, and Zn; also included because of the proximity of the Mountain Pass REE deposit were the rare earth elements Ce, Dy, Eu, La, Lu, Nd, Sm, Tb, and Yb.

Table 13 lists statistics for the selected elements that are based on samples from the EMNSA and the surrounding area from lat 34°30′N. to lat 35°45’N. and from long 114°45′W. to long 116°15′W. Threshold concentrations, defined as highest background concentrations, were selected by visual and statistical examination of the data, by observation of elemental concentrations near known mineralized areas, and by reference to published reports of specific geochemical studies of various wilderness-study areas within the EMNSA. The threshold concentrations listed in table 13 for the EMNSA are regional thresholds and do not take into account any variations in bedrock or other factors. Table 13 includes published threshold concentrations established for two wilderness-study areas within the EMNSA (Miller and others, 1985, tables 1, 2; Goldfarb and others, 1988, table 3), which are included for reference and to illustrate how threshold concentrations vary with scale of study, degree of local bedrock mineralization, and judgment of the individual investigator.

Selected percentiles are listed in table 13 and also in the captions of figures 54 to 73. First, the computer program ranks concentration values from lowest to highest, then it lists the concentration values at selected percentiles. Concentration values qualified by "N" (not detected at lower limit of determination) are ranked lowest; those qualified by "L" (detected below lower limit of determination) or "<" (less than lower limit of determination) are ranked next to the lowest; and those qualified by "G" or ">" (both signify concentration values greater than upper limit of determination) are ranked highest. Unqualified values are ranked in the middle according to their magnitude. Concentration values listed in percentile columns in table 13 for RASS and PLUTO samples are rounded to the emission-spectrographic steps mentioned above (1.5, 2, 3, 5, 7, or 10, or powers of 10 of these numbers); those listed for NURE samples are rounded to two significant figures.

Because lower limits of determination for emission-spectrographic techniques are high relative to average crustal abundances for some elements (Ag, As, Au, Bi, Sb, Th, W), almost all detectable concentrations for these elements are anomalous, depending on sample type; some of the rare earth elements also fall in this category (Dy, Tb). For elements that have a wide range of detectable concentrations, a "high" category is plotted on figures 54 to 73 showing distribution of anomalous and high concentrations of various elements. Because some subjectivity is involved in establishing threshold concentrations, inclusion of a "high" category shows the appearances of geochemical patterns if lower thresholds are chosen.

The high proportion of samples that have anomalous concentrations of Ag, Ba, Cu, Mo, Pb, and Zn in rock and heavy-mineral-concentrate samples (table 13) is the result of the large number of samples collected in highly mineralized parts of the Providence Mountains.

Figures 54 through 73 show map distributions of anomalous and high concentrations of elements in the various sample media. Each figure plots no more than four elements; these are grouped by common elemental association and are represented by vertical, horizontal, and diagonal lines. Anomalous concentrations and high concentrations are shown as lines of longer and shorter length, respectively.

Any geochemical evaluation of a geologic terrane has to deal with the issue of determining which elemental concentrations are background and which are anomalous. This issue becomes more difficult when a wide range of rock types is present. For example, average Co concentration in mafic rocks is 48 ppm (parts per million), but, in granites, average Co concentration is 1 ppm (Rose and others, 1979, p. 554). If high Co concentrations are accompanied by high concentrations of other common constituents of mafic rocks such as Ni and Cr, high Co concentrations might be due to the presence of mafic rocks and, therefore, will probably not be anomalous. On the other hand, if high Co concentrations are accompanied by high concentrations of base metals but not by Ni and Cr, then hydrothermal activity may be the reason for the high concentrations; Co is part of the geochemical signature for a number of mineral-deposit types (porphyry copper, for example) that are not associated with mafic rocks (Cox and Singer, 1986). Therefore, the recognition of geochemical signatures is an important part of this geochemical evaluation of the EMNSA in view of the wide range of bedrock types. The following suggestions as to permissive mineral-deposit types in each of the areas discussed are based on both the general types of bedrock in a given area and the geochemical signature for the area.

A special problem in the identification of geochemical signatures in the EMNSA is that of the recognition of REE signatures, inasmuch as the rare earth elements tend to be present together (Levinson, 1980, p. 868), whether in accessory minerals, such as apatite or monazite, or in economic deposits, such as at the Mountain Pass Mine. Also, REE tend to be present in high concentrations in Proterozoic and Jurassic granites of the EMNSA (D.M. Miller, written commun., 1991), especially in syenite, a fairly common rock type in the EMNSA. Thresholds for REE listed in table 13 were established on the basis of concentrations in RASS–PLUTO stream-sediment and NURE sediment-soil samples collected within about 0.8 km of the Mountain Pass Mine and also downstream from it, 3.2 to 4.8 km away. These samples showed an association of REE, Ba, and Sr, all components of the ore in the Mountain Pass Mine (see subsection above entitled "Ultrapotassic Rocks, Carbonatite, and Rare Earth Element Deposit, Mountain Pass, Southern California").

On the basis of mineral-deposit occurrences and geologic studies of the EMNSA and surrounding areas, the EMNSA has potential for many types of mineral deposits, which include porphyry copper-molybdenum deposits, precious and base metals (polymetallic) in veins or replacement bodies, gold deposits of several types (for example, breccia-pipe gold and volcanic-hosted gold), various types of mineralized skarn, and U–Th–Nb–REE-bearing carbonatites or pegmatites. Table 14 summarizes the geochemical results on an area-by-area basis. The listing of elements for each area in table 14 is based only on samples from within the specific areas shown on figure 49. Therefore, the listings differ slightly from those reported in table 7 of U.S. Geological Survey (1991, p. 182–183), which also included some samples near but outside the areas. The combined RASS and PLUTO stream-sediment data sets are referred to as stream-sediment samples, whereas the combined NURE stream-sediment and soil samples are referred to simply as NURE samples.

The following discussions of areas apply the qualitative terms "not," "weakly," "mildly," "moderately," or "highly" anomalous to each of the areas as a whole. These qualitative terms are based on the number and proportion of samples that have anomalous concentrations, the number of elements present in anomalous concentrations, the intensity of the anomalous concentrations in individual samples, and the number of sample media that have anomalous concentrations. A preponderance of high but not necessarily anomalous concentrations is the basis for regarding some areas as at least weakly anomalous (table 14) in terms of a given element. The rationale is that a mineralizing system at depth might result in what appears to be a high background; the geochemical signature then determines where the area falls on the scale between "not anomalous" and "highly anomalous." As always, the mineral-resource potential of each area is determined by its geochemistry in conjunction with geologic, geophysical, and mineral-deposit studies, as well as other data. As stated before, the geochemical signatures for each area are defined without regard to possible grade or tonnage of any possibly included mineralized system.

Bedrock types in the following sections are listed according to relative abundance in each area. Elements are listed in the general order of (1) those associated with various sulfide deposits, (2) those associated with late-stage magmatic differentiates, and (3) those elements that are part of the REE association; obviously, considerable overlap of these three associations exists.

Soda Mountains

Bedrock of that part of the Soda Mountains that lies on the west border of the EMNSA (fig. 49) consists of Jurassic and Cretaceous granitoid rocks and Mesozoic volcanic and sedimentary rocks (pl. 1). Some stream-sediment samples from the Soda Mountains have anomalous concentrations of Zn, B, Mo, and Sn. Concentrate samples contain anomalous concentrations of Cu, Ag, Zn, Mn, Pb, Au, Ba, Co, Bi, B, Sn, Mo, Be, Th, Nb, La, Ce, Tb, Yb, and Dy. No rock samples were collected in the area. NURE samples have anomalous concentrations of Eu. The area is overall mildly anomalous geochemically. Possible deposit types include porphyry copper-molybdenum, polymetallic veins and replacement bodies, copper or lead-zinc skarns, and Th–Nb–REE-bearing pegmatite or carbonatite. The anomalous values of the Nb–REE elements in concentrate samples may have been derived from small outcrops of Proterozoic rocks too small to show at the scale of our geologic map (pl. 1). Inasmuch as most of the Soda Mountains are outside the EMNSA, types of deposit are not shown on the compilation of the types of mineral deposits (pl. 2).

Little Cowhole Mountain

Cambrian dolomite and Jurassic and (or) Cretaceous granitoid rocks of Cowhole Mountains and Cambrian dolomite are present in approximately equal amounts in the area of Little Cowhole Mountain (pl. 1). The granitoid rocks of Cowhole Mountains in places are cut by epidote-chlorite veins plus or minus quartz and pyrite, especially near their southwesternmost exposure in Little Cowhole Mountain. Stream-sediment samples do not contain anomalous concentrations of any of the elements analyzed. Concentrate samples contain anomalous concentrations of Cu, Bi, Sn, Mo, Be, Th, and Tb. No rock samples were collected. The area is geochemically mildly anomalous. From the available geochemistry, possible deposit types include copper and tin skarns and Th–Be–REE-bearing pegmatites. Known deposits at Little Cowhole Mountain include the copper skarns at the Anthony prospects and at the El Lobo Mine (pl. 2). At the Anthony prospects (U.S. Bureau of Mines, 1990a, map no. 338, pl. 1), copper skarn is seemingly zoned mineralogically from dense, steeply dipping, locally well bedded, light-green pyroxene skarn to olive-green to olive-brown compact masses of approximately 100 percent andradite that contains secondary copper minerals replacing chalcopyrite. Along the easternmost skarn at this locality, skarn is developed variably at least 500 m along the contact between the granitoid rocks of Cowhole Mountains (unit KJcm, pl. 1) and dolomite. The highest concentration of secondary copper minerals is associated directly with the most intense retrograde alteration of andradite to epidote. In detail, the contact between the granitoid rocks of Cowhole Mountains and wallrock is quite irregular, and the most continuously exposed pod of skarn has a width of approximately 100 to 150 m. In all, some skarn is exposed for more than 800 m along the contact. At the El Lobo Mine (U.S. Bureau of Mines, 1990a, map no. 339, pl. 1), extensive banded, brown-black garnet-pyroxene skarn in places is mantled by early-stage calc-silicate hornfels and cut by K–feldspar- and chalcedonic-quartz-bearing veins that include diffuse boundaries that fade into the surrounding groundmass of calc-silicate hornfels. Medial parts of the millimeter- to centimeter-sized veins are occupied by irregular concentrations of apple-green epidote. In places, ovoid pods of garnet-pyroxene skarn are approximately 100 m wide. The bulk of the sulfide minerals, mostly chalcopyrite, apparently is associated with epidote-altered garnet-pyroxene skarn. In addition, some coarsely crystalline sphalerite, in masses approximately 0.5 cm wide, is intergrown with epidote. The granitoid rocks of Cowhole Mountains, in the area immediately adjacent to the El Lobo Mine, mostly consist of partially chloritized hornblende diorite that includes less than 1 volume percent dispersed cubes of iron oxide replacing pyrite. One prospect pit at the El Lobo Mine shows intense development of siderite that is controlled strongly by minor structures striking north-south and dipping approximately 40° W. Some open spaces in brecciated siderite along these structures are filled by quartz (fig. 74). Nonetheless, the overall concentration of secondary copper minerals in the general area is relatively weak.

Cowhole Mountain

Bedrock of Cowhole Mountain consists of Jurassic and (or) Cretaceous granitoid rocks, Jurassic quartzarenite, Mesozoic volcanic and sedimentary rocks, Cambrian dolomite, Devonian to Permian limestone, and Early Proterozoic gneiss and granitoid rocks (pl. 1). The only element present in anomalous concentrations in samples from the Cowhole Mountain area is Mo in one concentrate sample. No rock samples were collected. The area is not geochemically anomalous, on the basis of RASS and PLUTO stream-sediment data sets and NURE samples. In addition to the polymetallic and iron skarn shown on plate 2 in the northern part of Cowhole Mountain (U.S. Bureau of Mines, 1990a, map nos. 343–344, pl. 1), the polymetallic skarn at the Mosaic Queen Mine (map no. 344) is the proximal occurrence of a fairly continuous zone of genetically related mineralized rocks that extend along a strike length of about 0.5 km in a northwest-southeast direction (fig. 75). At its southeasternmost end, unprospected mineralized rock, in places as much as 30 m wide, is dominated by massive replacement of Cambrian dolomite and Devonian to Permian limestone by specularite associated with epidote. Some coarsely crystalline specularite crystals are as much as 1 cm wide, and the specularite-replacement bodies show very sharp contacts with fractured and altered limestone. The iron-mineralized rock becomes dominated by a magnetite-garnet-pyroxene skarn alteration somewhat to the south of the Mosaic Queen, and some pendants of limestone have been converted almost entirely to massive epidote that includes some disseminated, fine-grained crystals of specularite. At the Mosaic Queen, sucrosic, gray-white marble that weathers pinkish tan includes less than 5 volume percent calc-silicate minerals. Immediately above the major prospect pit there, magnetite-hematite is intergrown with olive-green to olive-brown massive garnet. Magnetite definitely predominates over specularite. Samples analyzed by the U.S. Bureau of Mines (1990a) from this locality include as much as 3,900 ppm Zn, as much as 2,600 ppm Cu, and greater than 10,000 ppm Pb.

Cinder Cone Area

Approximately equal map areas of Cretaceous adamellite and Pliocene and Pleistocene basalt lava flows dominate the Cinder Cone area, located due east of Baker in the northwestern part of the EMNSA (pl. 1). Lesser amounts of Early Proterozoic gneiss and granitoid rocks, at and east of Seventeenmile Point, and Pliocene and Pleistocene basalt cinder deposits also are present. All sample media are represented in the samples collected in the

Cinder Cone area. Many elements are present in anomalous concentrations in all sample media. Stream-sediment samples contain anomalous concentrations of Zn, Mo, and Co. Concentrate samples have anomalous concentrations of Cu, Mn, Ag, Zn, Co, Bi, Sn, Mo, Be, Th, Nb, Tb, and Yb. Rock samples have anomalous concentrations of Cu, Pb, Ag, Zn, As, Sb, Mn, Bi, B, Sn, Mo, and W. NURE samples contain anomalous concentrations of Th, Ce, and Eu. Possible deposit types, which are based on geochemistry, include porphyry copper-molybdenum, polymetallic veins and replacement bodies, a variety of types of mineralized skarn, and Th–Nb–REE-bearing carbonatite and pegmatite. This large area is moderately anomalous, on the basis of the large number of elements present in anomalous concentrations even though the concentrations tend to be only weakly to moderately anomalous.

Types of deposits known in this general area include gold-silver quartz-pyrite veins, polymetallic veins, polymetallic fault, and polymetallic and tungsten skarn (pl. 2). Occurrences of polymetallic fault essentially are oxidized, base- and precious-metal-mineralized fault zones that include mostly brittle-style fault gouge and breccia and lack high concentrations of quartz and carbonate minerals as gangue. Most mineral occurrences are in the general area of Seventeenmile Point and the Paymaster and Oro Fino Mines; these epigenetic occurrences are hosted by Early Proterozoic rocks. Some likelihood exists that these areas may be parts of large slide blocks (H.G. Wilshire and J.E. Nielson, written commun., 1991). Approximately 50 percent of the occurrences have been classified as gold-silver quartz-pyrite veins. In general, widely spaced fractures that show northwesterly directed strikes are filled by brick-red iron oxides that locally include approximately 0.3–m-wide brecciated vein quartz. The attitudes of such mineralized fractures and veins are at very high angles to the ductile-style metamorphic foliation in the enclosing gneiss and granitoid. At the main workings of the Paymaster Mine (U.S. Bureau of Mines, 1990a, map no. 353, pl. 1), a 1– to 2–m-wide zone of brecciated gneiss and granitoid is densely veined by quartz (fig. 76). Some nearby veins pinch and swell, also at high angles to the metamorphic fabrics. At the Paymaster No. 3 Mine, mineralized gold-silver quartz-pyrite zones are as much as 2 to 3 m wide, have a strike of N. 10° W., and dip to the northeast. At the surface, these zones extend as much as 50 m from the main portal.

Exposures in the pediment area approximately 0.8 km due west of the Paymaster Mine contain epidotized granodiorite that may be the locus of emplacement of a widespread mineralized system that shows the general area of the gold-silver quartz-pyrite veins at the Paymaster Mine as a distal manifestation. In the pediment area, away from the major exposures of bedrock, small pods of 1– to 2–m-wide heavily epidotized granodiorite and, possibly, some dark-green, pyroxene-bearing calcic exoskarn are present where the epidotized granodiorite is in contact with marble.

Gold-silver quartz-pyrite veins also appear to be the predominant type of occurrence in the general area of the Oro Fino Mine (this particular mine is designated incorrectly as the Brannigan Mine on the Old Dad Mountain 15′ quadrangle). Such veins have been emplaced along a west-northwest-striking fault that includes recrystallized, well-bedded marble and brecciated limestone in the hanging wall. The fault zone is at least 2 to 3 m wide and shows evidence in outcrop of a brittle style of deformation; its dip is approximately 35° to 40° N. The brecciated-limestone body is terminated on the east by another north-northeast-striking fault that seems to have hosted most of the mineralization explored in the workings. Near the headframe at these workings, very steeply dipping and shattered rocks crop out for distances of as much as 5 to 6 m and have been explored by at least two shafts.

Some of the most intensely mineralized rock in this area is in the immediate vicinity of the Oro Fino Mine and its nearby workings (U.S. Bureau of Mines, 1990a, map no. 356, pl. 1). At the Oro Fino Mine, a west-northwest-striking mineralized fault includes recrystallized, well-bedded limestone and brecciated limestone in its hanging wall. Brecciated limestone, possibly indicative of some type of collapse, is fairly widespread in this area and is present also in some relatively thick sequences of rock exposed nearby (fig. 77). These rocks presumably are part of the Paleozoic sequence of rocks in the EMNSA, but they have not been mapped separately on the geologic map (pl. 1) because of limitations of scale. The mineralized fault zone is 2 to 3 m wide, dips 35° to 40° N., and includes gold-silver quartz-pyrite-type veins along it. On the east, the limestone megabreccia in the hanging wall is bounded by a north-northeast-striking mineralized structure that apparently hosted some of the most productive ore shoots at the mine and was explored by a major shaft and auxiliary levels. Heavily iron-oxide-stained quartz-pyrite veins show maroon- to brick-red colors that grade into ochre-dominated colors. In the area of the main headframe, very steeply dipping, shattered mineralized rocks along the north-northeast-striking mineralized structure are as much as 5 to 6 m wide and are explored by at least two shafts.

The workings of the Brannigan Mine are actually located close to the southeast corner of sec. 26, T. 13 N., R. 10 E. (U.S. Bureau of Mines, 1990a, map no. 362, pl. 1). Near these workings, some well-bedded quartzite includes a thin quartz-pebble conglomerate at its base, which in turn lies unconformably on gneissic metaquartzite that presumably is Proterozoic in age (fig. 25*A*). The quartzite is probably Late Proterozoic and Cambrian in age and has been included with the Early Proterozoic gneiss and granitoids (unit Xg) unit on the geologic map (pl. 1) because of its limited areal extent. At the main workings of the Brannigan Mine (termed the Brannigan East Mine by the U.S. Bureau of Mines (1990a) and subsequently restaked as the Rachele claim group), quartz-sulfide (pyrite) veins plus or minus chalcopyrite and tremolite and (or) actinolite appear to have been the ore worked in the past. Some veins show altered wallrocks that contain a coarsely crystalline, dark-green, possibly hedenbergitic, pyroxene. Such zones of alteration and mineralization closely follow bands of dolomite in the Paleozoic rocks. A sample analyzed by the U.S. Bureau of Mines (1990a) from this locality included 8.75 ppm Au and 160 ppm Ag, which is consistent with the high Ag/Au ratio that is characteristic of many polymetallic veins in the EMNSA.

In the Turquoise Mountain Mining District in the hills near Halloran Spring, 5 km northwest of the EMNSA, copper-molybdenum mineralization is related apparently to shallow-seated porphyritic intrusions (Hall, 1972). Little known mineralization exists in Proterozoic rocks of this area. Mineralization at the Telegraph Mine (U.S. Bureau of Mines, 1990a, map no. 121, pl. 1), near the southeast end of the hills near Halloran Spring, includes low-sulfide, vug-filling, gold- and silver-bearing quartz veins that were emplaced at approximately 10 Ma (Lange, 1988). These veins, which cut the informally named, Cretaceous Teutonia adamellite of Beckerman and others (1982) (Kt), are classified as gold-silver quartz-pyrite veins that are epithermal and related to wrench faulting. Early Proterozoic rocks in southeastern parts of the hills near Halloran Spring lie within the Cinder Cones Wilderness Study Area, where Wilshire and others (1987) found no evidence of mineralization. Wilshire and others (1987) assigned a low potential for gold and silver to areas underlain by Early Proterozoic rocks primarily because of their proximity to Cretaceous plutonic rocks, thought elsewhere in the region to be associated genetically with mineralization in Proterozoic wallrocks (Hewett, 1956). However, neither indications of mineralization in the vicinity of those contacts nor signs of prospecting were found by Wilshire and others (1987).

Marl Mountains

Bedrock geology of the Marl Mountains, approximately 6 km northeast of Kelso Peak, is dominated by Cretaceous adamellite (pl. 1). Early Proterozoic gneiss and granitoid rocks also are present. Stream-sediment samples from the Marl Mountains have anomalous concentrations of Pb, Ag, Zn, and Mo. Concentrate samples have anomalous concentrations of Cu, Ag, Zn, Au, Bi, Mo, Th, La, Ce, Nd, Sm, Tb, Yb, and Dy. No rock samples from the Marl Mountains are available. NURE samples have anomalous concentrations of Th and Dy. The area is moderately anomalous geochemically. Deposit types possible from these data include porphyry copper-molybdenum, polymetallic veins and replacement bodies, and REE–Th-bearing carbonatite and pegmatite. Cretaceous adamellite in the Marl Mountains is known to include four polymetallic-vein, one polymetallic-fault, and five gold-silver quartz-pyrite vein occurrences (pl. 2). We use the designation of polymetallic fault to refer to brittle-type fault zones, almost all heavily oxidized, that are mineralized by base and precious metals and lack silicate and carbonate veins.

Old Dad Mountain

No single rock type dominates Old Dad Mountain and its surrounding area (pl. 1). The promontory at Old Dad Mountain itself is underlain by a resistant knob of limestone that is part of the Devonian to Permian limestone (PDl, pl. 1) unit. Other lithic units present are Early Proterozoic gneiss and granitoid rocks (Xg), Jurassic Aztec Sandstone (Ja), Mesozoic volcanic and sedimentary rocks (Mzv), Late Proterozoic and Cambrian siliciclastic rocks (€Zs), and Tertiary volcanic rocks (Tv_1). Dunne (1972, 1977) mapped the Old Dad Mountain area but did not subdivide the Proterozoic rocks. Hewett (1956) reported the presence of granite, schist, and quartzite intruded by syenite dikes in the Proterozoic rocks in this general area.

Stream-sediment samples from Old Dad Mountain do not have anomalous concentrations of any of the elements considered. Concentrates have anomalous concentrations of Cu, Pb, Ag, Bi, Sn, Th, and Tb. Rocks have anomalous concentrations of Cu, Pb, Zn, Ag, Au, Co, Mo, Bi, B, and Be. The area is mildly anomalous geochemically. Porphyry copper-molybdenum deposits, polymetallic vein or replacement bodies, mineralized skarn, pegmatites, or carbonatites may be present on the basis of the elemental concentrations above. The area in the vicinity of Old Dad Mountain under discussion here extends approximately 16 km in a northwest-southeast direction from south of Seventeenmile Point to south of the Kelso Mountains (pl. 1). From northwest to southeast, the types of deposits in the vicinity of Old Dad Mountain include polymetallic faults at the Sweet (Reviella) claim group (U.S. Bureau of Mines, 1990a, map no. 366, pl. 1) and Lucky (ODM) claim group (U.S. Bureau Mines, 1990a, map no. 368, pl. 1), some polymetallic veins also at the Lucky (ODM) claim group, and iron skarn at the Old Dad Mountain iron deposit (U.S. Bureau Mines, 1990a, map no. 369, pl. 1) that also shows some minor amounts of polymetallic vein (fig. 78*A*). In addition, copper- and zinc-bearing magnetite skarn is present at the Golden M Mine (U.S. Bureau Mines, 1990a, map no. 372, pl. 1), located approximately 3 km southeast of the main promontory at Old Dad Mountain itself (pl. 2), that we classify as polymetallic skarn because of high concentrations of base metals at the occurrence.

Although these four mineralized occurrences extend almost across the entire length of the Old Dad Mountain area, surface indications of alteration are confined to the general areas of the mineralized occurrences. However, alteration is well exposed and widespread at one of the occurrences. At the Lucky (ODM) claim group, a zone of chloritic alteration as much as 150 m thick and containing abundant iron oxides (presumably after iron sulfide minerals of some type) is present in Late Proterozoic and Cambrian siliciclastic rocks (€Zs), which as mapped includes shattered and chloritized granodiorite. Some of this granodiorite contains fault zones filled by 0.3–m-wide ochre gossan. Recrystallized limestone, presumably part of the Devonian to Permian limestone (PDl) and seemingly in tectonic contact with the siliciclastic rocks, overlies the siliciclastic rocks and, in places, is laced with iron-oxide-stained fractures. Shattered siliciclastic rocks below the contact show fairly abundant secondary copper minerals on their weathered surfaces together with some glassy-appearing vein-type quartz. The exposed width of the shattered and mineralized rocks at this particular locality is as much as 150 m and the strike length is approximately 3.5 to 4 km. Some narrow, sulfide-impregnated, clay-altered rhyolite or rhyodacite dikes, which contain 5 to 15 volume percent phenocrystic quartz, have been emplaced into the shattered siliciclastic rocks and apparently are related genetically to the surrounding alteration (fig. 78*B*). A sample analyzed by the U.S. Bureau of Mines (1990a) from this locality included about 500 ppb Au. In many gold-rich porphyry-type systems, 500 ppb is the Au concentration in many ore zones (Sillitoe, 1979), and this Au value in samples is considered by many exploration geologists to constitute a threshold that warrants additional investigation. As a comparison, geochemical studies of the Kalamazoo porphyry copper deposit, located in Arizona, show that the ore there, not known particularly for its Au content, contains as much as 800 ppb Au along some extended intercepts of drill core (Chaffee, 1976). However, alteration in the general area of the Lucky (ODM) claim group suggests that other types of occurrences may be present, including porphyry gold and polymetallic replacement, in addition to those already listed above.

At the Old Dad Mountain iron deposit, massive magnetite-hematite replacement bodies show knife-edge contacts with the surrounding coarsely crystalline, brecciated white marble. The U.S. Bureau of Mines (1990a) estimated approximately 363,000 to 454,000 tonnes of magnetite-hematite-rich rocks remain in place at this locality. Much of the magnetite is intergrown with actinolite and seems to be related genetically to a highly schistose, chloritized granodiorite (not shown on plate 1 because of its relatively small size) that is cut by magnetite-actinolite-epidote veins. Blades of actinolite commonly are present in clusters as much as 2 to 4 cm wide. In addition, the schistose granodiorite shows development of some early-stage gray-green pyroxene hornfels in adjoining limestone. The apparently richest pods of magnetite-bearing rocks formed in limestone that crop out as much as 5 to 10 m away from the actual contact with schistose granodiorite. Overall, the mineralization at this locality is associated with a low-sulfur-bearing environment, although minor amounts of secondary copper minerals, probably chrysocolla, are present in some pods of magnetite as alteration products of chalcopyrite.

At the Golden M polymetallic-skarn occurrence, most mineralization is confined to an approximately 1–m-wide minor fault zone that strikes about N. 40° E., dips 80° to 90° S., and separates Devonian to Permian limestone (PDl) from a small mass of Proterozoic gneiss, which has been included with Mesozoic volcanic and sedimentary rocks (Mzv). The fault zone is at a high angle to foliation in the gneiss. Secondary copper minerals are present in most masses of magnetite-epidote, which form highly irregular replacement pods along a strike length of about 150 to 300 m. Some olive-green to brown garnet skarn is cut by reticulated, millimeter-sized veinlets of magnetite. In addition, much of the limestone close to the workings (two adits and an incline) is heavily stained by orange iron oxide minerals, suggestive of disseminated iron sulfide minerals. One sample analyzed by the U.S. Bureau of Mines (1990a) from this locality included more than 500 ppb Au.

Kelso Mountains

Bedrock of the Kelso Mountains includes Early Proterozoic gneiss and granitoid rocks (unit Xg, pl. 1), Late Proterozoic and Cambrian siliciclastic rocks (€Zs), and Cretaceous granitoid rocks, the latter of which includes fairly wide expanses of the informally named Teutonia adamellite of Beckerman and others (1982) (Kt) and some relatively small occurrences of biotite-rich granitoid (Kb). Concentrate samples have anomalous concentrations of Cu, Ag, Au, Sn, W, La, Ce, Nd, Sm, Tb, and Dy. NURE samples contain anomalous concentrations of La and Dy. No rock samples from the area are in the data bases. The area is geochemically mildly anomalous overall. Mineralized skarns and REE–bearing pegmatite and carbonatite are possible deposit types. The Kelso Mountains are characterized by a REE geochemical signature, although the presence of Cu, Ag, and Au may be indicative of the presence of polymetallic veins. Types of mineral occurrences known in the general area of the Kelso Mountains include polymetallic fault, gold-silver quartz-pyrite vein, and polymetallic vein (pl. 2). Most of these occurrences, 12 in all, are associated spatially with Late Proterozoic and Cambrian siliciclastic rocks that crop out in the southeastern part of the Kelso Mountains (pl. 1). The two gold-silver quartz-pyrite veins known here crop out in areas underlain by Early Proterozoic gneiss and granitoid rocks. These spatial associations between mineral occurrence and host rock suggest derivation of some of the Au and Ag from Early Proterozoic gneiss and granitoid rocks. The known mineralization in the general area of the Kelso Mountains is presumed to be related to Mesozoic magmatism. However, Jurassic and Cretaceous granitoid rocks (pl. 1) that crop out in the southern part of the Kelso Mountains area are not known to host any metallic-mineral occurrences. Analyses of mineralized rocks from the area of the Kelso Mountains further suggest that overall intensity of precious-metal mineralization here is less than that found elsewhere in the EMNSA (U.S. Bureau of Mines, 1990a). Only two analyzed samples of mineralized rocks contain more than 500 ppb Au at the 12 sites.

Bristol Mountains

Bedrock of the Bristol Mountains, located northwest of the Granite Mountains just outside of the EMNSA near its southwest corner, consists of Jurassic granitoid rocks. Stream-sediment samples in the Bristol Mountains contain anomalous concentrations of Mn, Pb, Zn, Sn, Mo, and B. Concentrate samples contain anomalous concentrations of Cu, Mn, Ag, Zn, Mo, Sn, Be, Nb, La, Nd, Sm, Eu, Yb, and Dy. NURE samples have anomalous Eu concentrations. The data bases contain no rock data. The area geochemically is mildly to moderately anomalous overall. Skarn, polymetallic vein or replacement bodies, and REE–bearing carbonatite or pegmatite are possible deposit types. We have not classified or shown the distribution of the types of mineral occurrences present in the Bristol Mountains because all of the bedrock in the mountains is outside of the EMNSA.

Clark Mountain Range

Bedrock of the Clark Mountain Range includes Early Proterozoic gneiss and granitoid rocks (unit Xg, pl. 1), Late Proterozoic and Cambrian siliciclastic rocks (€Zs), Cambrian dolomite (€d), and Devonian to Permian limestone (PDl). The Clark Mountain Range is moderately to highly anomalous geochemically. Many elements are present in anomalous concentrations in all sample media (table 13). Present and past mining activities emphasize the anomalous geochemistry of the area. The presence of the carbonatite-hosted REE deposit at Mountain Pass is reflected by anomalous concentrations of REE in concentrate and NURE samples. Other possible deposit types in the Clark Mountain Range include porphyry copper-molybdenum, polymetallic vein and replacement bodies, skarn, and pegmatite, on the basis of anomalous metal concentrations. Types of mineral occurrences and deposits in the Clark Mountain Range include the following: (1) silver-copper veins in brecciated dolostone; (2) polymetallic veins; (3) gold breccia pipe at the Colosseum Mine; (4) tungsten veins; (5) barite veins; (6) polymetallic replacement; (7) copper skarn at the Copper World Mine (fig. 79*A*); (8) zinc-lead skarn; (9) gold-silver quartz-pyrite vein; (10) placer gold and platinum-group elements; and (11) polymetallic skarn (pl. 2). As described in the sections that follow, many deposits and mineral occurrences apparently are linked genetically, as exemplified by many occurrences that surround the gold breccia pipe at the Colosseum Mine (Sharp, 1984). Silver-copper brecciated dolostone, tungsten veins, and barite veins apparently are related to emplacement of the gold breccia pipe at the Colosseum Mine during the Cretaceous. All tungsten vein occurrences are present on the east side of the range and are hosted by Early Proterozoic younger granitoids (Xg_1). In addition, on the west side of the range, some polymetallic replacement deposits and occurrences are present in another areally extensive mineralized environment where they are distal to polymetallic, copper, and zinc-lead deposits and occurrences associated with emplacement of Cretaceous granitoid rocks (Kg_2). Also, mineralization at the Conquistador No. 2 Mine (U.S. Bureau of Mines, 1990a, map no. 70, pl. 1) apparently is related to development of the metamorphic fabric in the enclosing Late Proterozoic and Cambrian siliciclastic rocks (pl. 1). At this locality, a series of shafts and approximately 15 trenches and shallow prospects explore a vein that strikes N. 35° E. and dips 35° to 45° N. This vein system is exposed discontinuously along a strike length of about 300 m. Where well exposed in the shafts, individual veins commonly are as much as 1 m wide and show bleaching of the surrounding siliciclastic rocks for distances of about 3 m on either side of the trace of the vein segments. Quartz in the veins is milky white and typically includes some iron oxide minerals that replace pyrite, which at one time constituted probably as much as 2 volume percent of the vein. The fabric of the vein quartz parallels the schistosity in the surrounding siliciclastic rock. Elsewhere in the general area of the Conquistador No. 2 Mine, wispy, apparently deformed stringers of vein quartz cut across the well-developed slaty cleavage in the siliciclastic rocks. The occurrences at the Conquistador No. 2 Mine are one of the few places in the EMNSA where mineralization seems to be associated with the metamorphic deformation. Nonetheless, cursory examination of exposures of the siliciclastic rock in the general area of the Conquistador No. 2 Mine suggests that this type or style of mineralization is fairly isolated. No widespread development exists of a pervasive low-sulfide gold-quartz type of vein mineralization, as we classify the Conquistador No. 2 Mine following the criteria of Berger (1986a) for these types of deposit. The geologic environment and overall extent of mineralization at the Conquistador No. 2 Mine may be more analogous to low-sulfide gold-quartz veins of the Chugach, Alaska, type (Bliss, 1992b), which are restricted to nonbatholithic terranes, than to those reported previously by Berger (1986a).

Mescal Range

Bedrock of the Mescal Range includes Cambrian dolomite (unit Ꞓd, pl. 1), Late Proterozoic and Cambrian siliciclastic rocks (ꞒZs), Jurassic sandstone (Ja), Devonian to Permian limestone (PDl), and Jurassic Ivanpah granite of Beckerman and others (1982) (Ji). Concentrations of Pb, Zn, and Tb are anomalous in concentrate samples. The data bases have no rock samples from the area shown as the Mescal Range on figure 49. Polymetallic veins or replacements are the most likely deposit types in the area because Early Proterozoic rocks hosting REE–bearing pegmatite and carbonatite do not crop out in this area. Known deposits and occurrences in the general area of the Mescal Range are predominantly zinc and lead bearing. They include zinc and lead skarn (exemplified by the Mohawk Mine), polymetallic skarn, polymetallic replacement, and polymetallic vein, and they are concentrated in the general area of several small bodies of Cretaceous monzogranite that crop out near the west end of Mohawk Hill in the northwestern part of the area of the Mescal Range (pl. 2). Lead-zinc-mineralized garnet-pyroxene skarn in direct contact with clay-altered biotite monzodiorite is well exposed near the main headframe at the Mohawk Mine (fig. 79*B*). In addition, a small number of gold-silver quartz-pyrite veins is present, as well as one placer-gold occurrence present in gravels near the Mohawk Mine. The widespread presence of zinc-lead-bearing types of deposit here contrasts markedly with the copper-bearing types, classified mostly as copper skarn (pl. 2), just to the north of Mohawk Hill in the general area of the Copper World Mine. However, the predominance of zinc-lead types of occurrences here does not exclude the possibility of significant precious-metal deposits being present. Some fairly widespread exposures of coarse-grained monzogranite porphyry that is intensely propylitically and argillically altered in association with emplacement of pyrite-bearing quartz veins and stockworks are present in the southern part of the Mescal Range. These exposures of altered monzogranite, shown as unit Kg_1 on plate 1, are in the general area of the Iron Horse (Bonanza), Lead Lady, and Blue Buzzard Mines (U.S. Bureau of Mines, 1990a, map nos. 144–146, pl. 1). The mostly polymetallic-replacement-type mineralization at these three deposits appears to be related to the altered monzogranite. However, analyses by the U.S. Bureau of Mines (1990a) of mineralized rock samples from these three deposits all show Au concentrations of less than 500 ppb (pl. 6). Nonetheless, many jasperoids in the general area of these deposits include Au concentrations in excess of 1,000 ppb, and related targets were being drilled during 1991 by the exploration group of Phelps Dodge Mining Co. (John D. Forrester, oral commun., 1991). Additional discussion concerning genetic linkages among types of deposits is included in the section below entitled “Evaluation of Metallic Mineral Resources.”

Ivanpah Mountains

Bedrock of the Ivanpah Mountains includes Jurassic granite (unit Ji, pl. 1); Early Proterozoic granitoid rocks, gneiss, and migmatite (Xm); Devonian to Permian limestone (PDl); Late Proterozoic and Cambrian siliciclastic rocks (€Zs); and Cambrian dolomite (Cd). Thick sequences of thin-bedded Paleozoic carbonate rocks are exposed conspicuously in the Striped Mountain block of the Ivanpah Mountains area (fig. 80; pl. 1). Stream-sediment samples from the Ivanpah Mountains contain anomalous concentrations of Cu, Ag, Zn, Mo, Sn, and W. Other sample media contain anomalous concentrations of many elements that suggest the presence of polymetallic veins or replacement bodies, porphyry copper-molybdenum deposits, skarns, and carbonatites or pegmatites containing deposits of REE or Th. Concentrate samples have anomalous concentrations of Cu, Mn, Pb, Ag, Au, Co, Bi, Sb, Mo, W, Sn, Be, Th, La, Ce, Nd, Sm, Tb, and Dy. Rock samples have anomalous concentrations of Cu, Zn, Co, Mn, Pb, Ag, As, Bi, W, Sn, Mo, Be, and B. NURE samples contain anomalous concentrations of La, Ce, Lu, Sm, Eu, Tb, Yb, and Dy. Overall, the Ivanpah Mountains geochemically are moderately to highly anomalous.

Known deposit types in this area include tungsten skarn, polymetallic fault, polymetallic vein, copper skarn (pl. 2), and one unnamed occurrence of low-sulfide gold-quartz vein in the Late Proterozoic and Cambrian siliciclastic rocks (U.S. Bureau of Mines, 1990a, map no. 16, pl. 1). At the gold-quartz-vein locality, shattered rocks approximately 1 m wide show local emplacement of quartz-pyrite-minor chalcopyrite veins at a high angle to the regional attitude of foliation in the surrounding siliciclastic rock. However, the vein quartz is itself deformed and shows a foliated fabric that includes lineated margins in its selvages. Approximate attitude of the veins is a N. 40° W. strike and a 55° S. dip. Massive epidote skarn is present at the Silverado-Tungstite Mine at the east end of Striped Mountain (fig. 79*C*), from which a small tonnage of silver ore was shipped prior to 1900 (U.S. Bureau of Mines, 1990a). Mineralization at this locality is probably associated with the adjoining Jurassic Striped Mountain pluton (Jsm), which is present as a narrow intrusion of hornblende diorite along the west side of the Ivanpah Mountains (pl. 1). Silver mineralization at the Silverado-Tungstite Mine may be associated with retrograde quartz, which fills open spaces and cuts prograde garnet skarn (fig. 79*D*). In addition, some endoskarn is well developed near the Silverado-Tungstite Mine as diffuse epidote skarn that shows relict igneous textures. Jasperoid along a 2– to 3–m-wide, steeply dipping fault that strikes N. 35° W. at the Express Mine (U.S. Bureau of Mines, 1990a, map no. 171, pl. 1) has been explored by a 10– to 12–m-wide open cut and is classified by us as a polymetallic fault (pl. 2). In addition, the area of Striped Mountain contains a vast resource of limestone (U.S. Bureau of Mines, 1990a).

The bulk of the mineralization in terms of numbers of occurrences in this part of the EMNSA is present in Jurassic granitoid rocks as polymetallic veins, gold-silver quartz-pyrite veins, polymetallic faults, zinc-lead skarns in pendants too small to show at the scale of the geologic map, and one fluorite vein (pl. 2). The gold-silver quartz-pyrite veins show no apparent lateral zonation relative to the distribution of polymetallic veins in this general area. The tin (tungsten) skarn mineralization at the Evening Star Mine (U.S. Bureau of Mines, 1990a, map no. 193, pl. 1) apparently is related to emplacement of Jurassic granitoid rocks, although the main mass of the Jurassic granitoid rocks crops out approximately 1 to 5 km east of the workings at the Evening Star Mine (pl. 1). Narrow dikes at the Evening Star Mine and at the nearby Standard Mine No. 2 are similar lithologically to Jurassic granitoid rocks east of these two occurrences. At the Evening Star Mine, chalcopyrite-bearing tremolite hornfels is present near the outer limits of skarn development and is mantled by a zone of recrystallized limestone that includes fine-grained crystals of magnetite and (or) pyrite. In places, the marble has been dolomitized as much as 10 m away from some zones of heavily sulfidized, structurally controlled skarn. South-southwest of the Evening Star Mine, Jurassic granitoid rocks have been converted to an epidote endoskarn that shows relict outlines of plagioclase. Magnetite is abundant in many pods of skarn at the Evening Star Mine, and the magnetite seems to be one of the earliest postsilicate phases to crystallize in the open-space environment of the skarns.

Cima Dome

Bedrock of the Cima Dome area includes two bodies of Cretaceous adamellite, the Teutonia adamellite and the Kessler Springs adamellite, both of which are informally named units of Beckerman and others (1982), and an elongate, northwest-trending body of Jurassic granite (pl. 1). Geochemical samples in the area of Cima Dome are represented by only one sample, a rock that contains an anomalous concentration of Tb. The only known mineral occurrence in the area of Cima Dome is present at the Teutonia Mine (pl. 2; see also U.S. Bureau of Mines, 1990a, map no. 210, pl. 1).

At the Teutonia Mine, polymetallic-vein mineralization is concentrated along a zone that strikes N. 60° W. in the Kessler Springs adamellite. Alteration in the area of the mine extends approximately 20 to 30 m from some of the major strands of vein exposed by several currently inaccessible shafts. Alteration consists mainly of conversion of plagioclase to clay minerals, possibly including some halloysite. Some 4– to 5–cm-wide, greasy-appearing, gray veins of quartz show early-stage sulfide minerals, now oxidized to ochre-brown iron oxide minerals, primarily along the walls of the veins, but some late-stage sulfide minerals also are present along the medial parts of the veins. A sample of ore obtained from a dump at the Teutonia Mine was examined using the scanning electron microscope. Silver-bearing minerals identified include galena, argentite, and tetrahedrite. Contents of silver in galena are highly variable even at the scale of the several-hundred-micron-wide domains examined. Some silver-bearing galena, as narrow, 5–µm-wide rims that discontinuously surround much larger crystals of sphalerite, is confined to short segments of the rims; the remaining galena is apparently free of any detectable silver. Some tetrahedrite detected is argentiferous, and it seems to be paragenetically intermediate between early-stage sphalerite and late-stage, notably non-silver-bearing galena. Other minerals detected during the scanning-electron-microscope study are aurichalcite (ideally, $2(Zn,Cu)CO_2 \cdot 3(Zn,Cu)OH_2$), barite, possibly specular hematite, covellite, and argentite. Argentite is present as feathery 2– to 3–mm-long crystals on the borders of irregularly shaped crystals of galena. The argentite is mantled by covellite in places. Overall, the locality shows relatively sparse concentrations of secondary copper minerals, including both malachite and chrysocolla. Although some veins also include iron-carbonate minerals, overall the veins still retain a high quartz–carbonate-mineral ratio. No carbonate minerals were noted in the walls of the veins. In places, vein material is coxcombed, brecciated, and filled by jasperoidal material. We have classified the mineralization at the Teutonia Mine as a silver-rich variety of polymetallic vein (pl. 2). Production from the Teutonia Mine includes approximately 46.9 kg Ag during 1880 (U.S. Bureau of Mines, 1990a).

New York Mountains

Bedrock of the New York Mountains includes extensive areas of Cretaceous adamellite (namely, the informally named Mid Hills adamellite (unit Kmh, pl. 1) of Beckerman and others (1982)) and Early Proterozoic migmatite and granitoid rocks (Xm), as well as lesser amounts of Tertiary andesite and basalt (Tab), Devonian to Permian limestone (PDl), Cretaceous granodiorite (Klo), Tertiary dacite flows (Td), Mesozoic volcanic and sedimentary rocks (Mzv), Triassic sedimentary rocks (TRm), Cambrian dolomite(Єd), and Miocene rhyolite ash-flow tuff (Tw). Numerous elements are present in anomalous concentrations in all sample media from the New York Mountains. The area is one of the most highly anomalous geochemically in the EMNSA. Stream-sediment samples contain anomalous concentrations of Cu, Mn, Pb, Ag, Zn, Mo, W, Co, B, and Be. Concentrate samples have anomalous concentrations of Cu, Mn, Pb, Ag, Zn, Co, Ba, Bi, Sn, Mo, W, Be, B, Th, La, Ce, Nd, Sm, Eu, Tb, Yb, and Dy. Rock samples have anomalous concentrations of Cu, Pb, Ag, Zn, Au, As, Co, Sb, Ba, Bi, La, Mo, and B. NURE samples have anomalous concentrations of Th, Ce, Dy, Lu, Eu, and Yb. Possible deposit types include porphyry copper-molybdenum, polymetallic vein and replacement bodies, disseminated gold, skarn of all types, and U–Th–Nb-bearing carbonatite and pegmatite.

A number of different types of mineralized systems are present in the New York Mountains. The Mid Hills adamellite hosts the Big Hunch stockwork molybdenum system (Ntiamoah-Agyakwa, 1987; U.S. Bureau of Mines, 1990a, map no. 290, pl. 1) that shows intensely developed quartz stockworks cropping out across an area of approximately 5 km^2 near the southwest edge of the New York Mountains (pl. 2). This system initially was thought to contain as much as approximately 363,000,000 kg Mo in about 1.6 billion tonnes of rock (U.S. Bureau of Land Management, 1980). However, subsequent investigations have shown that this amount of Mo should be revised substantially and that a content of approximately 21,000,000 kg Mo probably is a more reasonable estimate on the basis of results of drilling to date (Wetzel and others, 1992). In addition, the New York Mountains include the following other types of deposit: (1) polymetallic fault, gold-silver quartz-pyrite vein, and polymetallic vein in Early Proterozoic migmatite; (2) copper skarn and polymetallic skarn in Devonian to Permian limestone; and (3) polymetallic vein, polymetallic fault, gold-silver quartz pyrite vein, and tungsten vein in the Mid Hills adamellite. The polymetallic veins at the Golden Quail Mine near the southeast edge of the New York Mountains (pl. 2; see also U.S. Bureau of Mines, 1990a, map no. 417, pl. 1) were known to include an identified resource of 12,500 kg Au in 1992 (Wetzel and others, 1992). Elsewhere in the New York Mountains, the most intense concentration of mineral occurrences and deposits is present in Early Proterozoic migmatite. Analyses of mineralized rock samples from a cluster of these occurrences and deposits, in an area of about 20 km^2 near the site of Vanderbilt, show Au concentrations higher than 500 ppb (pl. 6).

Mid Hills

The Cretaceous Mid Hills adamellite (unit Kmh; pl. 1) and Rock Springs monzodiorite (Krs), both informally named units of Beckerman and others (1982), and Early Proterozoic granitoid rocks (Xg_2) are the predominant rock types in the Mid Hills. Tertiary tuffs (Tw) also are present. Stream-sediment samples from the Mid Hills contain anomalous concentrations of Zn, Mo, and B. Concentrate samples contain anomalous concentrations of Mn, Ag, Ba, Bi, Mo, W, Nb, La, Ce, Eu, and Nd. Rock samples contain anomalous concentrations of Zn, Mn, Pb, Ag, and Bi. NURE samples contain anomalous concentrations of Ce. Possible deposit types include porphyry copper-molybdenum, polymetallic vein and replacement bodies, skarns, and REE–Th–Nb-bearing pegmatites and carbonatites (pl. 2). The area is mildly to moderately anomalous geochemically overall.

The Mid Hills area includes some polymetallic vein; gold-silver quartz-pyrite vein; and polymetallic fault types of occurrences and deposits, together with a small number of polymetallic-skarn and copper-skarn occurrences hosted by pendants of Devonian to Permian limestone enclosed within the Mid Hills adamellite. Most occurrences are present near the mapped outer intrusive margin of the Mid Hills adamellite. Analyses of mineralized rock samples from several polymetallic-vein and polymetallic-fault occurrences in the general area of the Gold Valley Mine (U.S. Bureau of Mines, 1990a, map no. 570, pl. 1) show Au concentrations in excess of 500 ppb (pl. 6). Although the Mid Hills adamellite in places shows intense mineralization at the surface, large areas of this pluton in the Mid Hills are unaltered.

Providence Mountains

The geology of the Providence Mountains is complicated by the presence of major faults that bound many of the map units (pl. 1). The area is dominated by Devonian to Permian limestone (unit PDl; pl. 1); Cambrian dolomite (Ꞓd); Jurassic granitoid rocks, which include the quartz monzonite of Goldstone (Jgo) and the quartz syenite of Winston Basin (Jwb); Early Proterozoic granitoid rocks (Xg_2); and Miocene rhyolite ash-flow tuff

(Tw). Significant amounts of Cretaceous porphyritic monzogranite (Kmh), Late Proterozoic and Cambrian siliciclastic rocks (ЄZs), and Jurassic hypabyssal and metavolcanic rocks (Jh) and diorite (Jd) also are present. The Providence Mountains are geochemically the most highly anomalous area in the EMNSA (figs. 50–73) and have been heavily sampled. All sample media contain anomalous concentrations of many elements. Stream-sediment samples contain anomalous concentrations of Cu, Mn, Pb, Ag, Zn, Co, Sn, Mo, Ba, and W. Concentrate samples have anomalous concentrations of Cu, Mn, Pb, Ag, Zn, Au, Ba, As, Co, Sb, Bi, Sn, Mo, W, Be, B, Th, Nb, La, Ce, Nd, Sm, Eu, and Tb. Rock samples contain anomalous concentrations of Cu, Mn, Pb, Ag, Zn, Au, Ba, Co, Sb, As, Bi, Sn, Mo, W, Be, B, Th, Nb, Nd, Eu, and La. NURE samples contain anomalous concentrations of Th, La, Lu, Eu, Yb, and Dy. Possible deposit types in the Providence Mountains include porphyry copper-molybdenum, polymetallic veins and replacement bodies, mineralized skarn of all types, disseminated gold, and REE–U–Th–Nb-bearing carbonatite and pegmatite.

Plate 2 shows the density and overall distribution of types of mineral occurrences in the Providence Mountains. The Providence Mountains contain the largest occurrence of known iron skarn in the EMNSA at the Vulcan Iron Mine (fig. 81*A*; pl. 2). Iron skarn formed here at the now-faulted contact (fig. 81*B*) between Jurassic albitized diorite and Cambrian dolomite (unit Єd, pl. 1; see also Goldfarb and others, 1988). Approximately 3 million tonnes of magnetite-rich skarn is still present in the ground at this locality (Goldfarb and others, 1988). That part of the northern Providence Mountains underlain by Early Proterozoic granitoids, mostly augen gneiss of granite and granodiorite composition, includes the densest concentration of metallic-mineral occurrences in the EMNSA. In this area, the metallic-mineral occurrences seem to be preferentially concentrated in a broadly elongate, north-northeast-trending zone centered along the trace of the East Providence fault (pl. 1). Polymetallic-vein, polymetallic-fault, and gold-silver-quartz-pyrite-vein occurrences are predominant (pl. 2). Near the center of this intensely mineralized area, two occurrences of possible low-fluorine stockwork-molybdenum systems also are present. These two possible stockwork-molybdenum systems are in and near Cretaceous intrusive breccia (part of unit Kmh) at Globe Wash (Goldfarb and others, 1988). Goldfarb and others (1988) describe these molybdenum occurrences as, in upper Globe Wash, massive felsic dikes or sills and irregularly shaped, silica-cemented breccias that are altered to quartz and sericite; widespread propylitic alteration in Proterozoic gneiss becomes more pervasive and intense near mineralized zones; and sericitic alteration of wallrock is common along quartz veins. The SS No. 17 prospect contains visible grains of molybdenite (one sample yielded 250 ppm Mo) along with large pyrite crystals and mostly native sulfur apparently after pyrite, in massive, white radial and ring quartz veins (fig. 82*A*) surrounding a felsic intrusive breccia. Another sample of gossan from a minor fault in the general area of the SS No. 17 prospect includes approximately 600 ppm Mo (table 11, analysis no. 46). The development of breccia in this general area may reflect explosive release of vapor concomitant with transition from a single phase to a two-phase fluid regime. Several companies have explored this area since 1970 on the basis of evidence that suggests a stockwork-molybdenum system at depth. The highest Mo concentrations were detected in chip samples collected near the SS Nos. 20–22 and 27–29 Mines, and the South (Star?) Mine, which are near the center of the area of molybdenum exploration. Goldfarb and others (1988) further suggest that there is unknown potential for a molybdenum-porphyry system in upper Globe Wash. The brecciated, porphyritic, leucocratic, informally named, Cretaceous Mid Hills adamellite of Beckerman and others (1982), which intrudes Proterozoic gneiss to the west of the East Providence fault zone, shows extensive propylitic and argillic alteration; local sericitic alteration and pyritization are common near silicified breccia zones (fig. 82*B*). One prospect pit contains molybdenite rosettes in white quartz veins of both ring and radial geometry; the veins have anomalous F, Pb, and Zn concentrations.

Although the age of mineralization of the polymetallic veins and other occurrences hosted by the Early Proterozoic (intermediate-age) granitoids has not been established, they may be related to, and zoned around, a large Cretaceous porphyry-type system centered on the molybdenite occurrences at Globe Wash described above. However, the lateral extent of the quartz stockworks at Globe Wash at the inferred center of the system is quite small compared to the areal size and intensity of quartz stockworks known in many other similar stockwork-molybdenum systems (Theodore and Menzie, 1984; Theodore and others, 1992). In fact, at Globe Wash, brecciated fragments of sericitically altered leucogranite have been flooded secondarily by quartz and some molybdenite (Goldfarb and others, 1988) across only a relatively small area in the bottom of Globe Wash. The vein quartz is not coextensive with the mapped Cretaceous granite there (Kmh). Therefore, we questionably designate these occurrences of molybdenite as part of a stockwork-molybdenum system and, further, suggest that if this is the central part of a very large porphyry system, then the most heavily molybdenum- and (or) copper-mineralized parts would be at approximately 4 to 5 km depths below the surface.

Granite Mountains

Bedrock of the Granite Mountains is dominated by Cretaceous granitoid rocks (units Kpm, Kgd, pl. 1), mostly 70 to 75 Ma in age. Lesser amounts of Jurassic diorite and granitoid rocks (Jd, Jqd) are also present. Concentrate and rock samples have anomalous concentrations of many elements: Cu, Pb, Ag, Zn, Co, Ba, Bi, Sn, Mo, W, Be, Th, La, La, Ce, Nd, Tb, and Yb are present in anomalous concentrations in concentrate samples; rock samples have anomalous concentrations of Cu, Mn, Ag, As, Pb, Co, Sn, Zn, Ba, Bi, Mo, B, Nb, Nd, Tb, Yb, Ce, and Dy. NURE samples contain anomalous concentrations of La and Eu. The area is only mildly to moderately anomalous geochemically because, although many elements are present in anomalous concentrations, they are generally weakly anomalous or else only a small proportion of samples from the area have anomalous concentrations of a given element. Porphyry copper-molybdenum, polymetallic veins and replacements, and REE–Th–Nb-bearing pegmatites are possible deposit types on the basis of available geochemistry. Only a small number of mineral occurrences are present in the Granite Mountains area (pl. 2). These include two polymetallic veins, one iron skarn, and one gold-silver quartz-pyrite vein, all widely separated from one another and not showing any apparent zonal relations. Moreover, most exposed granitoid rocks in the Granite Mountains area are not altered visibly at the surface.

Van Winkle Mountain

Van Winkle Mountain, near the south-central edge of the EMNSA, is largely made up of Miocene air-fall tuff and lava flows (unit Tal, pl. 1). Miocene tuff breccia (Ttb) and Cretaceous monzogranite (Kpm) make up small parts of the area. The only sample from the area shown as Van Winkle Mountain on figure 49 is a NURE sample. The only element present in an anomalous concentration is La. The area is weakly anomalous geochemically, on the basis of limited information. Three mineral occurrences are known in the area of Van Winkle Mountain (pl. 2). Only one of these has sufficient data available upon which to make a deposit-type classification, and that one occurrence has been classified as a polymetallic fault that cuts Miocene air-fall tuff and lava flows.

Grotto Hills

Most of the Grotto Hills is composed of Miocene shallow-intrusive rocks (unit Ti, pl. 1) and rhyolite, basalt, and dacite (Tv_1) that crop out in an area of about 6 km^2. The smaller, western hills are composed of Cambrian dolomite (Ꞓd) and Devonian to Permian limestone (PDl), which cover an area of about 0.5 km^2. Stream-sediment samples from the Grotto Hills contain anomalous concentrations of Ag, Zn, and Mo. Concentrate samples contain anomalous concentrations of Cu, Mn, Zn, Co, and Mo. No rock samples were collected in the Grotto Hills. NURE samples from the area do not have anomalous concentrations of any element. Possible types of occurrences include polymetallic veins and replacements. The area is geochemically weakly anomalous. No known mineral occurrences are present in the Grotto Hills (pl. 2).

Pinto Mountain

Pinto Mountain is underlain mainly by Miocene rhyolite ash-flow tuff (fig. 83), but a small area underlain by the informally named Cretaceous Mid Hills adamellite of Beckerman and others (1982) also is present (pl. 1). The only elements present in anomalous concentrations near Pinto Mountain are Mo in concentrate samples and Eu in NURE samples. Molybdenum in the concentrate samples may be derived from the general area of the Big Hunch stockwork-molybdenum system, which is directly upstream from the Pinto Mountain area (pl. 2). No rock samples in the RASS and PLUTO data bases were collected from the area. The area is not geochemically anomalous. No mineral occurrences are known in the immediate area of Pinto Mountain.

Table Mountain

Most of the Table Mountain area is underlain by Cretaceous granitoid rocks (units Krs, Kmh, pl. 1); small areas are underlain by Early Proterozoic granitoid rocks (Xg_1) and Tertiary tuff (Tw). Stream-sediment samples from Table Mountain contain anomalous concentrations of Zn and Mo. Concentrate samples contain anomalous concentrations of Ag. Rock samples contain anomalous concentrations of Cu, Pb, Ag, Sb, Sn, Mo, and Eu. NURE samples contain anomalous concentrations of Th, La, Ce, and Dy. The area is geochemically mildly anomalous. Possible deposit types suggested by the geochemical results include polymetallic veins and REE–Th-bearing pegmatites. Three mineral occurrences are present in the area of Table Mountain, and they consist of two polymetallic vein systems and one polymetallic fault (pl. 2). A rock sample collected at one of these occurrences contains more than 500 ppb Au (pl. 6; see also U.S. Bureau of Mines, 1990a).

Woods Mountains

Bedrock of the Woods Mountains is dominated by Miocene rhyolite ash flows and domes (unit Tts, pl. 1). Lesser areas of bedrock are composed of Miocene rhyolite ash-flow tuff (Tw) and basalt flows (Tb). No rock samples from the Woods Mountains are in the data sets examined. The only anomalous element concentrations are Ag and La in concentrate samples and Dy in NURE samples. The area is weakly anomalous geochemically. No metallic mineral occurrences are known in the Woods Mountains area (pl. 2; see also U.S. Bureau of Mines, 1990a).

Hackberry Mountain

Bedrock of Hackberry Mountain is mostly Miocene volcanic rocks of trachyte, trachydacite, and rhyolite (unit Ths, pl. 1); rhyolite ash-flow tuff (Tw); and rhyolite lava flows and ash flows, tuffaceous sedimentary rocks, tuff breccia, basalt flows, and andesite flows (Tv_2). A small area of Early Proterozoic gneiss and granitoid rocks (Xg) also is present. Stream-sediment samples from Hackberry Mountain contain anomalous concentrations of Ba. Concentrate samples have anomalous concentrations of Mn, Ag, Zn, Ba, and Mo. NURE samples contain anomalous concentrations of Ce, Eu, Yb, and Dy. No rock samples were collected. The area is geochemically mildly anomalous. Possible deposit types include polymetallic vein, polymetallic fault, and REE–bearing pegmatite. Seven of 16 mineral occurrences known in the area of Hackberry Mountain (pl. 2) have been classified as polymetallic fault, although the base-metal-enriched signatures of these occurrences may be reflections of a Creede-type quartz-adularia precious-metal system at depth (Mosier and others, 1986). Most of these seven polymetallic faults are concentrated in a northeast-trending zone along the southeast flank of Hackberry Mountain. Analyses of mineralized rock samples from the seven polymetallic faults all contain less than 500 ppb Au (pl. 6; see also U.S. Bureau of Mines, 1990a). One sample from a locality classified as a polymetallic vein (U.S. Bureau of Mines, 1990a, map no. 600, pl. 1), however, does contain more than 500 ppb Au. This particular locality is well south of the locus of most recent exploration activities by private industry (Gottlieb and Friberg, 1984). These exploration activities center on widely dispersed silicification in the general area of the seven occurrences of polymetallic faults described above. In addition, these seven occurrences coincide with (1) a magnetic low (pl. 5), suggestive of demagnetization resulting from hydrothermal alteration, and (2) an anomaly of limonitic and argillic alteration, as well as silicification, detected by our analysis of the Landsat Thematic Mapper image (fig. 36).

Our field examinations noted abundant silicification along the southeast flank of Hackberry Mountain, but none of this silicification appears to be comparable to the intensity of the pervasive silicification and stockwork veining described below in the general area of the Hart Mining District. Most silicification at Hackberry Mountain is present in rhyolite flows or densely welded ash-flow tuffs. In addition, pervasive bleaching of these rocks is found in association with the argillic alteration, which is confined mostly to a northeast-trending zone on the southeast flank of Hackberry Mountain where the polymetallic faults are present. These mineralized faults at Hackberry Mountain contain elevated abundances of Pb, As, Sb, and some Zn. Production of approximately 1,730 kg Pb is credited to the Dewey Mine, one of the seven occurrences classified as a polymetallic fault (U.S. Bureau of Mines, 1990a). Furthermore, Gottlieb and Friberg (1984) describe results of exploration activities as follows:

> The Hackberry Mountain prospect is a late Tertiary disseminated precious metal deposit hosted by rhyolites and ash-flow tuffs. Geochemical and lithologic logging of four drill holes down to 900 ft [274 m] show an upper [essentially] unaltered zone down to 200 ft [61 m] with occasional native Au in hematite-replaced sanidine. An altered zone extends to 800 ft [244 m], and an unaltered zone extends from 800 to 900 ft [244 to 274 m]. The altered zone is mainly ash-flows and the unaltered zones are mainly rhyolite lava flows.
>
> Surface and drill hole samples [in the Hackberry Mountain prospect] show varying degrees of alteration and mineralization. The ore consists of fine grained native Au surrounded by bladed stibnite, chalcedony and hematite. Argillic alteration is dominant, with lesser amounts of silicification. In the argillically altered rock the phenocrysts are altered to clay minerals, and the groundmass, which had devitrified to quartz and potassium feldspar prior to alteration, remains fresh. Silicified rocks are altered to quartz plus Fe and Mn oxides. Major element chemistry indicates Si and Mn increase in altered rocks, Al, Fe, and K remain constant, and Mg, Ti, Na, and Ca decrease. Ca is the best indicator of alteration. Minor element chemistry shows that Zn increases with alteration, Ba, Cr, and V remain constant, and Sr decreases. Sr, believed to be contained in plagioclase, is an accurate indication of alteration whereas Ba, contained in the more stable sanidine was not mobilized. Trace elements La, Y, and Yb remain constant with respect to alteration. Au varies from 0.001 to 0.088 oz/ton [0.03 to 2.75 g/t].

Vontrigger Hills

Bedrock of the Vontrigger Hills is mostly Early Proterozoic granitoid rocks (unit Xg_1, pl. 1), dated at between 1,660 and 1,695 Ma, and migmatite (Xm). Small areas of Miocene volcanic rocks (Tv_1) and Cretaceous granitoid rocks (Kpg) are found mainly in the western part of the area. Stream-sediment samples from the Vontrigger Hills do not contain anomalous concentrations of any elements. However, concentrate samples have anomalous concentrations of Ag and Ba, and rock samples have anomalous concentrations of Cu, Mn, Pb, Zn, Ag, As, Bi, Mo, Be, B, and Nb. The area is geochemically moderately anomalous overall. Possible deposit types include porphyry copper-molybdenum, polymetallic veins and replacement bodies, and REE–Nb-bearing pegmatites.

Six mineral occurrences in the Vontrigger Hills include three polymetallic veins, two low-sulfide gold-quartz veins, and one polymetallic fault (pl. 2). All occurrences are far removed from the Cretaceous granitoid that crops out near the southwest end of the Vontrigger Hills (pl. 1), and all the occurrences are hosted by Early Proterozoic younger granitoid rocks. Mineralization is extremely widespread at some localities (pl. 2), such as in the general area of the Rattlesnake Mine (U.S. Bureau of Mines, 1990a, map no. 592, pl. 1), where numerous prospect pits, shafts, and a partially reclaimed open cut approximately 100 m wide follow favorable indications of gold mineralization of various attitudes and types in an area of about 3 km^2. Much of the gold mineralization initially exploited at the Rattlesnake Mine, classified as polymetallic vein, is along a 10–m-wide zone of intensely silicified and highly fractured, foliated Early Proterozoic younger granitoid rocks. This mineralized zone has a strike of about N. 70° W. and is present at the north edge of a porphyritic monzogranite of undetermined size (not shown on pl. 1). Numerous unmineralized porphyritic granite dikes containing K–feldspar phenocrysts cut the Early Proterozoic younger granitoid rocks.

At the True Blue Mine (U.S. Bureau of Mines, 1990a, map no. 588, pl. 1), discontinuous, narrow stringers of vein quartz in places partly fill open cavities developed in Early Proterozoic younger granitoid rocks and elsewhere. The open cavities are lined by chrysocolla, azurite, and iron oxide minerals that replace pyrite. These veins typically are 1 to 2 cm wide and approximately 10 to 16 cm long; they cut the foliation in the surrounding Early Proterozoic younger granitoid rocks at high angles.

Piute Range

The southern part of the Piute Range is dominated by Cretaceous granitoid rocks (unit Kpg, pl. 1) but also contains substantial areas of Early Proterozoic younger granitoid rocks (Xg_1) and Miocene basalt flows (Tb). The middle and northern parts of the range are almost exclusively Miocene dacite to andesite flows, domes, and breccias (Td) but also contain small areas of underlying Early Proterozoic granitoid rocks (Xg), Miocene welded ash-flow tuff (Tps), and Early Proterozoic younger granitoid rocks (Xg_1). Stream-sediment samples from the southern and middle parts of the Piute Range contain anomalous concentrations of Pb, Zn, Mn, Co, Mo, and B. Stream-sediment samples from the northern part of the range do not have anomalous concentrations of any element. Concentrate samples from the southern and middle parts of the range have anomalous concentrations of Cu, Pb, Zn, Ag, Ba, B, Bi, Sn, W, Be, Mo, La, Sm, and Tb. Rock samples from the southern part of the range contain anomalous concentrations of Cu, Pb, Ag, Zn, Au, Sb, Bi, Mo, and W. NURE samples from the southern part of the range have anomalous concentrations of Th. Rock and concentrate samples from the northern part of the range contain anomalous concentrations of Be. Concentrate samples from the northern part of the range also have anomalous concentrations of Sn. NURE samples from the north part of the range contain anomalous concentrations of Ce, Lu, Sm, Eu, Yb, and Dy. Overall, the Piute Range is geochemically moderately to highly anomalous. Possible deposit types include porphyry copper-molybdenum, polymetallic veins and replacement bodies, disseminated gold, and REE–bearing carbonatite or pegmatite.

No mineral occurrences were reported by the U.S. Bureau of Mines (1990a) in the northern and central part of the Piute Range. Much of this part of the range includes relatively thick sequences of Miocene dacite to andesite flows, domes, and breccias (pl. 1). However, numerous prospects and previously mined areas are present in the southern part of the range, particularly to the west-northwest of Signal Hill and to the east-northeast of Billie Mountain (pl. 2). This area, known as Tungsten Flat and coinciding with the Signal Hill Mining District, includes several polymetallic-vein localities but only a small number (U.S. Bureau of Mines, 1990a) of the actual tungsten-vein localities are present. However, prospects and other workings of various types are extensively developed in an area of about 6 to 7 km^2 at Tungsten Flat that contains widespread exposure of Cretaceous granitoid rocks. Wolframite-bearing quartz veins typically are 1 to 2 m wide, strike N. 20° W., and dip steeply to the northeast; these veins are concentrated mostly in the northern part of the district. They are generally discontinous and have been extensively explored by shallow prospect pits and underground workings as much as 100 m long along strike. Secondary copper minerals are common in many of the workings. Intense clay alteration is confined to rocks generally within 5 to 7 m of the veins. The Leiser Ray Mine, near the south end of the mining district, shows elevated abundances of galena and chalcopyrite relative to occurrences at the north end of the district. The Leiser Ray Mine is a polymetallic-vein occurrence that has a past production of 6,877 kg Cu, 755 kg Pb, 36.8 kg Ag, and 0.8 kg Au (U.S. Bureau of Mines, 1990a). The main vein at the Leiser Ray Mine probably was discovered before 1891 (Hewett, 1956). The metal zonation in the Tungsten Flat Mining District seems to show silver-bearing polymetallic veins on the south, distal to tungsten veins on the north. Mineralization in the Tungsten Flat Mining District lies astride the projected east-northeast trend of the hinge line of the Piute Anticline (Hewett, 1956).

Castle Mountains

Bedrock of the Castle Mountains is mainly Miocene dacite and rhyolite shallow intrusions and extrusive domes, flows, and breccia (unit Tdr, pl. 1). Smaller areas of bedrock are composed of Early Proterozoic migmatite (Xm) and Miocene basalt and andesite lava flows (Tab) and rhyolite ash-flow tuffs (Tps). Stream-sediment samples from the Castle Mountains contain anomalous concentrations of Mn, Pb, Zn, Co, B, and Mo. Concentrate samples have anomalous concentrations of Cu, Mn, Zn, Ba, Co, Bi, Mo, B, Th, La, Ce, Nd, Sm, Eu, Yb, and Dy. Rock samples contain anomalous concentrations of Mn, Ag, Sb, Pb, Ba, Mo, B, Nb, Eu and Tb. NURE samples contain anomalous concentrations of Dy and Eu. The Castle Mountains geochemically are moderately to highly anomalous. Possible deposit types include porphyry copper-molybdenum, polymetallic vein and replacement bodies, epithermal gold, and REE–Th–Nb-bearing carbonatite and pegmatite. The Castle Mountains include the economically significant epithermal quartz-alunite quartz-adularia gold deposits at the Castle Mountains Mine, hosted by Tertiary volcanic rocks that show a diagnostic vuggy silica, acid-sulfate-type alteration (fig. 84; pls. 1, 2). These deposits constitute one of the largest economic reserves of minable gold known in 1995 in southern California.

Homer Mountain

Bedrock of Homer Mountain, located outside the east edge of the EMNSA, is composed of Early Proterozoic granitoid rocks (unit Xg_1, pl. 1). Stream-sediment samples from Homer Mountain contain anomalous concentrations of Ag and Mo. Concentrate samples have anomalous concentrations of Mn. NURE samples have anomalous concentrations of Eu and Dy. The area is geochemically weakly anomalous. Possible deposit types include polymetallic vein and REE–Nb-bearing pegmatite. Inasmuch as the area of Homer Mountain is outside the EMNSA, we have not included herein a discussion of its mineral occurrences.

U.S. Bureau of Mines Data Base

Assembly of Data Base

In this section of this report, we examine some of the metallic-mineral-resource implications of geochemical data obtained by the U.S. Bureau of Mines (1990a, tables 2*A*, *B*) on 1,050 rocks analyzed from the EMNSA. Most rock samples are from mineralized occurrences known within the EMNSA; approximately 98 percent of the rock samples can be assigned to the mineralized sites, or their immediate vicinity, that are classified by us as belonging to a particular type of deposit model (table 15). As such, the analyses that make up this data base provide sampling across the EMNSA of many of the various types of mineral deposits which are known to be present there. These samples yield data that can be used to determine local geochemical thresholds to be expected for various metals and suites of metals present in various systems, to determine zonal relations of metals among genetically linked types of deposits, and to determine metal associations in variously grouped samples of the data base.

Rock samples are classified as chip, random chip, grab, and select by the U.S. Bureau of Mines (1990a, table A–1). The chip samples, which consist of small rock chips taken in a regular series continuously along a line across a mineralized zone or other exposure, contain the most information for determination of the presence or absence of metal concentrations in a volume of rock. Select samples are generally judged to be most representative of the best mineralized parts of a mineralized vein or exposure and are typically used to help determine the presence or absence of a particular minor metal or metals in a mineralized system (for example, gold in a sample of sulfidized skarn).

Most samples that make up the data base are from the mesothermal environment, which is widespread in the EMNSA. Only seven samples of the 1,050 in the data base are from sites that have been assigned by us as belonging to an epithermal, quartz-alunite or quartz-adularia, gold-type system that is volcanic hosted and Tertiary in age. The overwhelming bulk of the samples are associated with Mesozoic metallogenic environments. However, the data base does not include any samples from the Providence Mountains in the south-central part of the EMNSA (pl. 6) because the number of elements per sample analyzed from this area is much less than the number of analyzed elements in the rest of the data base. The distribution of the sampling sites is an important point that must be kept in mind during the discussion below of various subsets of the data base. The Providence Mountains contain some of the most widely distributed and intensely concentrated mineral occurrences, both mined and unmined (U.S. Bureau of Mines, 1990a), in the EMNSA. In the Providence Mountains, approximately 200 mineralized sites have been examined and described by the U.S. Bureau of Mines (1990a; see also Moyle and others, 1986) and by the U.S. Geological Survey and the U.S. Bureau of Mines (Goldfarb and others, 1988) in an area of about 250 km^2. Most mineralized sites are polymetallic veins (pl. 2). In the Providence Mountains Wilderness Study Area, past production has been recorded from 13 nonferrous-metallic lode deposits, the largest production coming from the Bonanza King Mine from 1901 to 1960 (Goldfarb and others, 1988, table 1). The Bonanza King Mine yielded 4,811 or more tonnes of ore that included 1.8 kg Au, 2,571 kg Ag, 415 kg Cu, 31,489 kg Pb, and 1,051 kg Zn. Production recorded from the remaining 12 mines is minimal. The Vulcan Iron Mine produced 2.4 million tonnes iron ore from an iron skarn from 1942 to 1947 (Moyle and others, 1986; Goldfarb and others, 1988).

Although the report by the U.S. Bureau of Mines (1990a) includes analyses for 33 elements, we have selected 20 elements (Ag, As, Au, Ba, Ce, Co, Cr, Cs, Fe, La, Mo, Ni, Sb, Sc, Sm, Ta, Th, U, W, and Zn) upon which to base our statistical calculations described below. These studies are primarily an attempt to determine elemental associations in the sampled mineral deposits and mineral occurrences. One cannot make any inference about sizes of known or unknown deposits from the presence of a particular element, regardless of its concentration and its association with other elements, if one has only a small number of samples from a site. As noted by Barton (1986), “the presence of a given element seldom if ever proves the existence of an ore deposit.” As indicated in table 16, many of the 20 elements selected include large numbers of undetermined concentrations; primarily, the undetermined values of elemental concentration are less than some threshold. In fact, detection thresholds for individual elements vary highly among the samples for many of the reported analyses. For example, 56 different detection thresholds exist for Au in the less than 0.002 to less than 4.9 ppm range. However, 158 of 253 samples reported as containing Au concentrations at less-than-detection thresholds actually have a detection threshold of 2 ppb. To study elemental interrelations in the 20–element-by-1,050–rock matrix, as well as to maximize the number of samples for which supposedly valid values are available, we substituted a concentration that is 50 percent of the value of the most sensitive detection level for the entire data base (that is, 0.001 ppm for Au) for each concentration reported as “less than” a particular value. A completely filled matrix is required for sampling adequacy by some of the correlation techniques that use principal-components factor analysis that we describe below in the subsection entitled “Nonparametric Correlations.” Following these outlined procedures for elemental substitutions, we were able to assemble a completely filled composite 20–element-by-1,050–sample geochemical matrix. Only one “greater than” value was substituted from the raw data reported by the U.S. Bureau of Mines (1990a). This reported concentration, greater than 10,000 ppm As, was substituted with a value of 10,000 ppm As in the geochemical matrix, although values much higher than this are present in many of the other samples.

Some elements that are important to an analysis of economic resources, such as Cu and Pb, are present in a wide variety of geologic environments in the EMNSA but are judged not to be suitably represented in the raw-data matrix. Such a judgment reflects primarily the large number of samples for which unreported concentrations for these elements exist. Among the 1,050 rock samples, Cu concentrations are not available for 485 samples (U.S. Bureau of Mines, 1990a), and another 113 samples show Cu concentrations in excess of the uppermost reporting limit (10,000 ppm). In addition, 563 samples show no reported values for Pb, and 76 samples contain Pb concentrations higher than the uppermost reporting limit (10,000 ppm). Therefore, we do not examine Cu or Pb relations to the 20 elements listed above.

Some elements we chose to include in the matrix, nonetheless, do show a high percentage of values below detection relative to the 1,050 rock samples analyzed. Included among these are the following seven elements (the number of values below detection are shown paranthetically after each element): Ag (481), Ce (402), Co (642), Cs (549), Ni (801), Ta (687), and Zn (477). However, a very high percentage of the reported concentrations below detection in the raw-geochemical-data matrix (U.S. Bureau of Mines, 1990a, tables 2*A*, *B*) for each of the seven elements are at the most sensitive detection threshold. For example, detection thresholds are 2 ppm Ag for 468 of the 481 analyses shown on table 16 as having a value below detection in the raw-data matrix. Therefore, a replacement value of 1 ppm Ag for each of the 481 analyses should not distort the resulting matrix significantly. In addition, the presence of Co, a metal which in 1993 is considered to have some strategic importance, in highly anomalous concentrations at several localities in the EMNSA (U.S. Bureau of Mines, 1990a) is considered by us to be important geochemically, and so we chose to examine its relations to other elements and to type of deposit in the EMNSA even though concentrations below detection are more than 60 percent of the total number of Co concentrations reported (table 16; see also U.S. Bureau of Mines, 1990a). The most sensitive detection threshold for Co was 5 ppm, and 609 of the 642 values below detection are reported to be less than 5 ppm (U.S. Bureau of Mines, 1990a).

Frequency Distributions of Elements

Frequency distributions of the untransformed geochemical data obtained by the U.S. Bureau of Mines (1990a, tables 2*A*, *B*) are strongly skewed positively; that is, the most frequently occurring values are in the lowermost ranges of the reported concentrations and show long “tails” in the distribution of elemental concentrations toward high values. They are thus strongly nonnormal in overall distribution. To perform standard statistical calculations, the geochemical data in the composited 20–element-by-1,050–sample matrix were transformed by common logarithms to thereby approximate a closer fit to lognormality. Figure 85 shows frequency diagrams for the transformed data of the 20 elements. We should emphasize again that these data represent samples obtained from a wide variety of geologic environments and types of deposits in the EMNSA but outside the general area of the Providence Mountains. Somewhat more deposit-type-specific relations among elemental suites are included below in the descriptions of several deposits present in the EMNSA. Tests of kurtosis and skewness values (table 16), frequently used measures of goodness of fit for normality, at the 95 percent confidence level show that all 20 elemental distributions tested in the log-transformed data set deviate from lognormality. Positive values of skewness indicate that the right "tail" of the distribution is longer than the left "tail," which also is readily apparent in the plotted histograms (fig. 85). Kurtosis refers to relations among the peak, the center, and the tails of a distribution (for example, a deviation from normality that might be due to an extremely flat peak with relatively flat tails). A zero value of both kurtosis and skewness indicates a normal distribution. Among the 20 elements tested, visual inspection of the log-transformed distributions for Fe and U show them to have the closest approaches to normality; Sb also approaches a normal distribution (fig. 85). The fact that the original data represent a compositing of geochemical information from a wide variety of deposit types that show a wide range of concentrations of elements, coupled with a censoring of the data for many elements because thresholds of detection are higher than the actual distribution, have certainly contributed to yield the elemental distributions found. Nonetheless, distribution of Au values in the geochemical-data matrix shows that approximately 200 of the 1,050 rocks analyzed from the EMNSA by the U.S. Bureau of Mines (1990a) include concentrations of Au higher than, or equal to, 500 ppb, a value considered by many exploration geologists as suggestive for pursuing evaluations in mesothermal geologic environments. Similar conclusions were reached by the U.S. Bureau of Mines (1990a). In light of questions that might be raised concerning correlation calculations that employ statistical methods requiring normal distributions in the sampled population, nonparametric Spearman correlations were calculated below for the 20 elements transformed by logarithms to the base 10 (table 17).

The distribution of concentrations of Ag, As, Au, and Sb in the 20–element-by-1,050–rock matrix by deposit type for 12 of the 20 types of deposit we recognize in the EMNSA is shown graphically on figure 86. Most samples that show elevated concentrations of Au are from mineralized occurrences classified as polymetallic vein, polymetallic fault, and gold-silver quartz-pyrite vein (fig. 86*A*). The number of samples analyzed for each of these three types of deposits are 286, 75, and 97, respectively. Silver is especially enriched in the silver-copper brecciated-dolostone type of vein occurrence that is distal, and related genetically, to emplacement of the gold breccia pipes at the Colosseum Mine (fig. 86*B*; see also Sharp, 1984). Arsenic apparently is most strongly concentrated in polymetallic veins and, to a somewhat lesser degree, in the polymetallic-replacement deposits (fig. 86*C*). High concentrations of Sb are common in silver-copper brecciated dolostone, polymetallic vein, and, to a lesser degree, lead-zinc skarn (fig. 86*D*). However, only seven analyses are available from the lead-zinc-skarn environment.

If values of Mo were shown on a similar distribution plot, high values would be present in polymetallic veins, polymetallic replacement, and in two of the three samples analyzed from the known Big Hunch stockwork-molybdenum system in the EMNSA. Additional analyses of rock from the Big Hunch system are reported below in the section entitled "Low-Fluorine Porphyry-Molybdenum Deposits." Furthermore, as already noted, the U.S. Bureau of Mines (1990a) data base to which we refer does not include samples from the Providence Mountains, which have been demonstrated to show some elevated abundances of Mo at Globe Wash (Moyle and others, 1986). Lastly, if concentrations of Zn were shown on a similar plot, they would be fairly common throughout the range of values reported in figure 86 in those samples obtained from the polymetallic-replacement occurrences, polymetallic veins, and copper skarns.

Nonparametric Correlations

A nonparametric correlation statistic for all trace-element pairs available for the 20–element data set was calculated as Spearman correlation coefficient r (Davis, 1986), where $r=1-[6\Sigma(RX-RY)^2/(n(n^2-1))]$, RX and RY are the two sets of rankings, and n is the number of trace-element pairs (table 16). Each value is ranked, and corrections are made for tied observations.

Scatter plots for Ag and Fe versus Au are given in figures 87*A*–*B*. Gold shows the strongest positive Spearman correlation coefficients for Ag and Fe, 0.323 and 0.319, respectively, in the 1,050–sample data base. Such relatively reduced values of Spearman correlation coefficients for Au to other elements in the data set are probably a result of the presence of Au in a large number of types of deposits in the EMNSA, such as polymetallic vein, low-sulfide gold-quartz vein, polymetallic replacement, distal disseminated gold-silver, gold breccia pipe, silver-copper brecciated dolostone, gold-silver quartz-pyrite vein, polymetallic fault, polymetallic skarn, tungsten skarn, tin (tungsten) skarn, and copper skarn (table 15). Gold shows a somewhat enhanced association for Ag, having an r value of 0.4 in a 97–sample subset composited from 47 localities of gold-silver quartz-pyrite vein occurrences in the EMNSA. A stepwise-regression analysis (Davis, 1986) shows that only about 10 percent of the variance in the log values of Au can be predicted from the log values of Fe alone in the 1,050–sample data base. Similarly, stepwise regression analysis, which includes log values for Ag, Ba, Cr, Fe, Sb, Sc, Ta, and U, accounts for about 31 percent of the variance of the log values of Au in the 1,050–sample data base, reflecting primarily the geologic inhomogeniety of the data. Plots showing strong, positive associations between element pairs in the data set are exemplified by Sm–La (r=0.896), Sb–Ag (r=0.552), and Fe–Co (r=0.691) (figs. 87*C–E*; see also table 17). Finally, a plot of Ba versus U (fig. 87*F*) provides an example of an elemental association that is extremely weak (r=0.001; table 17). In all of these plots, most samples for which we substituted values at the detection threshold are readily apparent.

Associations Using Factor Analysis

Principal-components factor analysis, another multivariate statistical approach (Klovan, 1968; Davis, 1986), was used in an attempt to detect additional geologically significant elemental associations that may not have been resolved through the use of correlation coefficients. Our preliminary tests involved utilization of various other standard manipulations of the 20–element-by-1,050–sample data set (table 16). On the basis of our knowledge of the geologic environments sampled in the EMNSA, we conclude that the data set should primarily reflect contributions from the Proterozoic environment and the Mesozoic mesothermal environment. A simple factor analysis using two factors provides the following high loadings, which are measures of the degree of intercorrelation among the grouped elements (Klovan, 1968), for the geochemical data:

Factor 1: Ce, Th, Sc, Sm, Cs, Ta, Ba

Factor 2: Fe, Co, Zn, U

Factor 2 in this simple model also includes some moderate loadings for Au, As, Mo, and Ni. Therefore, in an attempt to resolve further the elemental associations masked by the simple two-factor model, we examined the data set using more than two factors. Of the options attempted, a relatively complex factor analysis using eight factors provides a geologically reasonable discrimination of the variances among the geochemical data. The R–mode principal components analysis, which emphasizes interrelations among elements under consideration (Krumbein and Graybill, 1965), reveals, using an orthogonal-transformation solution, the following high, positive loadings among elements in the eight-factor model (listed in order of decreasing loadings; notably lower elemental loadings in each factor are shown in parentheses):

Factor 1: La, Sm, Th, Ce, Sc, Ta, Ba, Cs

Factor 2: Co, Fe, (Sc)

Factor 3. Sb, As, Ag, Zn, (Mo)

Factor 4: Au, Ag

Factor 5: W, (Cs)

Factor 6: Ni

Factor 7: U, (Ta)

Factor 8: Cr, Mo, Ba

These loadings are considered to be firmly established statistically because total matrix-sampling adequacy has a value of 0.868 and thus meets minimum mathematical expectations of partial correlations that tend toward zero (Kaiser, 1970). For the eight-factor model adopted, calculated communalities suggest that anywhere from approximately 62 percent (for Cs) to approximately 93 percent (for W) of any elemental variance in the 20–element-by-1,050–sample data set is predictable from the remaining 19 other elements.

Elemental associations in the eight-factor model suggest dominance in their loadings by the following geologic processes or environments:

Factor 1: Proterozoic and Jurassic igneous rocks

Factor 2: Selected skarns and polymetallic veins

Factor 3: Gold breccia pipe and distal occurrences, selected skarns, and polymetallic veins and replacements

Factor 4: All deposit types in Mesozoic mesothermal environment

Factor 5: Tungsten vein and tungsten skarn

Factor 6: Iron skarn and polymetallic vein

Factor 7: Mesozoic polymetallic veins and skarns, and Jurassic igneous rocks

Factor 8: Polymetallic vein, fluorite veins, and stockwork-molybdenum occurrences

As pointed out in the subsection above entitled "Evaluation of Data," the EMNSA resides in a broad geologic province that apparently contains widespread elevated abundances of rare earth elements in rocks of highly diverse ages. As shown, many unaltered samples of Proterozoic and Jurassic granites are modestly enriched in La, Ce, Nd, Sn, Th, and several other elements (D.M. Miller, written commun., 1991). Therefore, the high loadings of many of these elements in Factor 1 must reflect their elevated abundances in Proterozoic and Jurassic granites in the EMNSA. In addition, the high loading of U and, to somewhat lesser degree, Ta in Factor 7 must also be at least a partial reflection of their modest but persistent elevated presence in Jurassic granites. Uranium is present in some unaltered samples of Jurassic granite in concentrations of as much as 20 ppm.

From the 1,050–sample data base, we assembled a smaller one (89 samples) that included all samples showing Co concentrations greater than or equal to 50 ppm. We then examined elemental relations in it to establish deposit types associated with high loadings of Co and its associated elements (Factor 2). Sixty-four samples in this smaller data base are from a geologic environment dominated by development of skarn (copper skarn, polymetallic skarn, iron skarn, tin-tungsten skarn, tungsten skarn, or zinc-lead skarn) and polymetallic-vein types of deposits. The highest concentration of Co detected is 859 ppm (U.S. Bureau of Mines, 1990a). Other types of deposit that include high concentrations of Co are gold-silver quartz-pyrite veins (two samples contain 799 and 460 ppm Co); polymetallic faults; vein barite; polymetallic replacement; and, finally, four samples from localities that cannot be classified into types of deposit on the basis of information available. Furthermore, Co in the 89–sample data base shows relatively weak overall Spearman correlation coefficients for other metals, the three highest being for Ni, Cs, and U, which range from 0.22 to 0.27. On the basis of these relations, mesothermal environments in the EMNSA that include the above-listed types of deposits can be considered to be permissive hosts for significant concentrations of Co. The known occurrences of these types of deposit in the EMNSA are shown on plate 2, and additional discussion of the types of deposits and their permissive areas and favorable tracts is included in the section below entitled "Evaluation of Metallic Mineral Resources."

A 131–sample data base, including all samples that contain more than 200 ppm Sb from the U.S. Bureau of Mines (1990a), also was prepared to evaluate Factor 3 loadings listed previously. Of the 131 samples, 55 are from vein occurrences distal to the Colosseum gold breccia pipe and genetically related to it (Sharp, 1984); 42 of these Sb–enriched samples are from sites included by us with the silver-copper brecciated-dolostone type of vein occurrence. In addition, some deposits of skarn, polymetallic vein, and polymetallic replacement also show abundances of Sb greater than 200 ppm elsewhere in the EMNSA (fig. 86*D*). In the 131 samples, Sb shows the highest positive correlation coefficients with Ag, As, and Au; figure 88 is a plot of Sb versus As for the 131 samples. Although we are not able to evaluate statistically the relations of Cu and Pb because of the large number of qualified values for these elements in the data base, Cu and Pb in the silver-copper brecciated dolostones that are marginal to the gold-bearing breccia pipes at the Colosseum Mine are uniformly high (U.S. Bureau of Mines, 1990a). If data were available for Cu and Pb, these elements undoubtedly would make up a strong component of Factor 3. The presence of elevated concentrations of Sb, As, and some Au in silver-copper brecciated dolostones in the Clark Mountain Range might be used as a favorable geochemical signature for gold-bearing breccia pipes at depth. In addition, the Ag/Au ratio in silver-copper brecciated dolostone distal to the Colosseum Mine is typically higher than 1,000, as is described in the subsection below entitled "Breccia Pipe and Related Deposits."

Factor 4 shows high loading for Au and Ag. Our evaluation of the 197 samples in the data base that contain abundances of Au in excess of 500 ppb indicates that no type of metallic-mineral deposit appears to exist in the Mesozoic mesothermal environment of the EMNSA which does not contain significant Au (pl. 6). By far, the most abundant deposit type whose samples contain Au in excess of 500 ppb is polymetallic vein, reflecting its predominance in the EMNSA (table 15). A select sample from the polymetallic veins at the Bighorn Mine near the south end of the Providence Mountains includes 22,000 ppb Au (table 11, analysis no. 15). In addition, skarns of all types show some analyses carrying at least 500 ppb Au or, corroborating the conclusions of Theodore and others (1991), that all types of skarns are, at a minimum, permissive sites of enhanced Au deposition.

Although Factor 6 shows a high loading only for Ni, the number of samples containing elevated concentrations of Ni is quite low. Only 31 of the 1,050 samples analyzed by the U.S. Bureau of Mines (1990a) contain higher than 100 ppm Ni, and only two of these are in excess of 500 ppm. These two samples are from mineralized sites classified as polymetallic vein (U.S. Bureau of Mines, 1990a, map no. 282) and iron skarn at the Old Dad Mountain deposit (U.S. Bureau of Mines, 1990a, map no. 369). Eleven of the 31 analyzed samples shown to contain more than 100 ppm Ni are from polymetallic veins. In addition, three of the silver-copper brecciated-dolostone occurrences that are distal, in a petrogenetic sense, to the gold breccia pipes at the Colosseum Mine also contain some rocks whose Ni contents are greater than 100 ppm.

Factor 7 shows a high loading for U and a moderate loading for Ta. Only 18 samples analyzed by the U.S. Bureau of Mines (1990a) contain in excess of 50 ppm U, and eight of these are from mineralized sites classified as some type of metallized skarn, of which four are iron skarn. The highest content of U found (1,590 ppm) in the EMNSA is from the general area of the REE–bearing carbonatites at the Esperanza group of claims in the northern part of the Ivanpah Mountains (U.S. Bureau of Mines, 1990a, map no. 156, pl. 1). Some polymetallic veins elsewhere in the EMNSA also contain high concentrations of U.

The high loading of Cr, Mo, and Ba in Factor 8, presumably reflecting polymetallic-vein, fluorite-vein, and stockwork-molybdenum occurrences in the EMNSA, may be an indication of interaction of fluids, which are associated with these types of occurrences, with mafic igneous rocks of the Proterozoic basement.

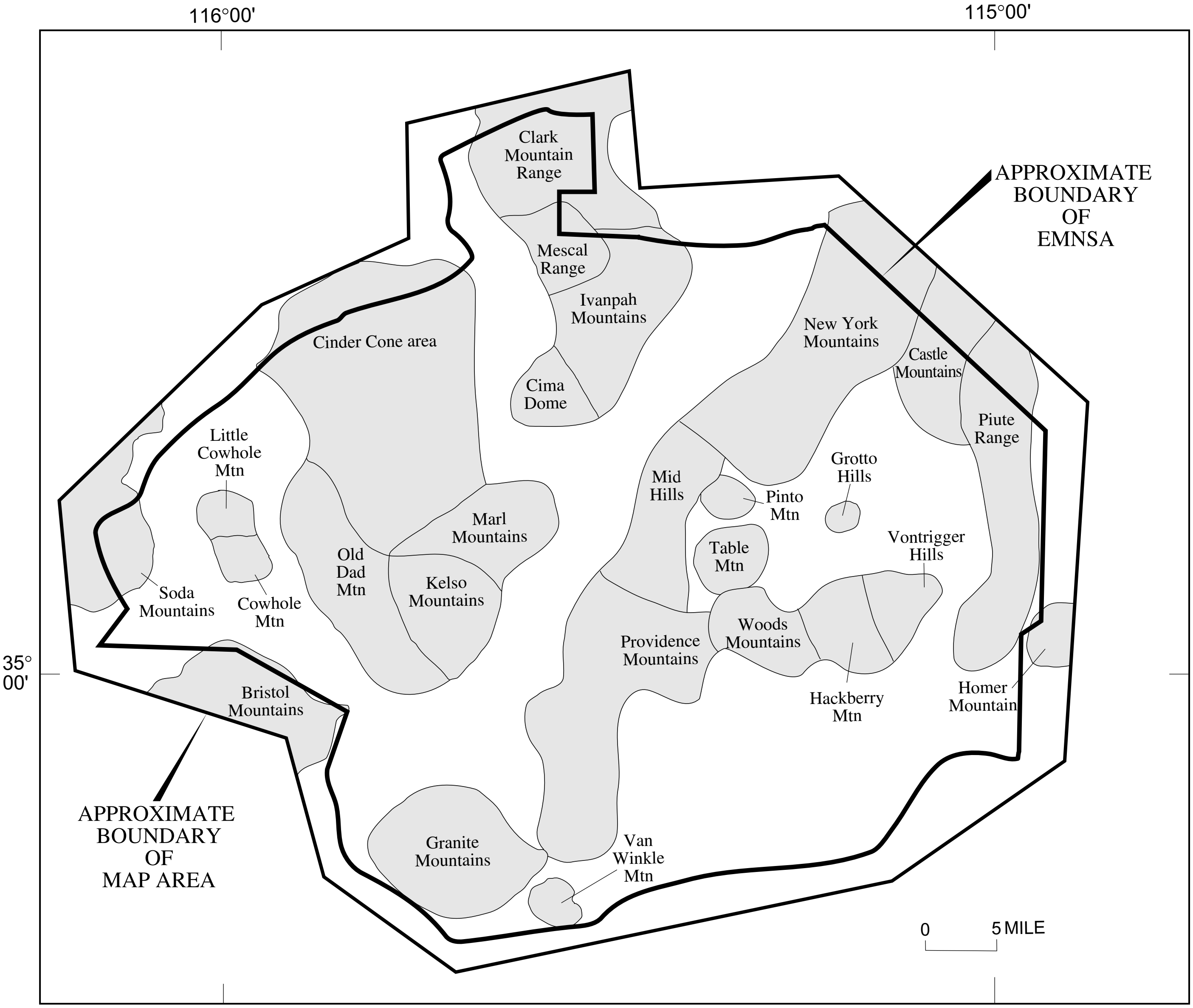

Figure 49. Map of East Mojave National Scenic Area (EMNSA), Calif., showing geographic areas (shaded) that were geochemically evaluated using data from Rock Analysis Storage System (RASS), geochemical data base for the United States (PLUTO), and National Uranium Resource Evaluation (NURE) data bases. Statistical data given in table 13; summary of geochemical anomalies given in table 14; sample localities shown on figures 50 to 53; data plotted on figures 54 to 73.

Figure 50. Sampling sites for Rock Analysis Storage System (RASS) and geochemical data base for the United States (PLUTO) stream-sediment samples from East Mojave National Scenic Area (EMNSA), Calif., and surrounding area. General outlines of geochemically evaluated areas (shaded) shown for reference; see figure 49 for location names. Statistical data given in table 13; summary of geochemical anomalies given in table 14; data plotted on figures 54 to 73.

Figure 51. Sampling sites for Rock Analysis Storage System (RASS) and geochemical data base for the United States (PLUTO) heavy-mineral-concentrate samples from East Mojave National Scenic Area (EMNSA), Calif., and surrounding area. General outlines of geochemically evaluated areas (shaded) shown for reference; see figure 49 for location names. Statistical data given in table 13; summary of geochemical anomalies given in table 14; data plotted on figures 54 to 73.

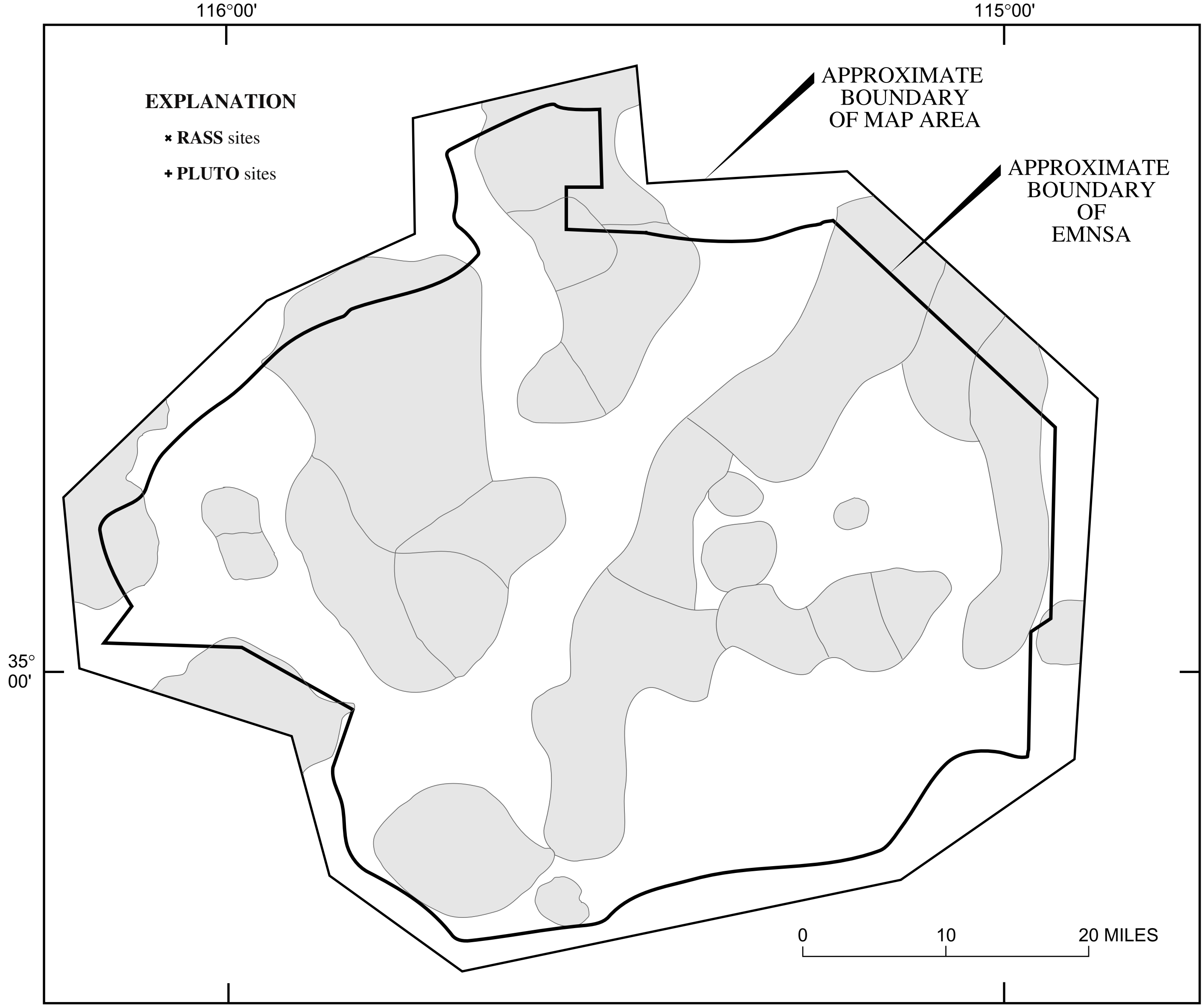

Figure 52. Sampling sites for Rock Analysis Storage System (RASS) and geochemical data base for the United States (PLUTO) rock samples from East Mojave National Scenic Area (EMNSA), Calif., and surrounding area. General outlines of geochemically evaluated areas (shaded) shown for reference; see figure 49 for location names. Statistical data given in table 13; summary of geochemical anomalies given in table 14; data plotted on figures 54 to 73.

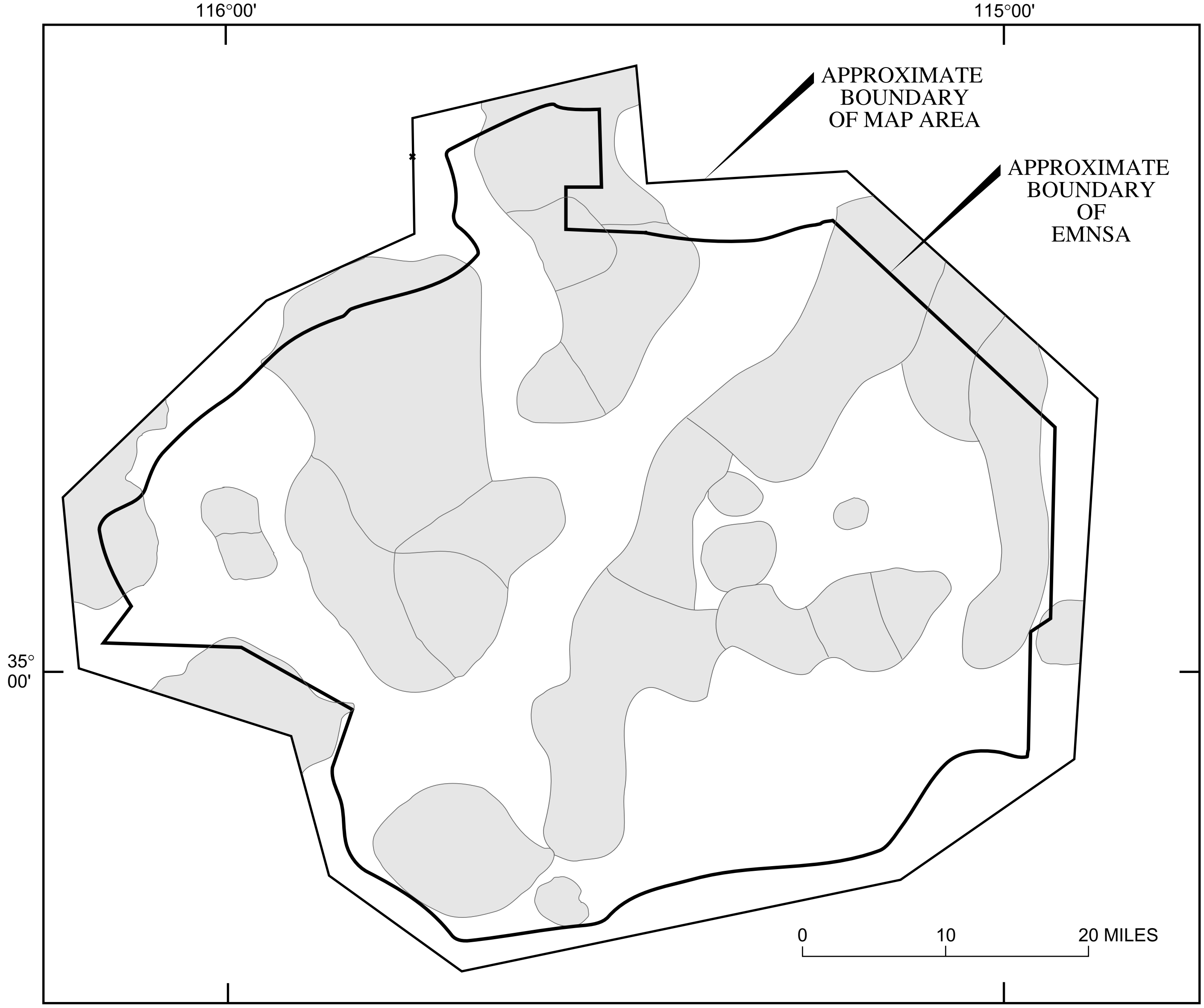

Figure 53. Sampling sites for National Uranium Resource Evaluation (NURE) stream-sediment and soil samples from East Mojave National Scenic Area (EMNSA), Calif., and surrounding area. General outlines of geochemically evaluated areas (shaded) shown for reference; see figure 49 for location names. Statistical data given in table 13; summary of geochemical anomalies given in table 14; data plotted on figures 54 to 73.

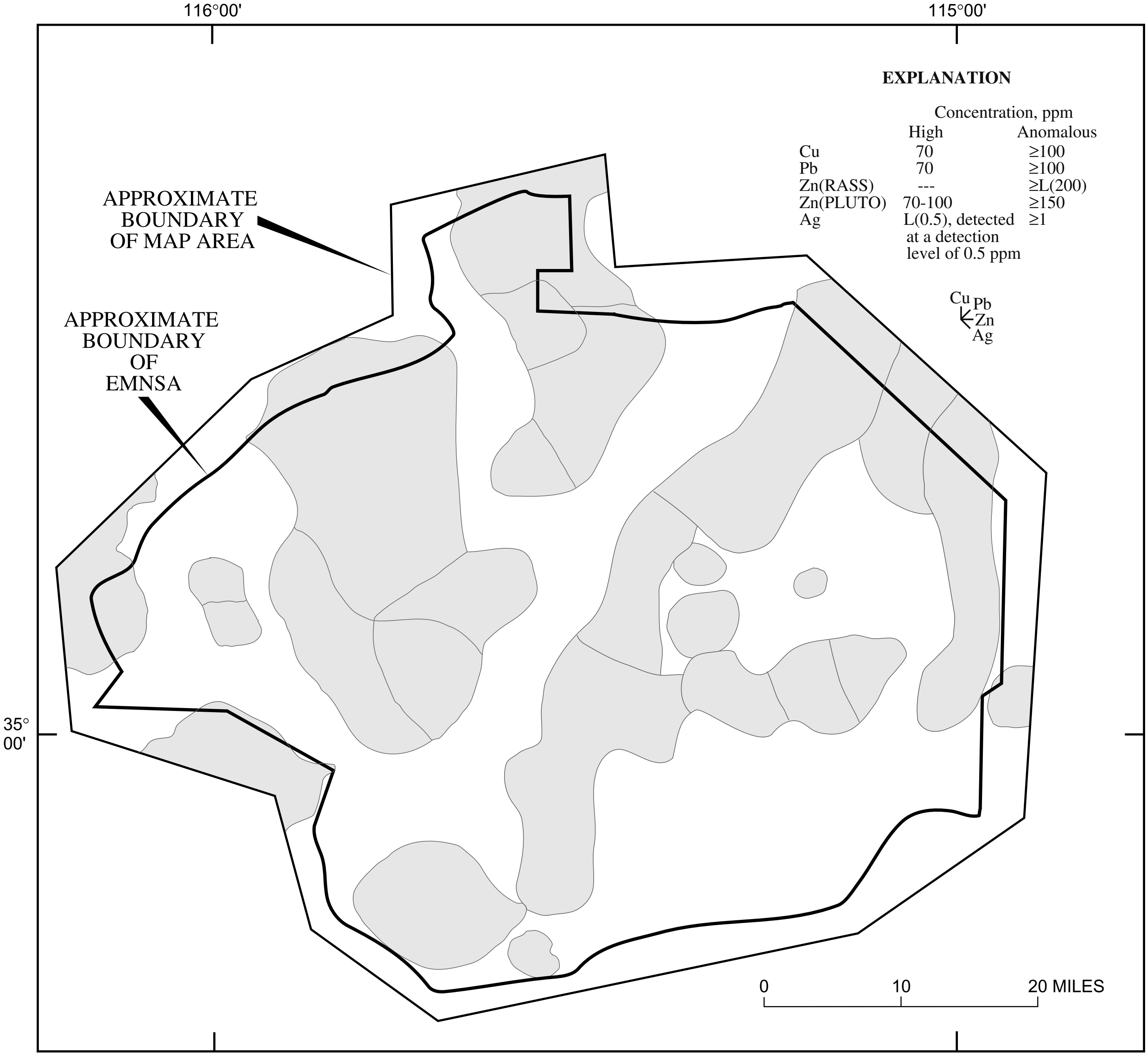

Figure 54. Distribution of anomalous and high concentrations, in parts per million, of Cu, Pb, Zn, and Ag in Rock Analysis Storage System (RASS) and geochemical data base for the United States (PLUTO) stream-sediment samples from East Mojave National Scenic Area (EMNSA), Calif., and surrounding area. For each locality, elements are shown by either vertical, horizontal, or diagonal lines emanating from a common locality point (overlapping lines represent more than one locality). Longer lines indicate anomalous concentrations; shorter lines, high concentrations. Concentration values shown are defined as follows: anomalous, above threshold values given in table 13; high, selected ranges that include threshold values as upper limits; L, detected below lower limit of determination (given in parentheses); ---, no value (any detectable concentration is anomalous). Percentiles for high concentrations are as follows: Cu, 90 to 95; Pb, 89 to 94; Zn, 67 to 79; Ag, 88 to 94. General outlines of geochemically evaluated areas (shaded) shown for reference; see figure 49 for location names. Statistical data given in table 13; summary of geochemical anomalies given in table 14; sample localities plotted on figure 50.

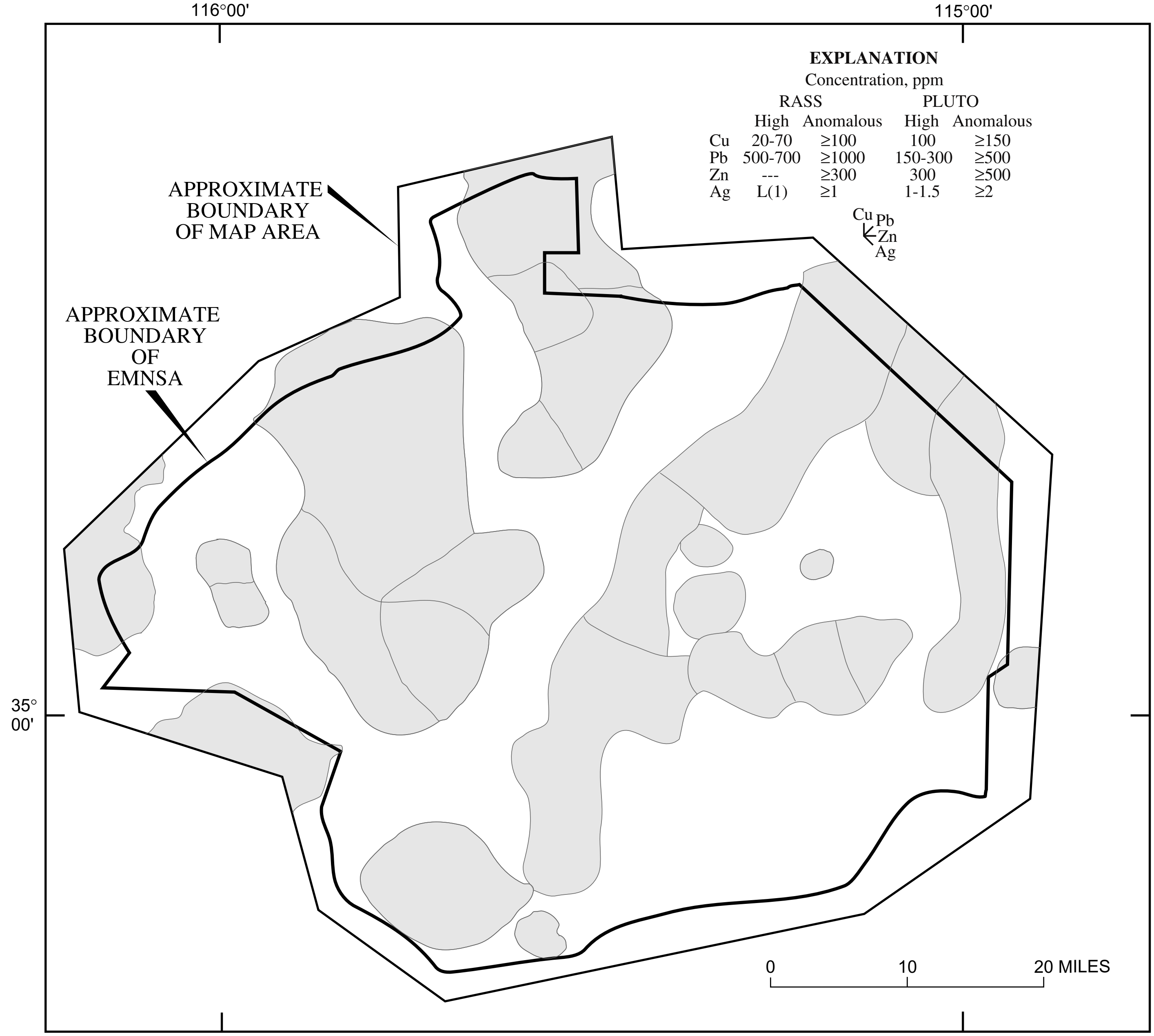

Figure 55. Distribution of anomalous and high concentrations, in parts per million, of Cu, Pb, Zn, and Ag in Rock Analysis Storage System (RASS) and geochemical data base for the United States (PLUTO) heavy-mineral-concentrate samples from East Mojave National Scenic Area (EMNSA), Calif., and surrounding area. For each locality, elements are shown by either vertical, horizontal, or diagonal lines emanating from a common locality point (overlapping lines represent more than one locality). Longer lines indicate anomalous concentrations; shorter lines, high concentrations. Concentration values shown are defined as follows: anomalous, above threshold values given in table 13; high, selected ranges that include threshold values as upper limits; L, detected below lower limit of determination (given in parentheses); ---, no value (any detectable concentration is anomalous). Percentiles for high concentrations in PLUTO samples are as follows: Cu, 77 to 92; Pb, 77 to 81; Ag, 81 to 86. Percentiles for high concentrations in PLUTO samples are as follows: Cu, 60 to 79; Pb, 74 to 97; Zn, 65 to 79; Ag, 54 to 77. General outlines of geochemically evaluated areas (shaded areas) shown for reference; see figure 49 for location names. Statistical data given in table 13; summary of geochemical anomalies given in table 14; sample localities plotted on figure 51.

Figure 56. Distribution of anomalous and high concentrations, in parts per million, of Cu, Pb, Zn, and Ag in Rock Analysis Storage System (RASS) and geochemical data base for the United States (PLUTO) rock samples from East Mojave National Scenic Area (EMNSA), Calif., and surrounding area. For each locality, elements are shown by either vertical, horizontal, or diagonal lines emanating from a common locality point (overlapping lines represent more than one locality). Longer lines indicate anomalous concentrations; shorter lines, high concentrations. Concentration values shown are defined as follows: anomalous, above threshold values given in table 13; high, selected ranges that include threshold values as upper limits; L, detected below lower limit of determination (given in parentheses); ---, no value (any detectable concentration is anomalous). Percentiles for high concentrations are as follows: Cu, 71 to 78; Pb, 61 to 75; Zn, 80 to 81; Ag, 65 to 73. General outlines of geochemically evaluated areas (shaded) shown for reference; see figure 49 for location names. Statistical data given in table 13; summary of geochemical anomalies given in table 14; sample localities plotted on figure 52.

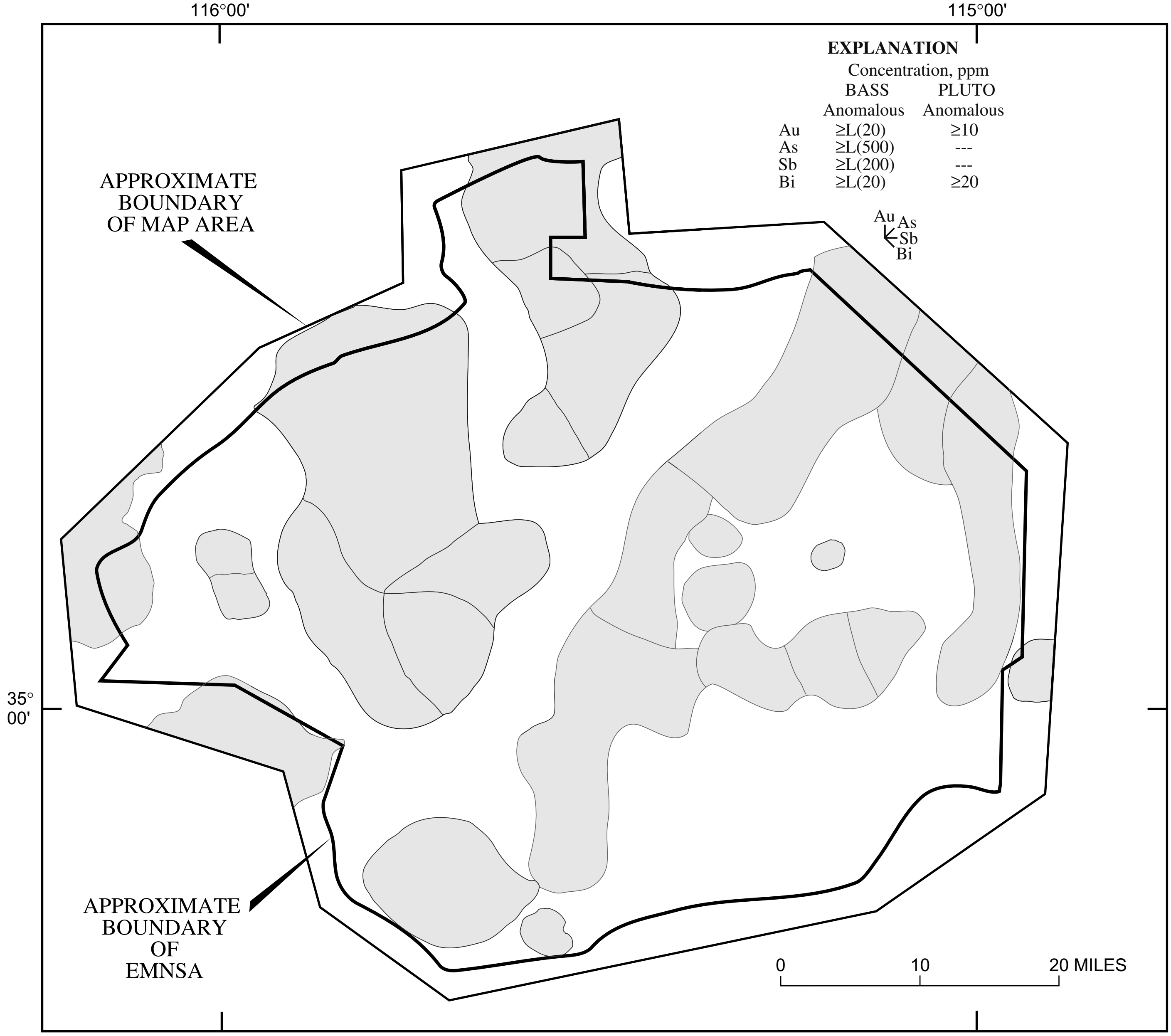

Figure 57. Distribution of anomalous concentrations, in parts per million, of Au, As, Sb, and Bi in Rock Analysis Storage System (RASS) and geochemical data base for the United States (PLUTO) heavy-mineral-concentrate samples from East Mojave National Scenic Area (EMNSA), Calif., and surrounding area. For each locality, elements are shown by either vertical, horizontal, or diagonal lines emanating from a common locality point (overlapping lines represent more than one locality). Anomalous concentration values shown are defined as those above threshold values given in table 13; L, detected below lower limit of determination (given in parentheses); ---, no data (As was not determined and Sb was not detected in PLUTO samples). General outlines of geochemically evaluated areas (shaded) shown for reference; see figure 49 for location names. Statistical data given in table 13; summary of geochemical anomalies given in table 14; sample localities plotted on figure 51.

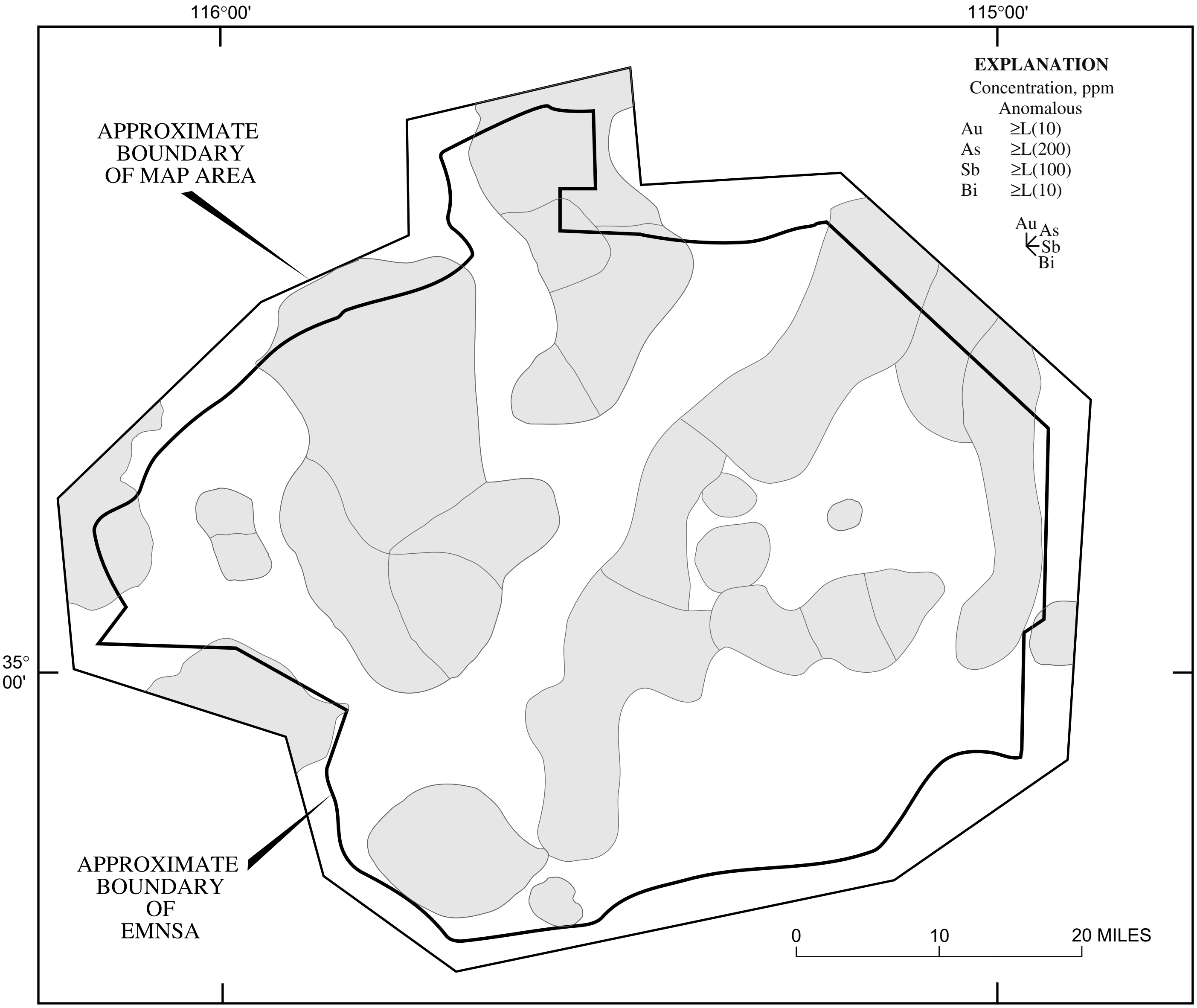

Figure 58. Distribution of anomalous concentrations, in parts per million, of Au, As, Sb, and Bi in Rock Analysis Storage System (RASS) and geochemical data base for the United States (PLUTO) rock samples from East Mojave National Scenic Area (EMNSA), Calif., and surrounding area. For each locality, elements are shown by either vertical, horizontal, or diagonal lines emanating from a common locality point (overlapping lines represent more than one locality). Anomalous concentration values shown are defined as those above threshold values given in table 13; L, detected below lower limit of determination (given in parentheses). General outlines of geochemically evaluated areas (shaded) shown for reference; see figure 49 for location names. Statistical data given in table 13; summary of geochemical anomalies given in table 14; sample localities plotted on figure 52.

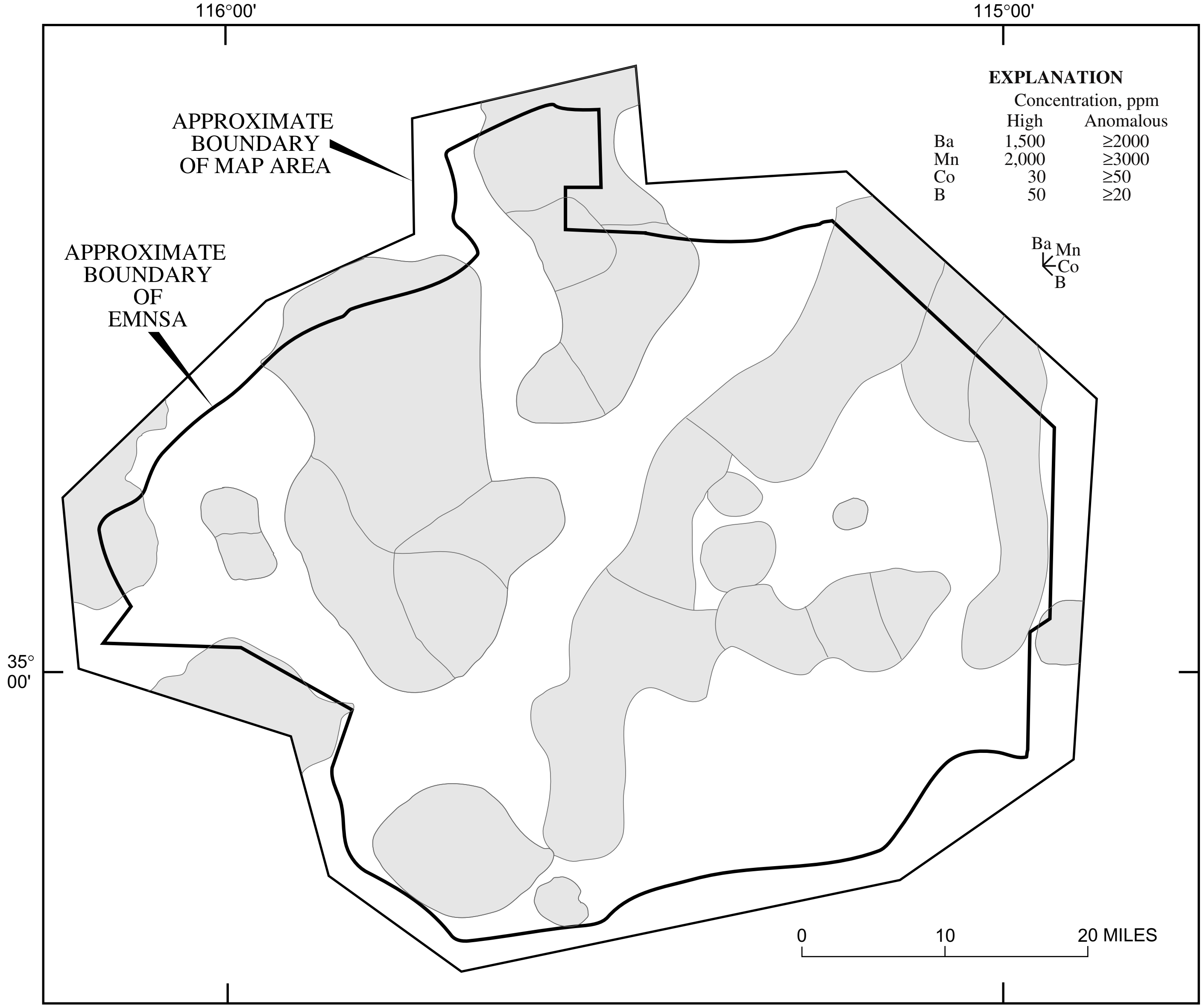

Figure 59. Distribution of anomalous and high concentrations, in parts per million, of Ba, Mn, Co, and B in Rock Analysis Storage System (RASS) and geochemical data base for the United States (PLUTO) stream-sediment samples from East Mojave National Scenic Area (EMNSA), Calif., and surrounding area. For each locality, elements are shown by either vertical, horizontal, or diagonal lines emanating from a common locality point (overlapping lines represent more than one locality). Longer lines indicate anomalous concentrations; shorter lines, high concentrations. Concentration values shown are defined as follows: anomalous, above threshold values given in table 13; high, selected ranges that include threshold values as upper limits. Percentiles for high concentrations are as follows: Ba, 95 to 97; Mn, 90 to 95; Co, 81 to 92; B, 90 to 95. General outlines of geochemically evaluated areas (shaded areas) shown for reference; see figure 49 for location names. Statistical data given in table 13; summary of geochemical anomalies given in table 14; sample localities plotted on figure 50.

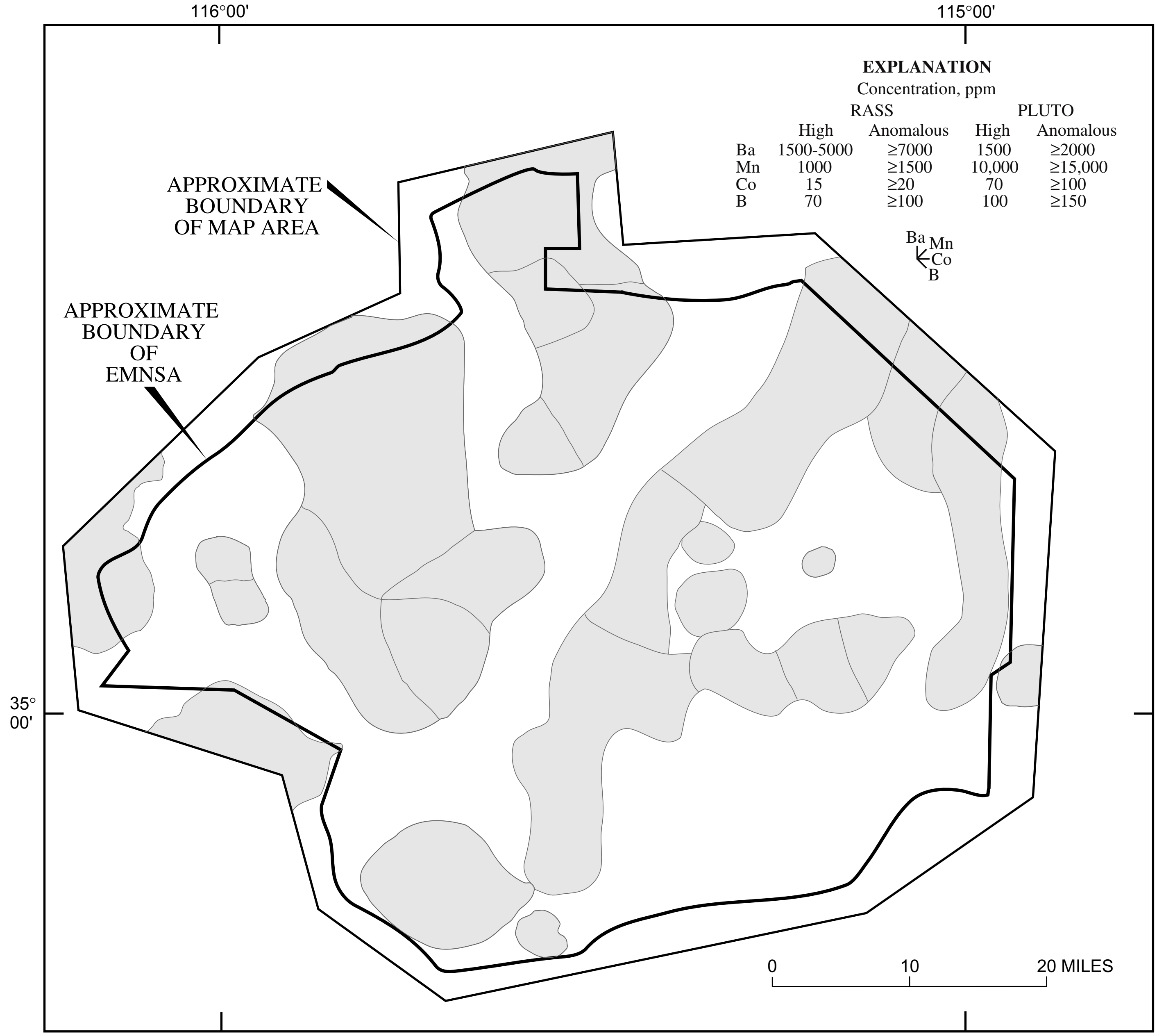

Figure 60. Distribution of anomalous and high concentrations, in parts per million, of Ba, Mn, Co, and B in Rock Analysis Storage System (RASS) and geochemical data base for the United States (PLUTO) heavy-mineral-concentrate samples from East Mojave National Scenic Area (EMNSA), Calif., and surrounding area. For each locality, elements are shown by either vertical, horizontal, or diagonal lines emanating from a common locality point (overlapping lines represent more than one locality). Longer lines indicate anomalous concentrations; shorter lines, high concentrations. Concentration values shown are defined as follows: anomalous, above threshold values given in table 13; high, selected ranges that include threshold values as upper limits. Percentiles for high concentrations in RASS samples are as follows: Ba, 58 to 79; Mn, 72 to 90; Co, 91 to 92; B, 92 to 94. Percentiles for high concentrations in PLUTO samples are as follows: Ba, 87 to 90; Mn, 74 to 94; Co, 77 to 87; B, 78 to 93. General outlines of geochemically evaluated areas (shaded) shown for reference; see figure 49 for location names. Statistical data given in table 13; summary of geochemical anomalies given in table 14; sample localities plotted on figure 51.

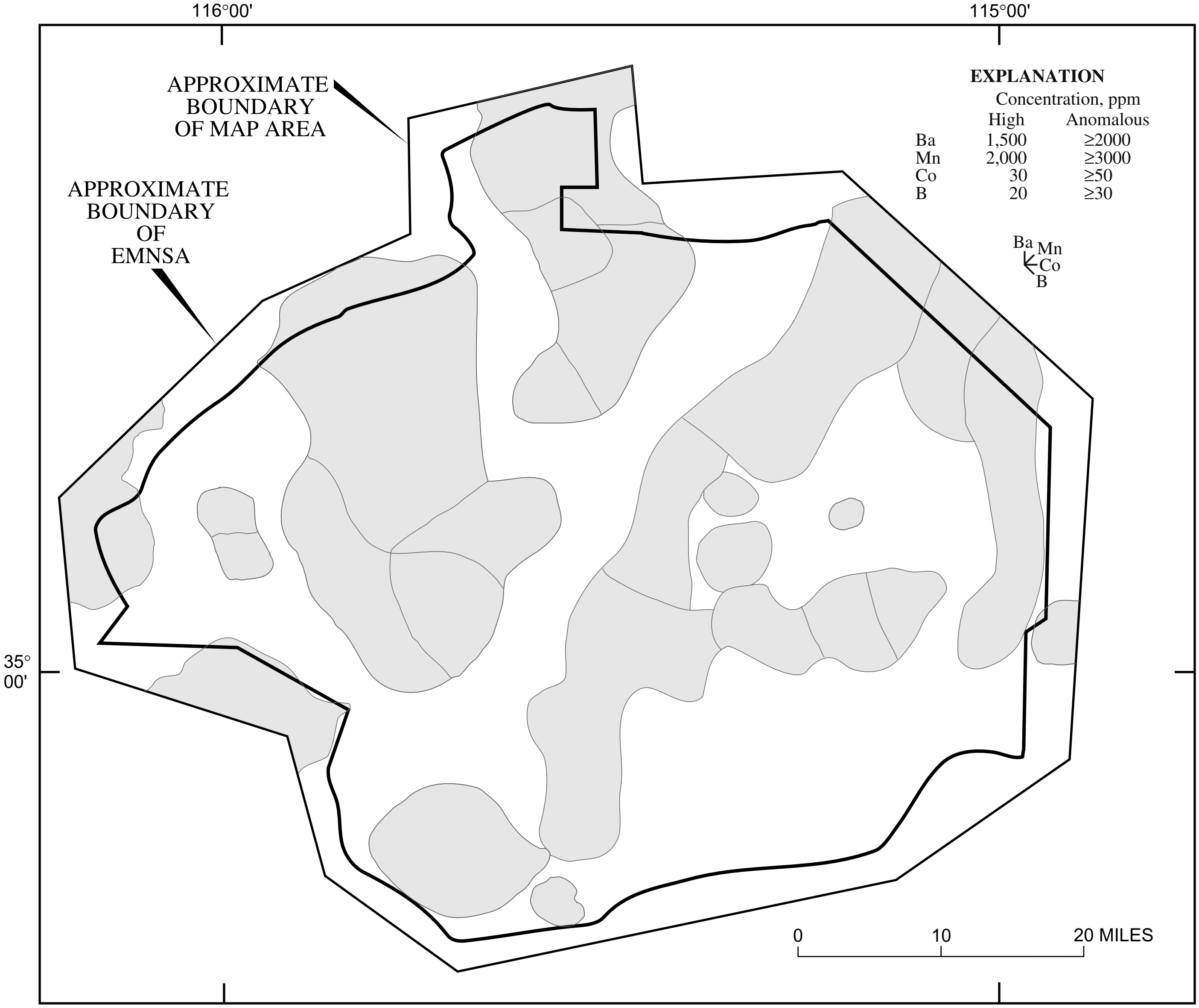

Figure 61. Distribution of anomalous and high concentrations, in parts per million, of Ba, Mn, Co, and B in Rock Analysis Storage system (RASS) and geochemical data base for the United States (PLUTO) rock samples from East Mojave National Scenic Area (EMNSA), Calif., and surrounding area. For each locality, elements are shown by either vertical, horizontal, or diagonal lines emanating from a common locality point (overlapping lines represent more than one locality). Longer lines indicate anomalous concentrations; shorter lines, high concentrations. Concentration values shown are defined as follows: anomalous, above threshold values given in table 13; high, selected ranges that include threshold values as upper limits. Percentiles for high concentrations are as follows: Ba, 83 to 92; Mn, 93 to 94; Co, 87 to 90; B, 83 to 88. General outlines of geochemically evaluated areas (shaded) shown for reference; see figure 49 for location names. Statistical data given in table 13; summary of geochemical anomalies given in table 14; sample localities plotted on figure 52.

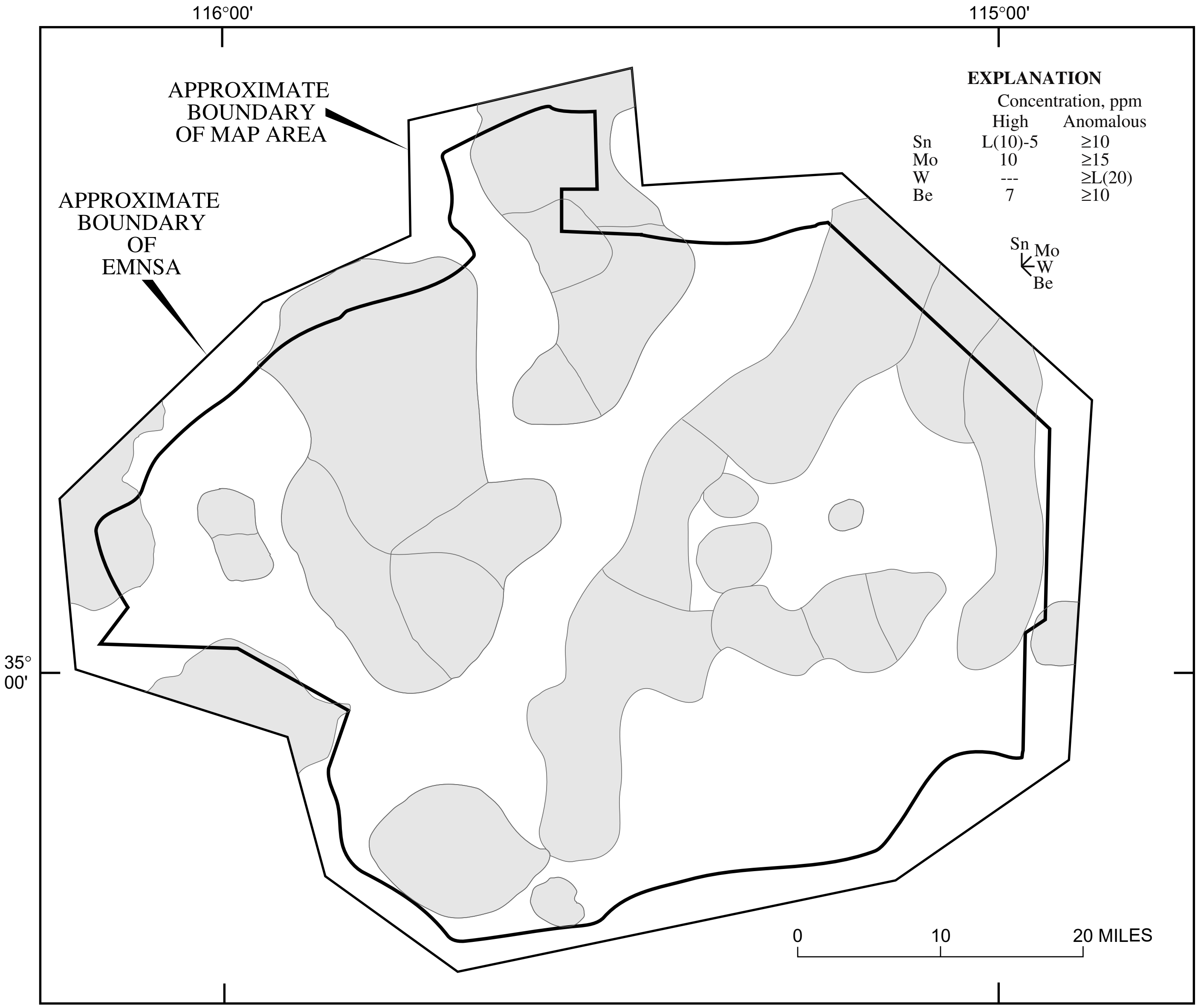

Figure 62. Distribution of anomalous and high concentrations, in parts per million, of Sn, Mo, W, and Be in Rock Analysis Storage System (RASS) and geochemical data base for the United States (PLUTO) stream-sediment samples from East Mojave National Scenic Area (EMNSA), Calif., and surrounding area. For each locality, elements are shown by either vertical, horizontal, or diagonal lines emanating from a common locality point (overlapping lines represent more than one locality). Longer lines indicate anomalous concentrations; shorter lines, high concentrations. Concentration values shown are defined as follows: anomalous, above threshold values given in table 13; high, selected ranges that include threshold ; L, detected below lower limit of determination (given in parentheses); ---, no value (any detectable concentration is anomalous). Percentiles for high concentrations are as follows: Sn, 96; Mo, 77 to 85; Be, 94 to 98. General outlines of geochemically evaluated areas (shaded) shown for reference; see figure 49 for location names. Statistical data given in table 13; summary of geochemical anomalies given in table 14; sample localities plotted on figure 50.

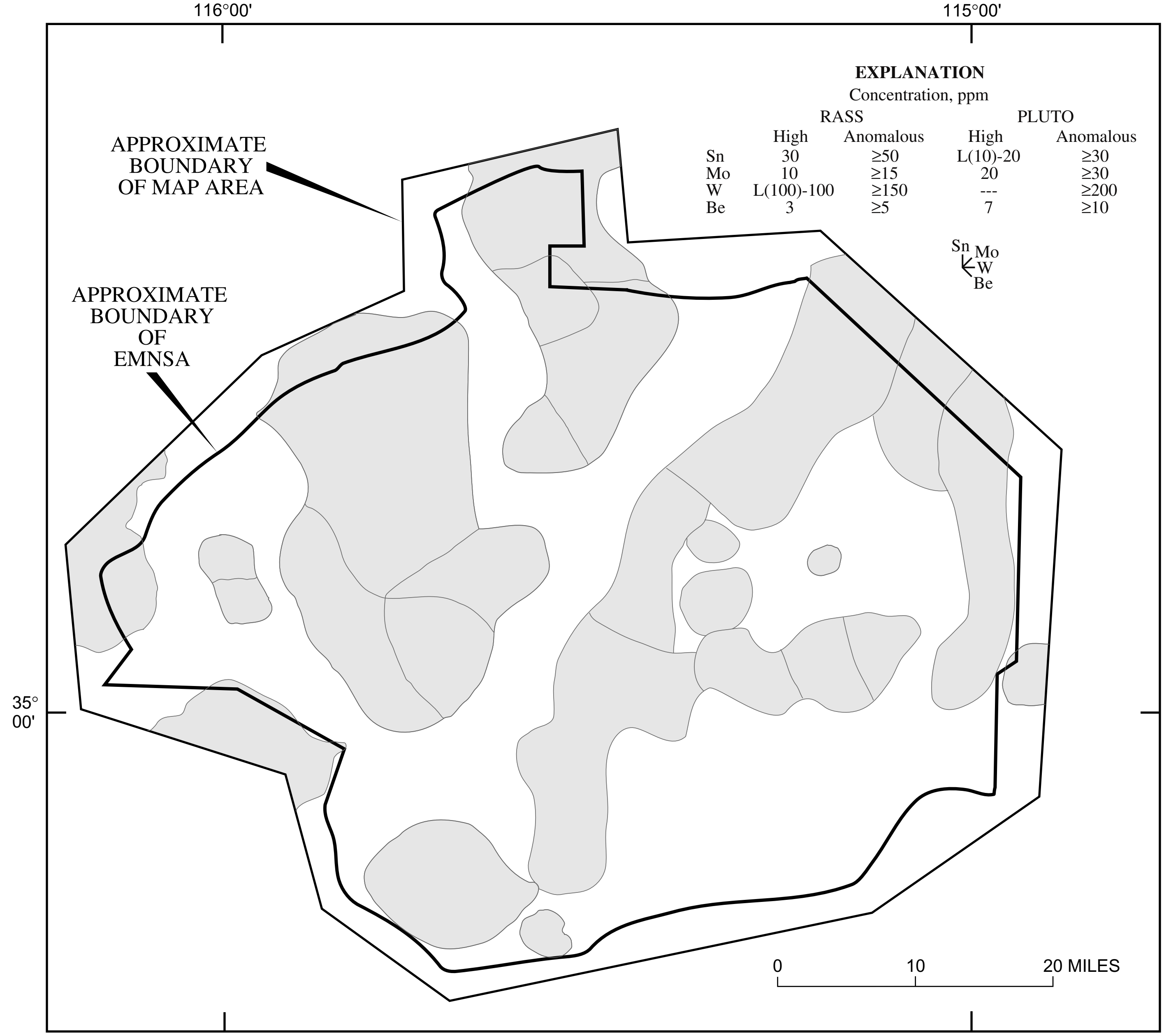

Figure 63. Distribution of anomalous and high concentrations, in parts per million, of Sn, Mo, W, and Be in Rock Analysis (RASS) and geochemical data base for the United States (PLUTO) heavy-mineral-concentrate samples from East Mojave National Scenic Area (EMNSA), Calif., and surrounding area. For each locality, elements are shown by either vertical, horizontal, or diagonal lines emanating from a common locality point (overlapping lines represent more than one locality). Longer lines indicate anomalous concentrations; shorter lines, high concentrations. Concentration values shown are defined as follows: anomalous, above threshold values given in table 13; high, selected ranges that include threshold values as upper limits; L, detected below lower limit of determination (given in parentheses); ---, no value (any detectable concentration is anomalous). Percentiles for high concentrations in RASS samples are as follows: Sn, 79; Mo, 84; W, 74 to 83; Be, 90 to 95. Percentiles for high concentrations in PLUTO samples are as follows: Sn, 50 to 85; Mo, 62 to 76; Be, 71 to 94. General outlines of geochemically evaluated areas (shaded) shown for reference; see figure 49 for location names. Statistical data given in table 13; summary of geochemical anomalies given in table 14; sample localities plotted on figure 51.

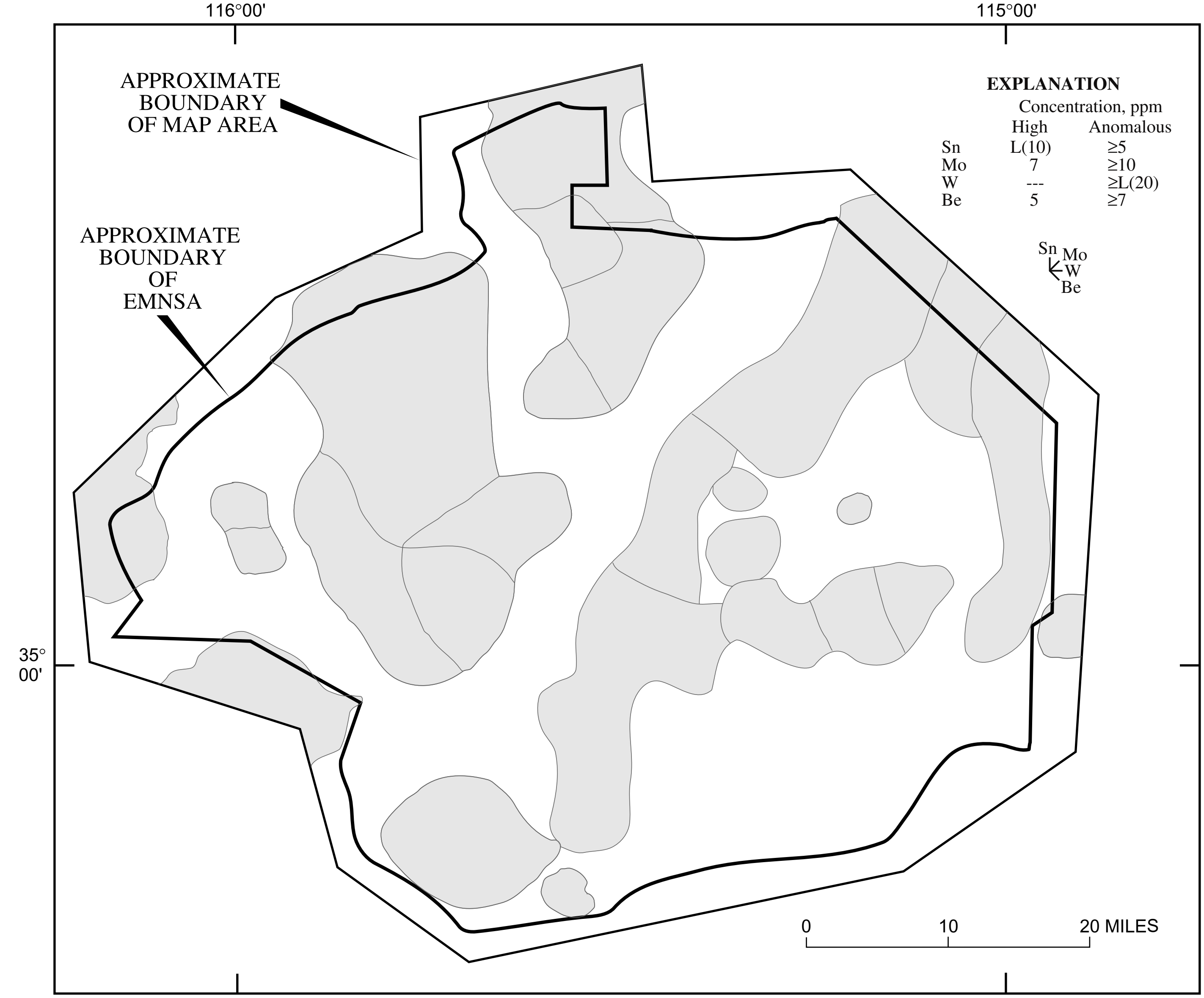

Figure 64. Distribution of anomalous and high concentrations, in parts per million, of Sn, Mo, W, and Be in Rock Analysis Storage System (RASS) and geochemical data base for the United States (PLUTO) rock samples from East Mojave National Scenic Area (EMNSA), Calif., and surrounding area. For each locality, elements are shown by either vertical, horizontal, or diagonal lines emanating from a common locality point (overlapping lines represent more than one locality). Longer lines indicate anomalous concentrations; shorter lines, high concentrations. Concentration values shown are defined as follows: anomalous, above threshold values given in table 13; high, selected ranges that include threshold values as upper limits; L, detected below lower limit of determination (given in parentheses); ---, no value (any detectable concentration is anomalous). Percentiles for high concentrations are as follows: Sn, 95 to 96; Mo, 82 to 86; Be, 95 to 97. General outlines of geochemically evaluated areas (shaded) shown for reference; see figure 49 for location names. Statistical data given in table 13; summary of geochemical anomalies given in table 14; sample localities plotted on figure 52.

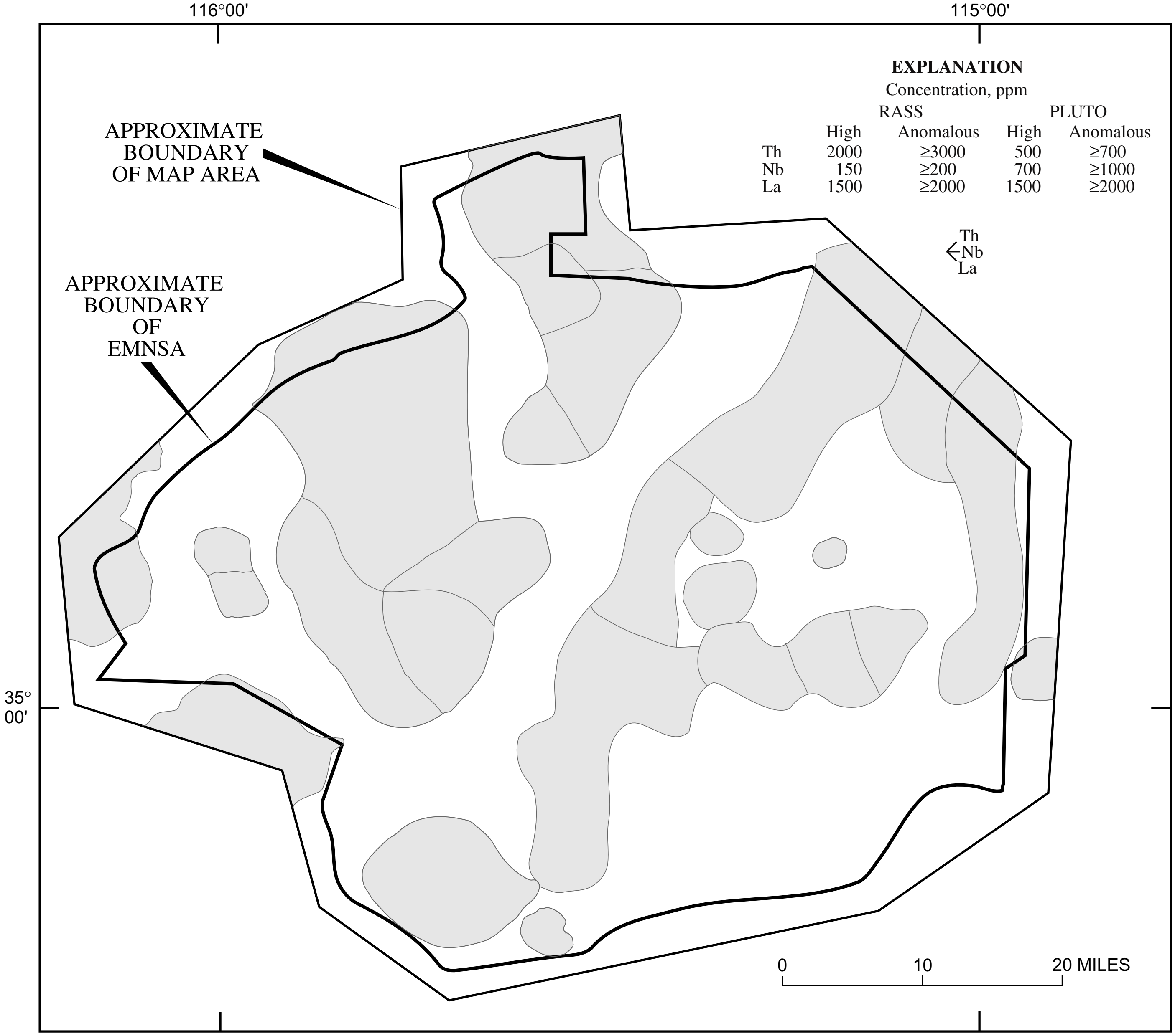

Figure 65. Distribution of anomalous and high concentrations, in parts per million, of Th, Nb, and La in Rock Analysis Storage System (RASS) and geochemical data base for the United States (PLUTO) heavy-mineral-concentrate samples from East Mojave National Scenic Area (EMNSA), Calif., and surrounding area. For each locality, elements are shown by either horizontal or diagonal lines emanating from a common locality point (overlapping lines represent more than one locality). Longer lines indicate anomalous concentrations; shorter lines, high concentrations. Concentration values shown are defined as follows: anomalous, above threshold values given in table 13; high, selected ranges that include threshold values as upper limits. Percentiles for high concentrations in RASS samples are as follows: Th, 92 to 94; Nb, 93 to 96; La, 94 to 96. Percentiles for high concentrations in PLUTO samples are as follows: Th, 88 to 92; Nb, 95 to 96; La, 78 to 85. General outlines of geochemically evaluated areas (shaded) shown for reference; see figure 49 for location names. Statistical data given in table 13; summary of geochemical anomalies given in table 14; sample localities plotted on figure 51.

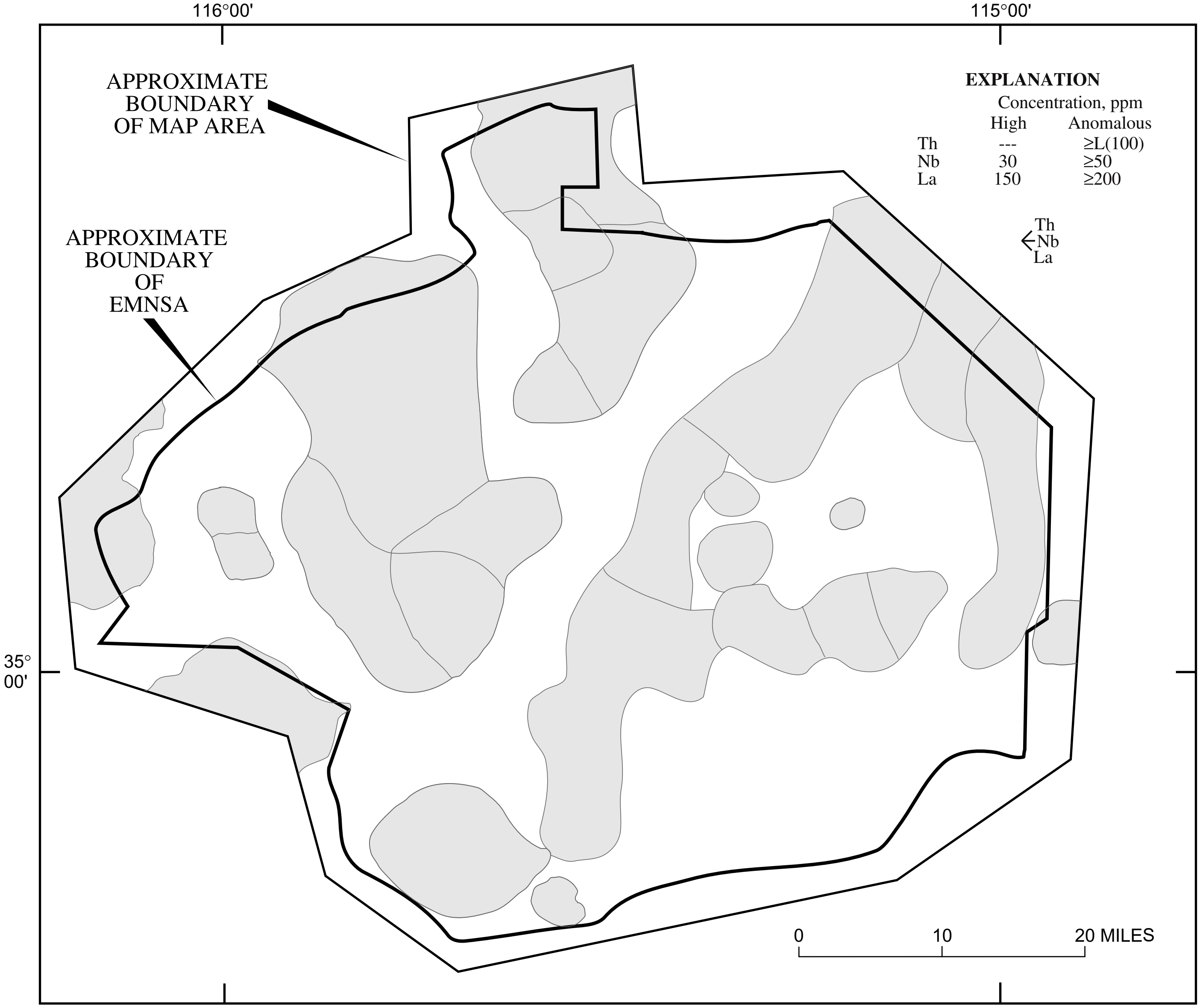

Figure 66. Distribution of anomalous and high concentrations, in parts per million, of Th, Nb, and La in Rock Analysis Storage System (RASS) and geochemical data base for the United States (PLUTO) rock samples from East Mojave National Scenic Area (EMNSA), Calif., and surrounding area. For each locality, elements are shown by either horizontal or diagonal lines emanating from a common locality point (overlapping lines represent more than one locality). Longer lines indicate anomalous concentrations; shorter lines, high concentrations. Concentration values shown are defined as follows: anomalous, above threshold values given in table 13; high, selected ranges that include threshold values as upper limits; L, detected below lower limit of determination (given in parentheses); ---, no value (any detectable concentration is anomalous). Percentiles for high concentrations are as follows: Nb, 95 to 98; La, 94 to 97. General outlines of geochemically evaluated areas (shaded) shown for reference; see figure 49 for location names. Statistical data given in table 13; summary of geochemical anomalies given in table 14; sample localities plotted on figure 52.

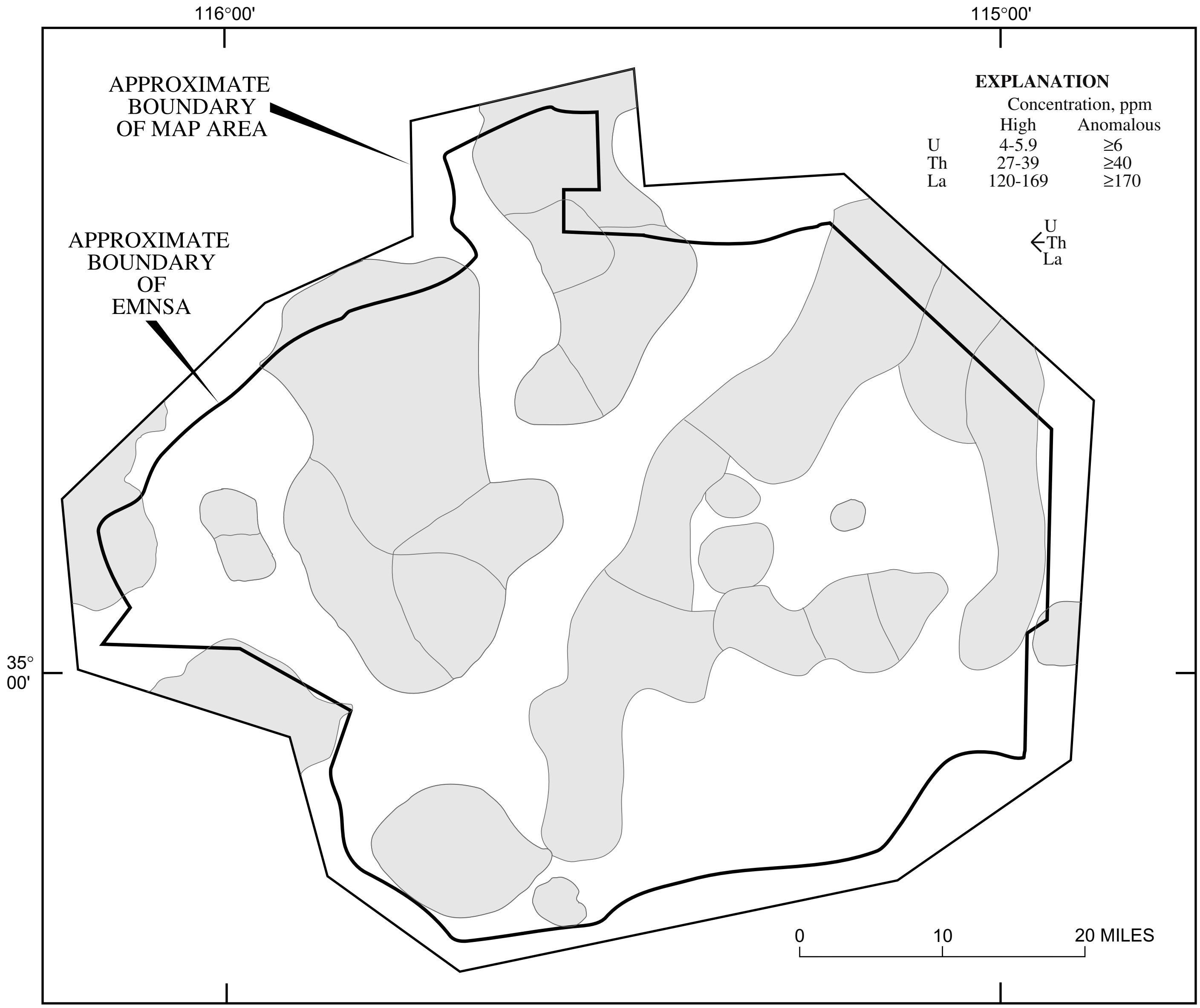

Figure 67. Distribution of anomalous and high concentrations, in parts per million, of U, Th, and La in National Uranium Resource Evaluation (NURE) stream-sediment and soil samples from East Mojave National Scenic Area (EMNSA), Calif., and surrounding area. For each locality, elements are shown by either vertical or diagonal lines emanating from a common locality point (overlapping lines represent more than one locality). Longer lines indicate anomalous concentrations; shorter lines, high concentrations. Concentration values shown are defined as follows: anomalous, above threshold values given in table 13; high, selected ranges that include threshold values as upper limits. Percentiles for high concentrations are as follows: U, 91 to 98; Th, 94 to 97; La, 97 to 98. General outlines of geochemically evaluated areas (shaded) shown for reference; see figure 49 for location names. Statistical data given in table 13; summary of geochemical anomalies given in table 14; sample localities plotted on figure 53.

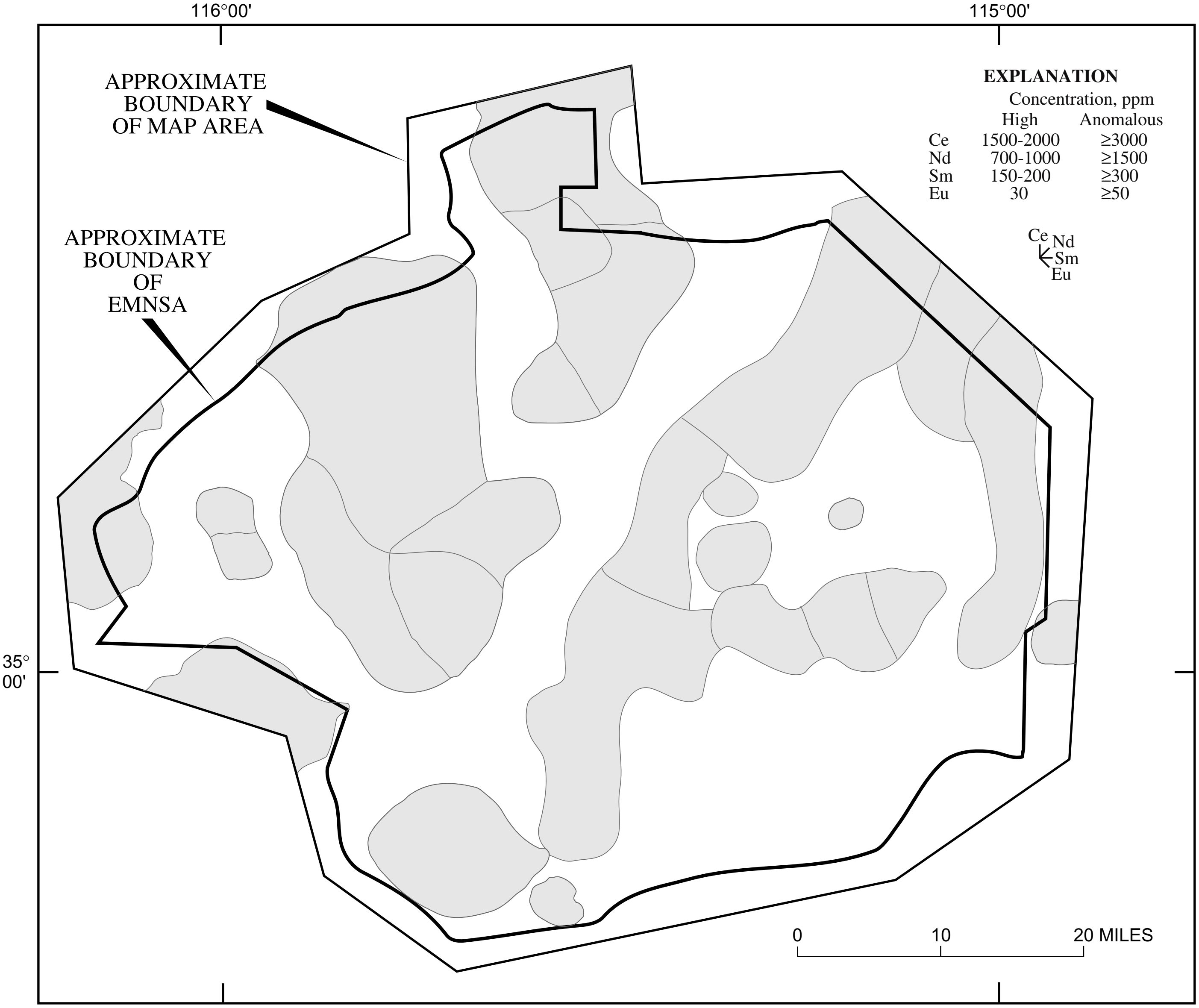

Figure 68. Distribution of anomalous and high concentrations, in parts per million, of Ce, Nd, Sm, and Eu in geochemical data base for the United States (PLUTO) heavy-mineral-concentrate samples from East Mojave National Scenic Area (EMNSA), Calif., and surrounding area. For each locality, elements are shown by either vertical, horizontal, or diagonal lines emanating from a common locality point (overlapping lines represent more than one locality). Longer lines indicate anomalous concentrations; shorter lines, high concentrations. Concentration values shown are defined as follows: anomalous, above threshold values given in table 13; high, selected ranges that include threshold values as upper limits. Percentiles for high concentrations are as follows: Ce, 74 to 88; Nd, 73 to 90; Sm, 75 to 92; Eu, 87 to 96. General outlines of geochemically evaluated areas (shaded) shown for reference; see figure 49 for location names. Statistical data given in table 13; summary of geochemical anomalies given in table 14; sample localities plotted on figure 51.

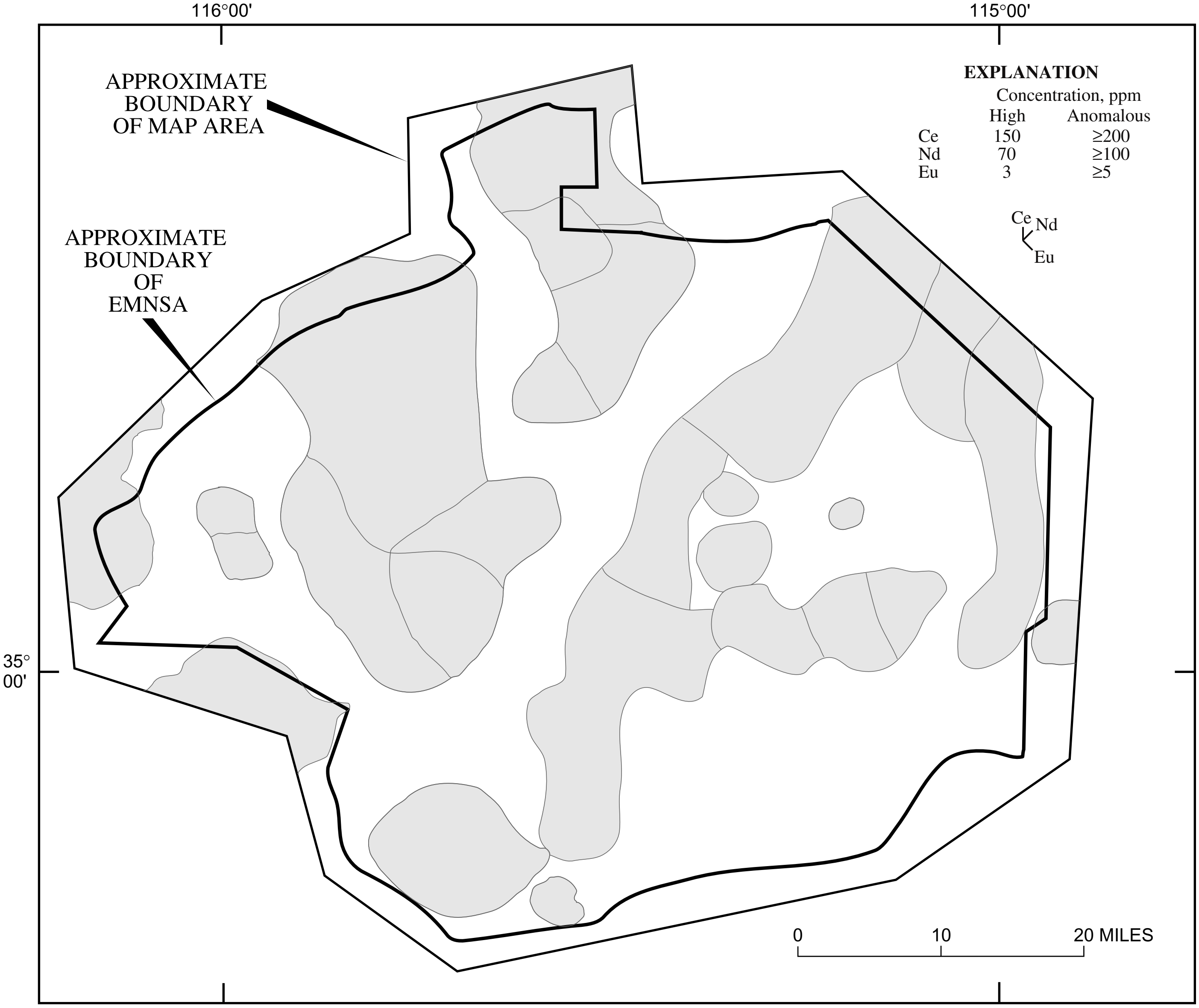

Figure 69. Distribution of anomalous and high concentrations, in parts per million, of Ce, Nd, and Eu in geochemical data base for the United States (PLUTO) rock samples from East Mojave National Scenic Area (EMNSA), Calif., and surrounding area. For each locality, elements are shown by either vertical or diagonal lines emanating from a common locality point (overlapping lines represent more than one locality). Longer lines indicate anomalous concentrations; shorter lines, high concentrations. Concentration values shown are defined as follows: anomalous, above threshold values given in table 13; high, selected ranges that include threshold values as upper limits. Percentiles for high concentrations are as follows: Ce, 88 to 95; Nd, 73 to 91; Eu, 68 to 95. General outlines of geochemically evaluated areas (shaded) shown for reference; see figure 49 for location names. Statistical data given in table 13; summary of geochemical anomalies given in table 14; sample localities plotted on figure 52.

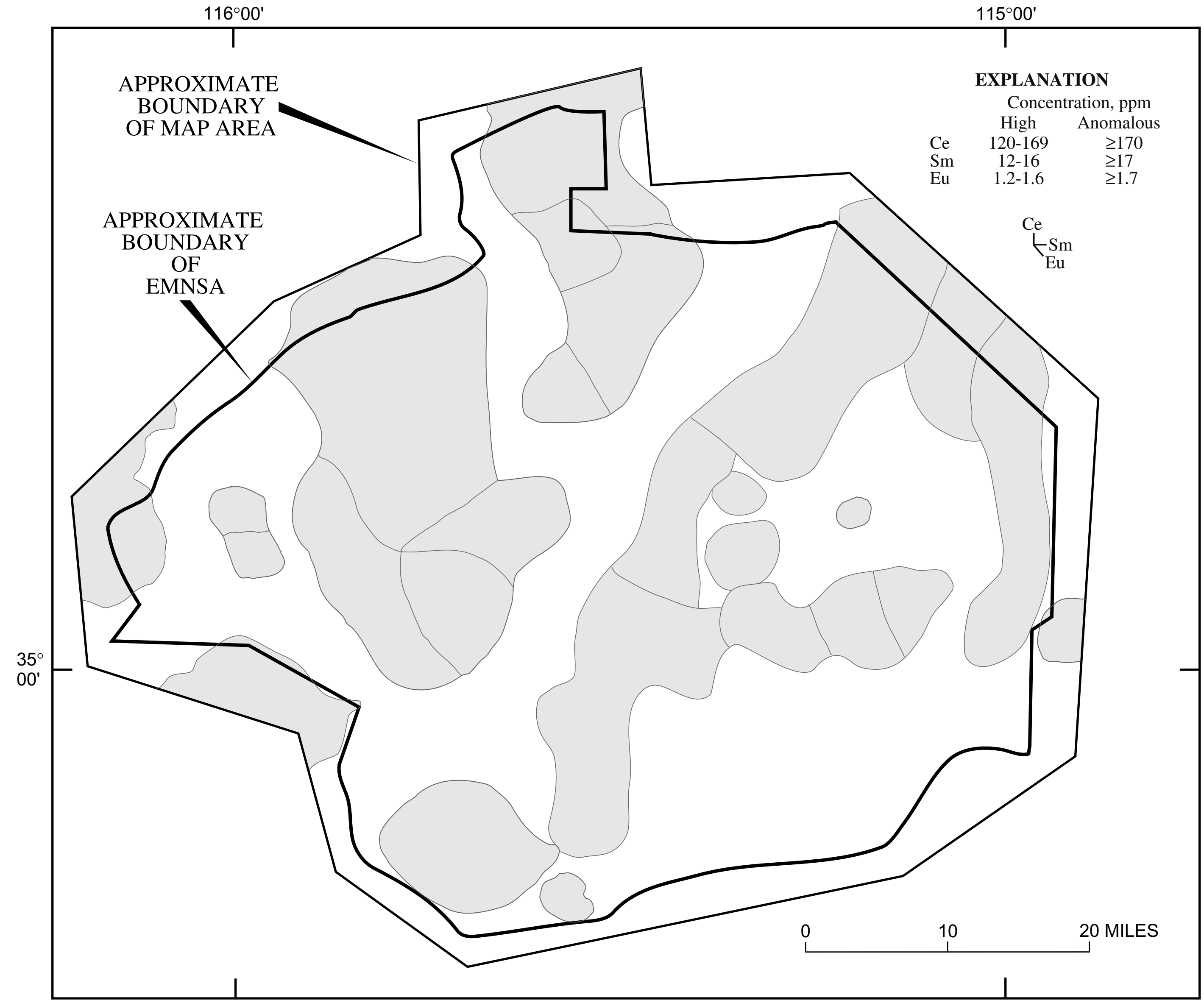

Figure 70. Distribution of anomalous and high concentrations, in parts per million, of Ce, Sm, and Eu in National Uranium Resource Evaluation (NURE) stream-sediment and soil samples from East Mojave National Scenic Area (EMNSA), Calif., and surrounding area. For each locality, elements are shown by either vertical, horizontal, or diagonal lines emanating from a common locality point (overlapping lines represent more than one locality). Longer lines indicate anomalous concentrations; shorter lines, high concentrations. Concentration values shown are defined as follows: anomalous, above threshold values given in table 13; high, selected ranges that include threshold values. Percentiles for high concentrations are as follows: Ce, 84 to 95; Sm, 89 to 95; Eu, 71 to 83. General outlines of geochemically evaluated areas (shaded) shown for reference; see figure 49 for location names. Statistical data given in table 13; summary of geochemical anomalies given in table 14; sample localities plotted on figure 53.

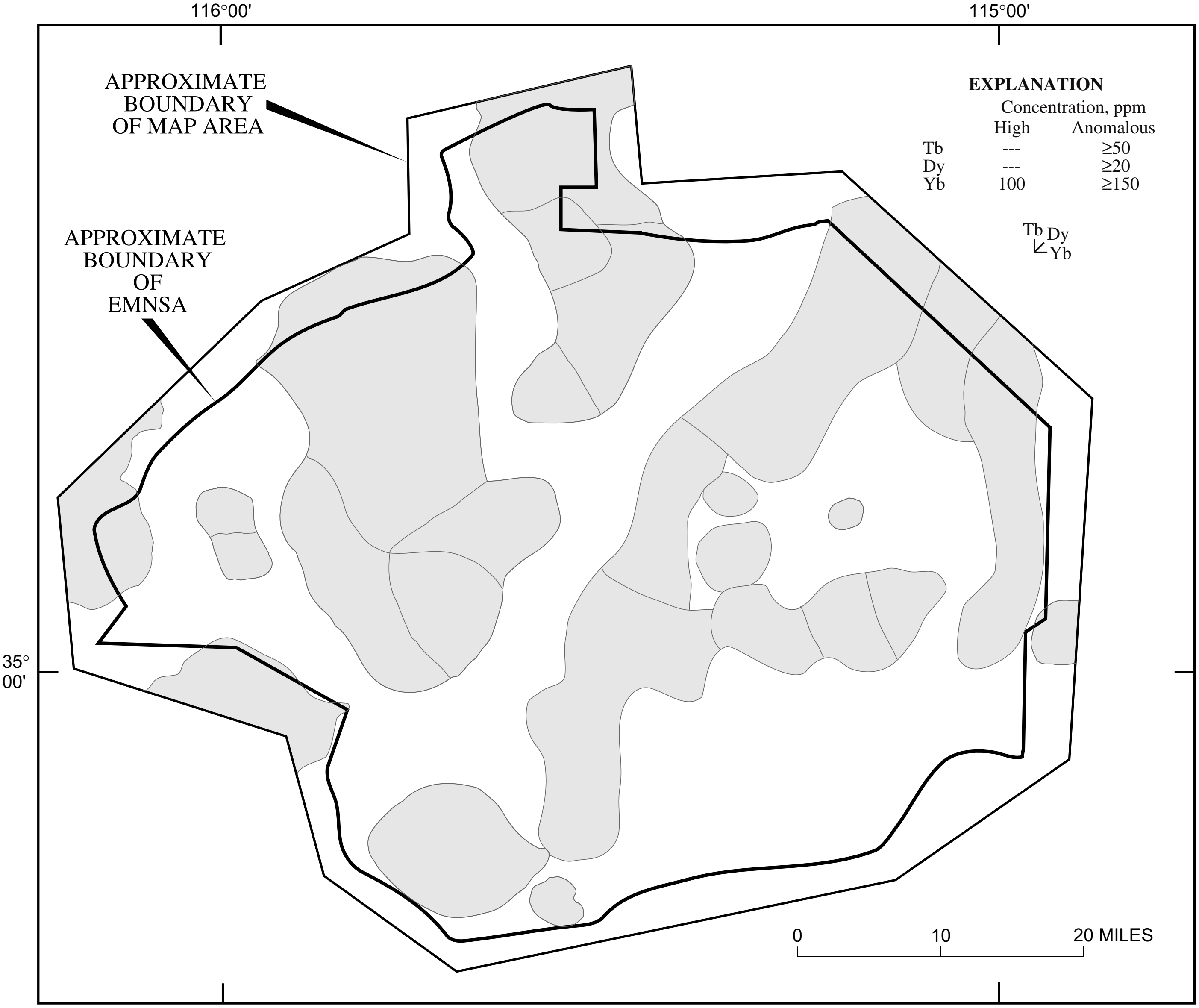

Figure 71. Distribution of anomalous and high concentrations, in parts per million, of Tb, Dy, and Yb in geochemical data base for the United States (PLUTO) heavy-mineral-concentrate samples from East Mojave National Scenic Area (EMNSA), Calif., and surrounding area. For each locality, elements are shown by either vertical, horizontal, or diagonal lines emanating from a common locality point (overlapping lines represent more than one locality). Longer lines indicate anomalous concentrations; shorter lines, high concentrations. Concentration values shown are defined as follows: anomalous, above threshold values given in table 13; high, selected ranges that include threshold values; ---, no value (any detectable concentration is anomalous). Percentiles for high concentrations are as follows: Yb, 76 to 92. General outlines of geochemically evaluated areas (shaded) shown for reference; see figure 49 for location names. Statistical data given in table 13; summary of geochemical anomalies given in table 14; sample localities plotted on figure 51.

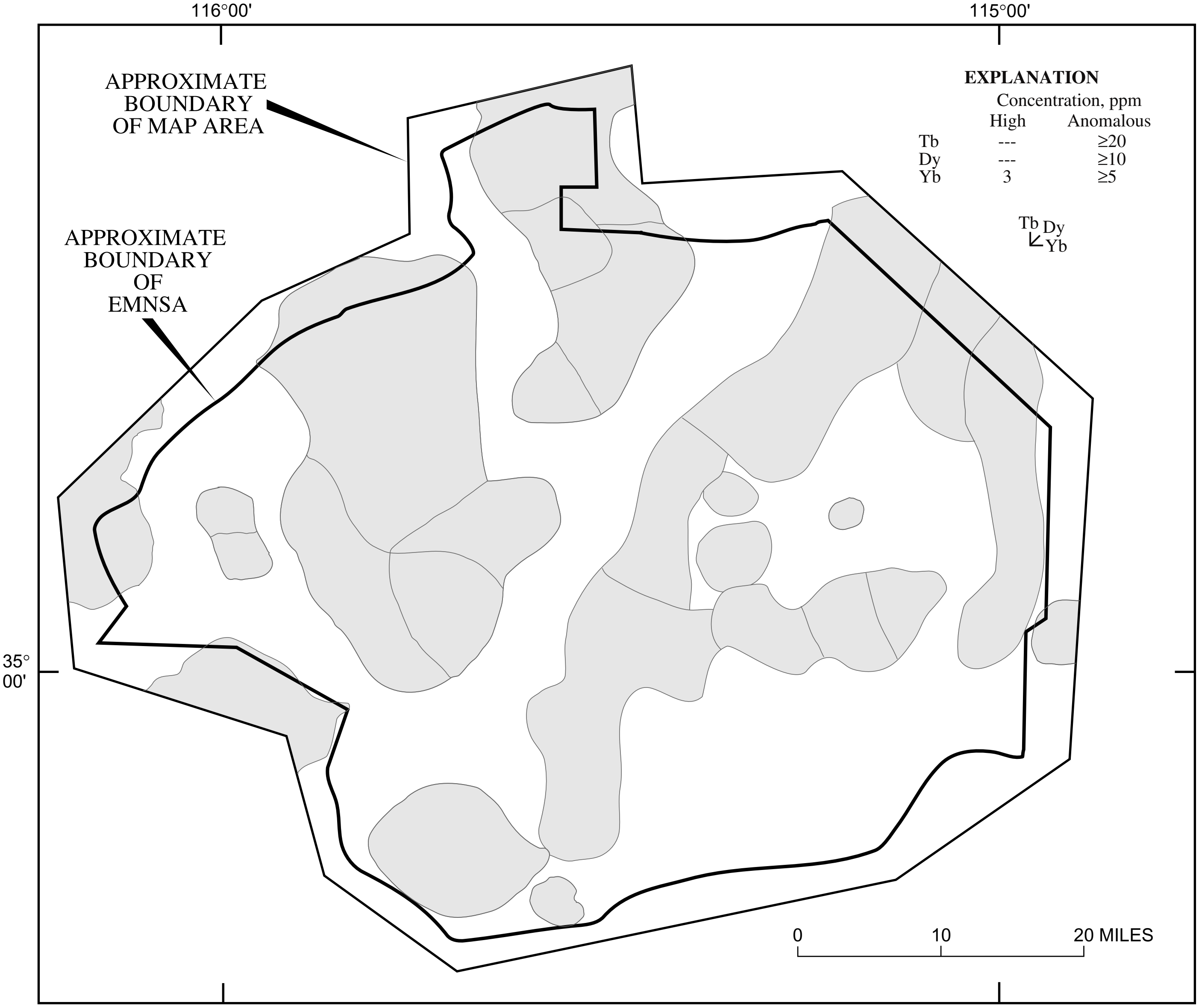

Figure 72. Distribution of anomalous and high concentrations, in parts per million, of Tb, Dy, and Yb in geochemical data base for the United States (PLUTO) rock samples from East Mojave National Scenic Area (EMNSA), Calif., and surrounding area. For each locality, elements are shown by either vertical, horizontal, or diagonal lines emanating from a common locality point (overlapping lines represent more than one locality). Longer lines indicate anomalous concentrations; shorter lines, high concentrations. Concentration values shown are defined as follows: anomalous, above threshold values given in table 13; high, selected ranges that include threshold values; ---, no value (any detectable concentration is anomalous). Percentiles for high concentrations are as follows: Yb, 88 to 96. General outlines of geochemically evaluated areas (shaded) shown for reference; see figure 49 for location names. Statistical data given in table 13; summary of geochemical anomalies given in table 14; sample localities plotted on figure 52.

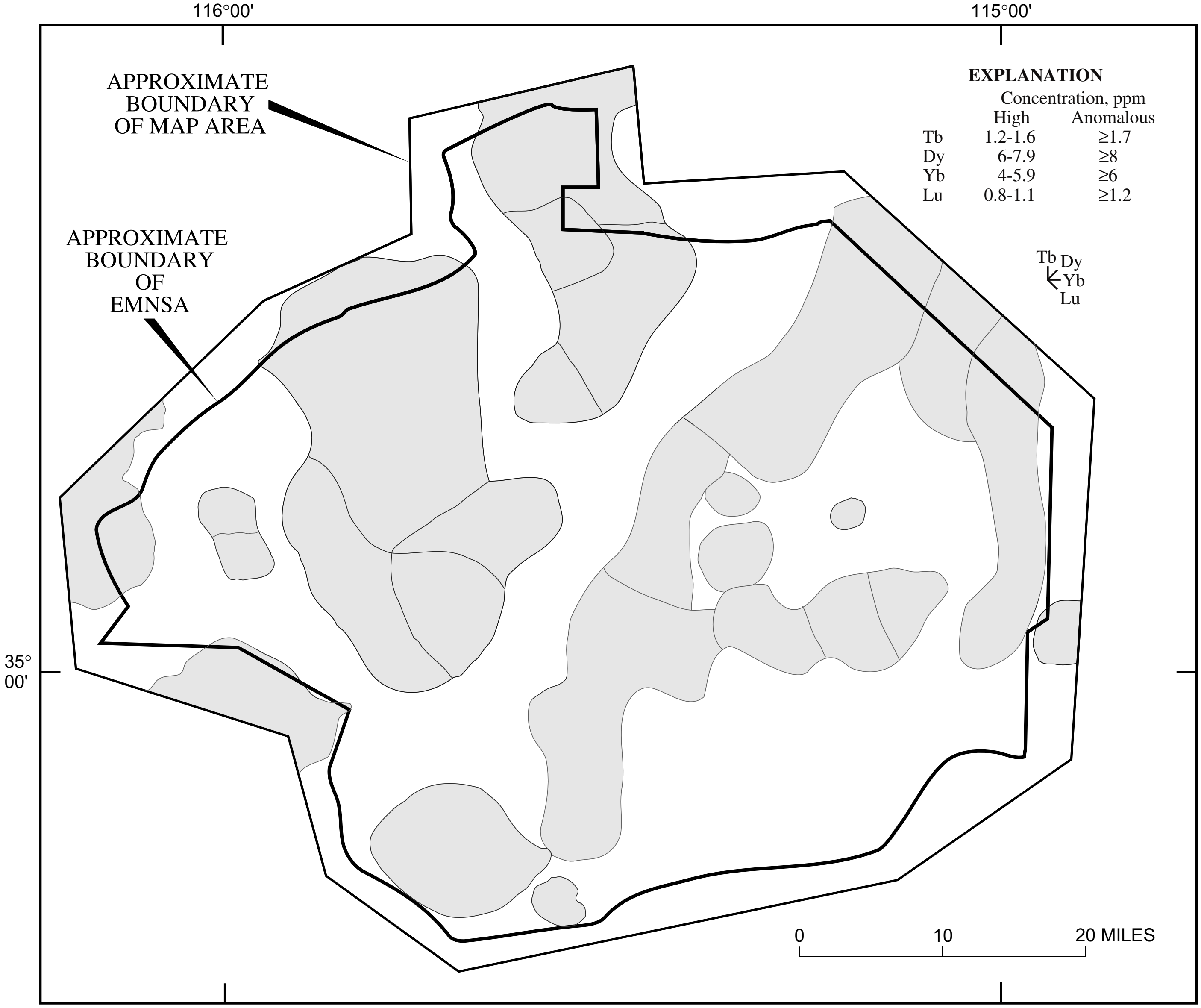

Figure 73. Distribution of anomalous and high concentrations, in parts per million, of Tb, Dy, Yb, and Lu in National Uranium Resource Evaluation (NURE) stream-sediment and soil samples from East Mojave National Scenic Area (EMNSA), Calif., and surrounding area. For each locality, elements are shown by either vertical, horizontal, or diagonal lines emanating from a common locality point (overlapping lines represent more than one locality). Longer lines indicate anomalous concentrations; shorter lines, high concentrations. Concentration values shown are defined as follows: anomalous, above threshold values given in table 13; high, selected ranges that include threshold values. Percentiles for high concentrations are as follows: Tb, 82 to 89; Dy, 82 to 91: Yb, 86 to 94; Lu, 87 to 96. General outlines of geochemically evaluated areas (shaded) shown for reference; see figure 49 for location names. Statistical data given in table 13; summary of geochemical anomalies given in table 14; sample localities plotted on figure 53.

Figure 74. Siderite brecciated along minor fault at El Lobo Mine, in Little Cowhole Mountain (fig. 49) near northwest boundary of East Mojave National Scenic Area, Calif.; open spaces filled partly by quartz.

Figure 75. Iron and polymetallic skarn formed in general area of Mosaic Queen Mine, Cowhole Mountain (fig. 49), East Mojave National Scenic Area, Calif. View toward N. 50° W. along approximately 0.5–km-long zone of skarn. Note approximately 2–m-wide prospect pit near bottom of photograph.

Figure 76. Brecciated Early Proterozoic gneiss and granitoid rocks veined by quartz (white, at hammer point) at main workings of Paymaster Mine near Seventeenmile Point (fig. 49), west-central part of East Mojave National Scenic Area, Calif.

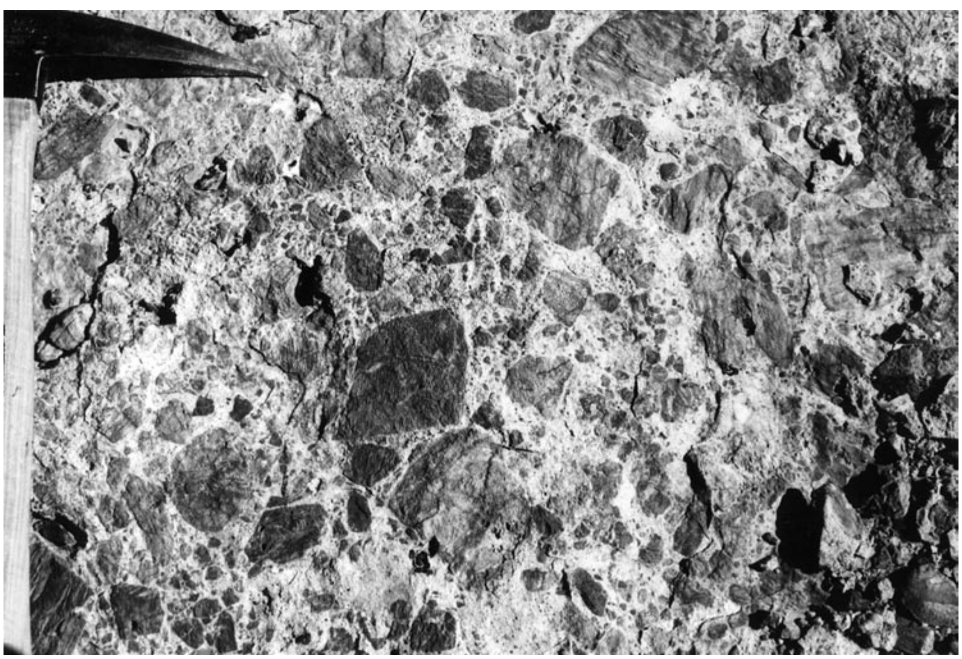

Figure 77. Brecciated Paleozoic limestone and dolomite in general area of Oro Fino Mine , approximately 3 km south of Seventeenmile Point (Old Dad Mountain, fig. 49), west-central part of East Mojave National Scenic Area, Calif.

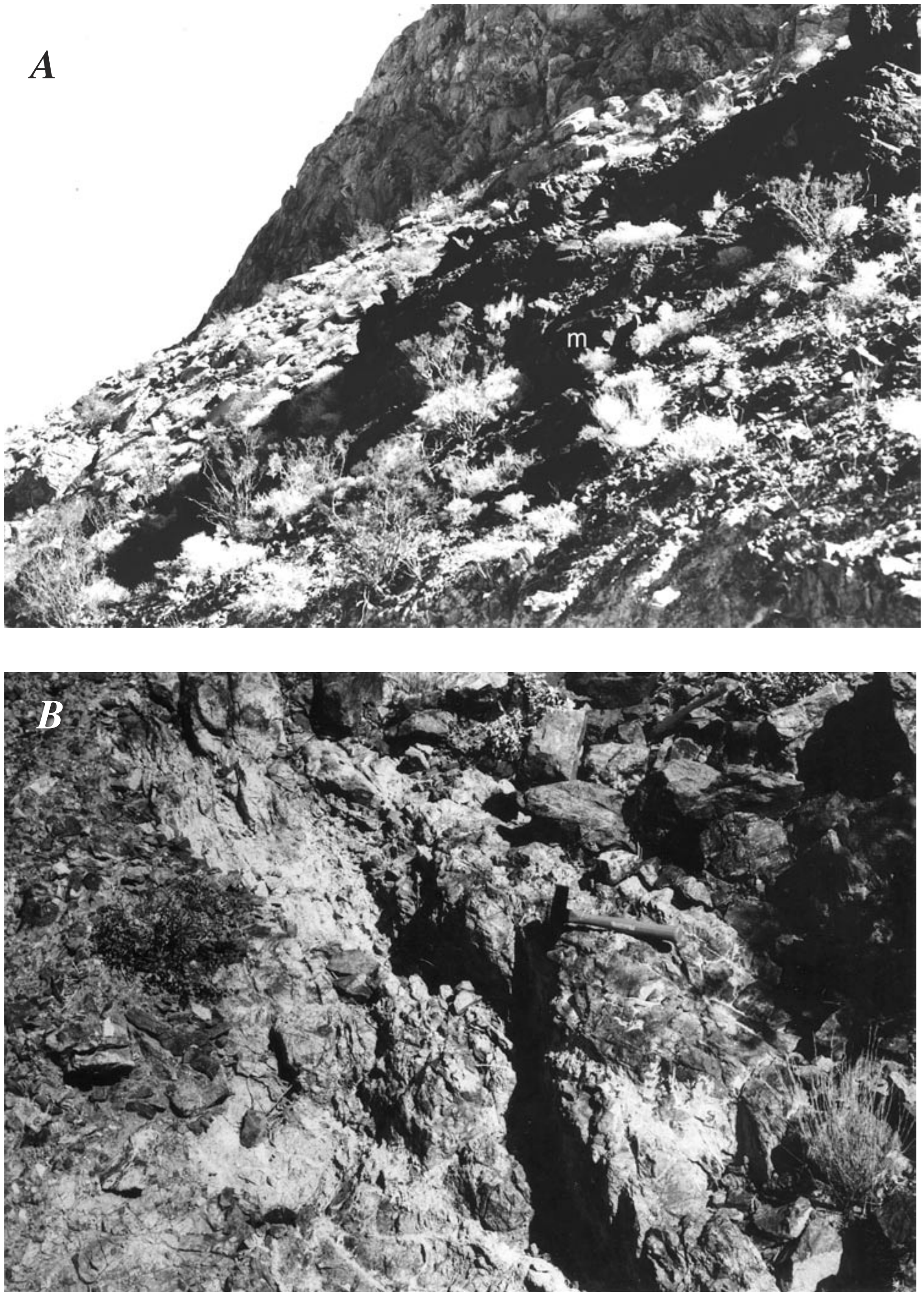

Figure 78. Mineral occurrences near Old Dad Mountain (fig. 49) in west-central part of East Mojave National Scenic Area, Calif. *A*, Massive magnetite (m) at Old Dad iron-skarn deposit, approximately10 m thick. In places, magnetite is associated with coarsely crystalline actinolite, which is present in clusters of radiating crystals. *B*, Shattered, sulfide mineral-impregnated silicic dike at Lucky (ODM) group of claims (NW 1/4 sec. 11, T. 12 N., R. 10 E.); dike is probably associated genetically with nearby widespread alteration.

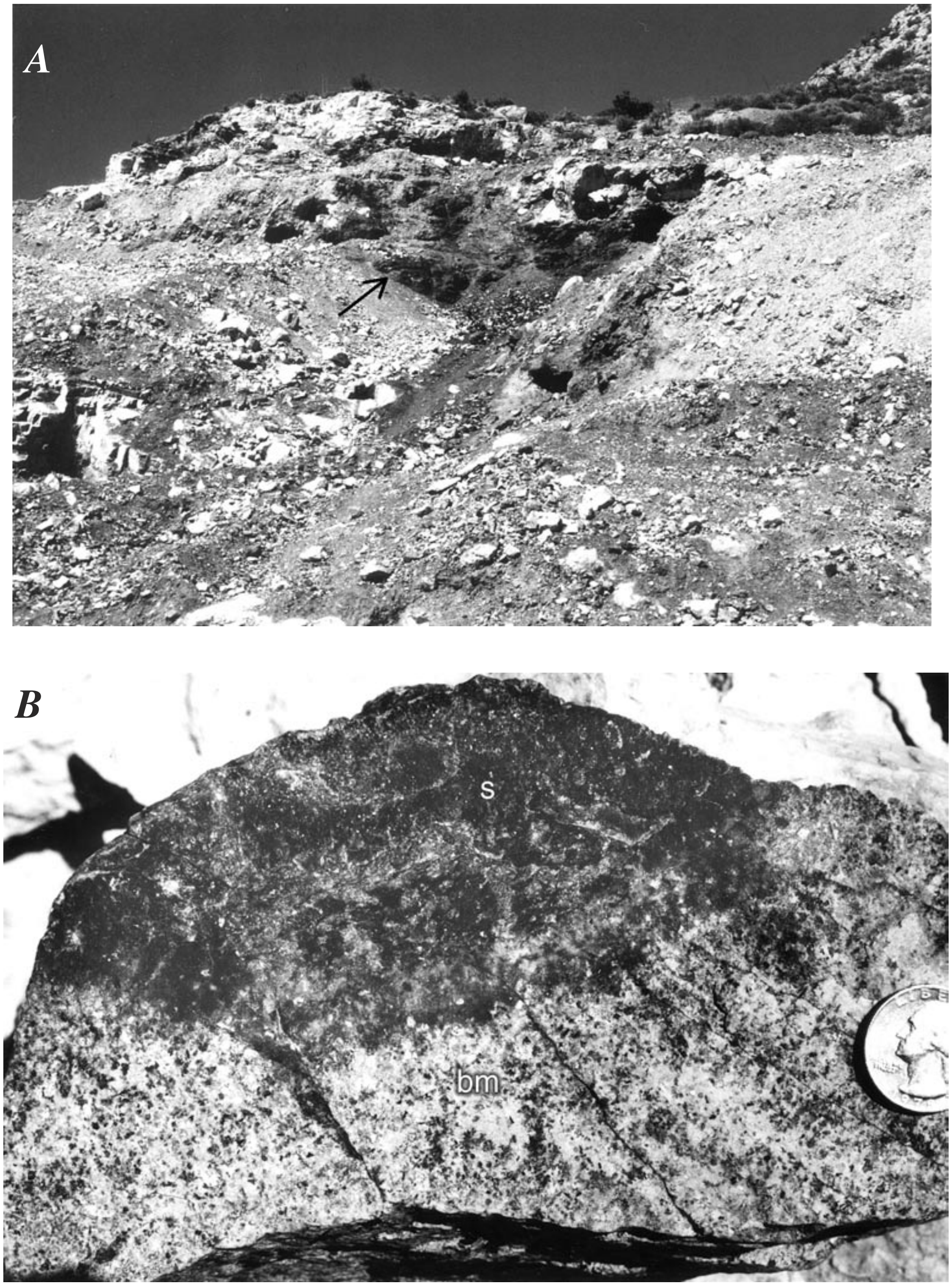

Figure 79. Skarn occurrences in north-central part of East Mojave National Scenic Area, Calif (fig. 49). *A*, Gossan (at head of arrow) formed in formerly iron-sulfide mineral-rich zones developed in layered marble and skarn adjacent to nonporphyritic hornblende diorite at Copper World Mine, south end of Clark Mountain Range. Dark area in center of photograph is approximately 30 m thick. *B*, Knife-edge contact between clay-altered biotite monzogranite (bm) and garnet-pyroxene skarn (s) at Mohawk Mine, near west end of Mohawk Hill at north end of Mescal Range. *C*, Massive epidote skarn (es) at Silverado-Tungstite Mine, showing sharp contact (at point of pick) with chloritic-altered hornblende diorite (hd) of Jurassic Striped Mountain pluton. *D*, Garnet-pyroxene skarn (s), possibly hedenbergitic, at Silvarado-Tungstite Mine, showing late-stage, open-cavity, and vein-type quartz (at head of arrow).

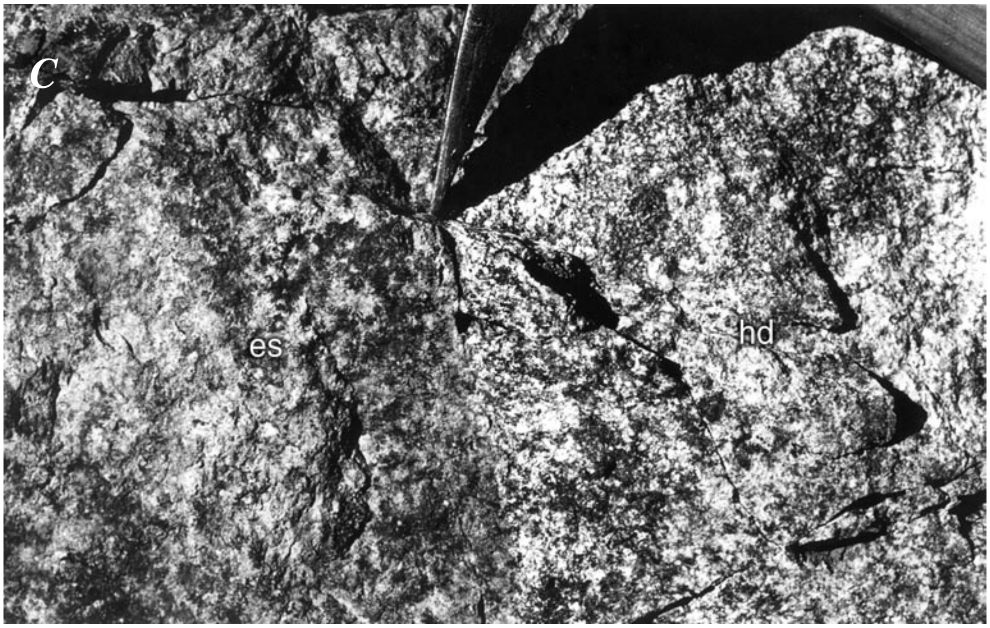

Figure 79. Skarn occurrences in north-central part of East Mojave National Scenic Area, Calif (fig. 49). *A*, Gossan (at head of arrow) formed in formerly iron-sulfide mineral-rich zones developed in layered marble and skarn adjacent to nonporphyritic hornblende diorite at Copper World Mine, south end of Clark Mountain Range. Dark area in center of photograph is approximately 30 m thick. *B*, Knife-edge contact between clay-altered biotite monzogranite (bm) and garnet-pyroxene skarn (s) at Mohawk Mine, near west end of Mohawk Hill at north end of Mescal Range. *C*, Massive epidote skarn (es) at Silverado-Tungstite Mine, showing sharp contact (at point of pick) with chloritic-altered hornblende diorite (hd) of Jurassic Striped Mountain pluton. *D*, Garnet-pyroxene skarn (s), possibly hedenbergitic, at Silverado-Tungstite Mine, showing late-stage, open-cavity, and vein-type quartz (at head of arrow).—Continued

Figure 80. Exposures of thin-bedded Paleozoic carbonate sequence at south end of Striped Mountain (fig. 49), East Mojave National Scenic Area, Calif. View to northeast.

Figure 81. Exposures of magnetite skarn at Vulcan Iron Mine, Providence Mountains (fig. 49), East Mojave National Scenic Area, Calif. *A*, Main entrance to open cut at Vulcan iron skarn showing gravels (g) and dolomite (d; unit €d, pl. 1) overlying faulted (dashed line) magnetite-rich skarn (m). View to north. *B*, Fault (dashed) between Jurassic albitized diorite (ad) and magnetite skarn (m). View to N. 60° W. along strike of fault. Outcrop is approximately 20 m high.

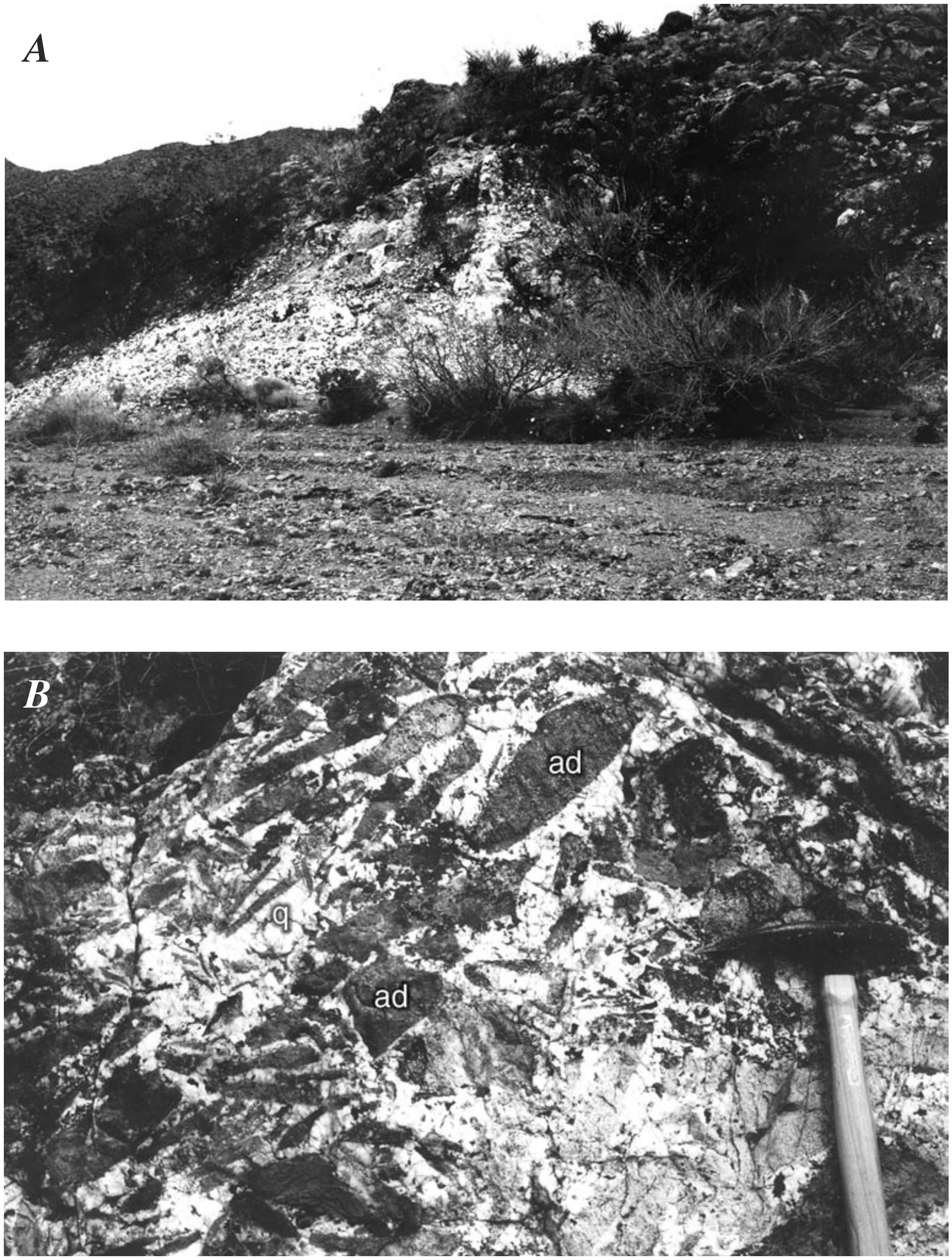

Figure 82. Massive quartz associated with molybdenite occurrence in Globe Wash, north-central Providence Mountains (fig. 49), East Mojave National Scenic Area, Calif. *A*, Exposure, approximately 30 m wide, of milky-white quartz in bottom of Globe Wash. View to north. *B*, Close-up view of 82*A* showing subangular fragments of leucogranite phase of informally named Cretaceous Mid Hills adamellite (ad) of Beckerman and others (1982) (unit Kmh, pl. 1) enclosed in massive quartz (q), which is characterized by widespread presence of brick-red iron oxide minerals.

Figure 83. Miocene ash-flow tuff (at head of arrow) at Pinto Mountain (fig. 49), East Mojave National Scenic Area, Calif. View to north.

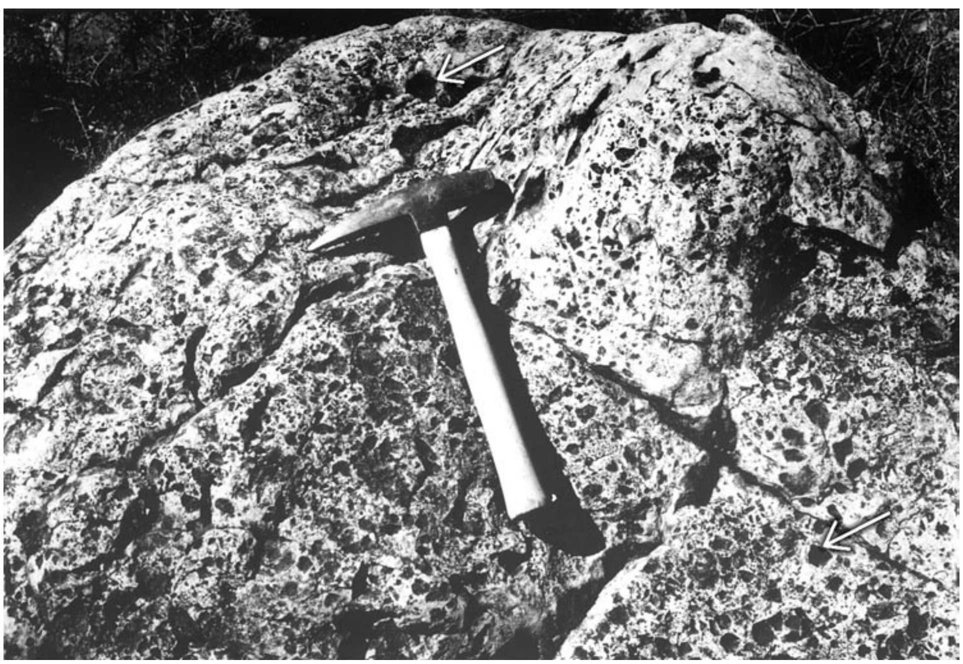

Figure 84. Exposure of vuggy-silica-altered Miocene rhyolite from Hart Mining District, Castle Mountains (fig. 49), East Mojave National Scenic Area, Calif. Vugs (at heads of arrows) result from acid leaching by meteoric fluids percolating through sulfur-enriched rocks.

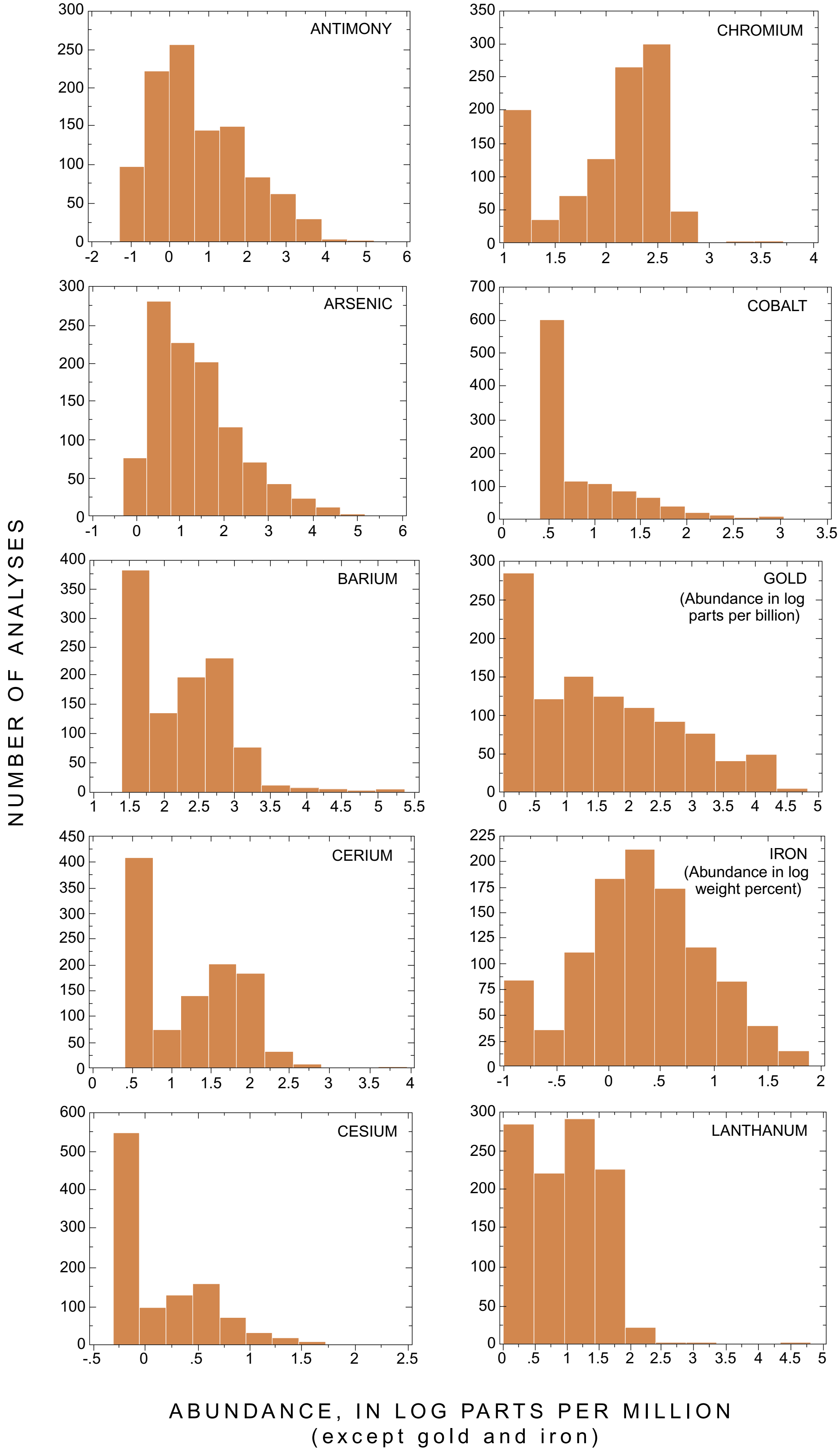

Figure 85. Frequency distribution of 20 elements in 1,050 rocks from East Mojave National Scenic Area, Calif. All abundances are in log parts per million, except gold, which are in log parts per billion, and iron, which are in log weight percent. Analyses by U.S. Bureau of Mines (1990a).

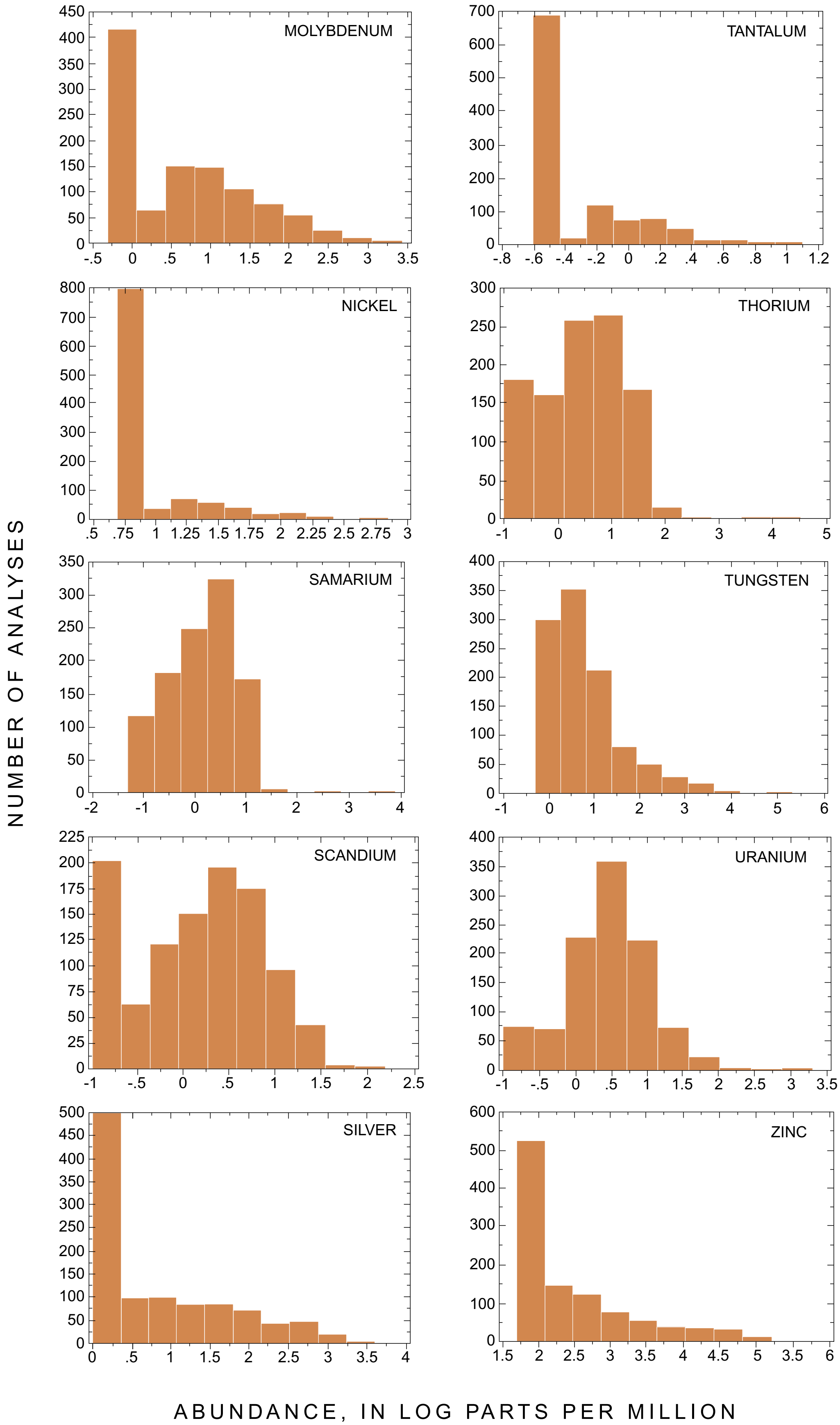

Figure 85. Frequency distribution of 20 elements in 1,050 rocks from East Mojave National Scenic Area, Calif. All abundances are in log parts per million, except gold, which are in log parts per billion, and iron, which are in log weight percent. Analyses by U.S. Bureau of Mines (1990a)—Continued.

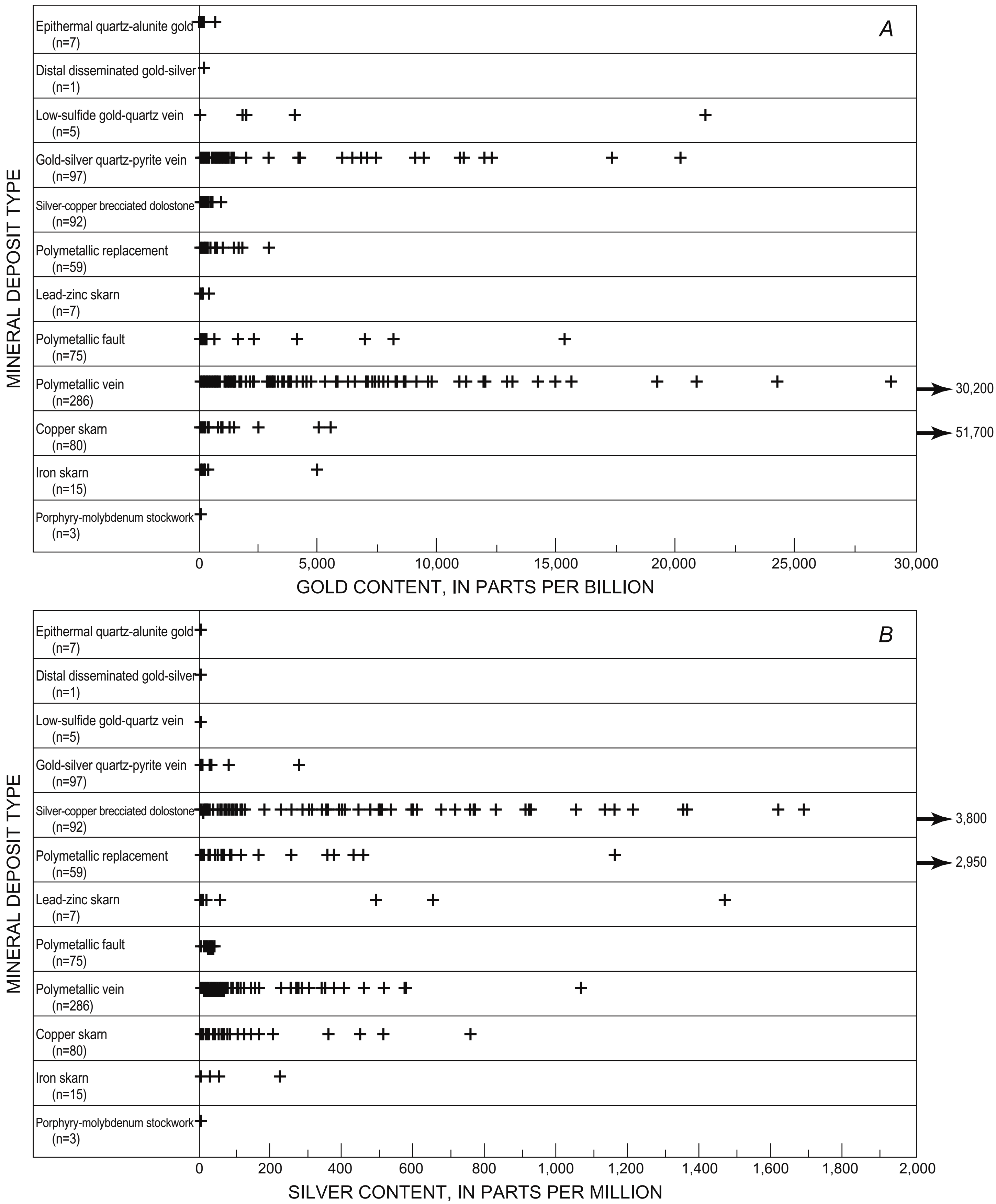

Figure 86. Plots showing detectable concentrations, grouped by deposit type, of four metals in mineralized rocks in East Mojave National Scenic Area, Calif. Analyses by U.S. Bureau of Mines (1990a); n, number of samples analyzed. *A*, Gold; *B*, Silver; *C*, Arsenic; *D*, Antimony.

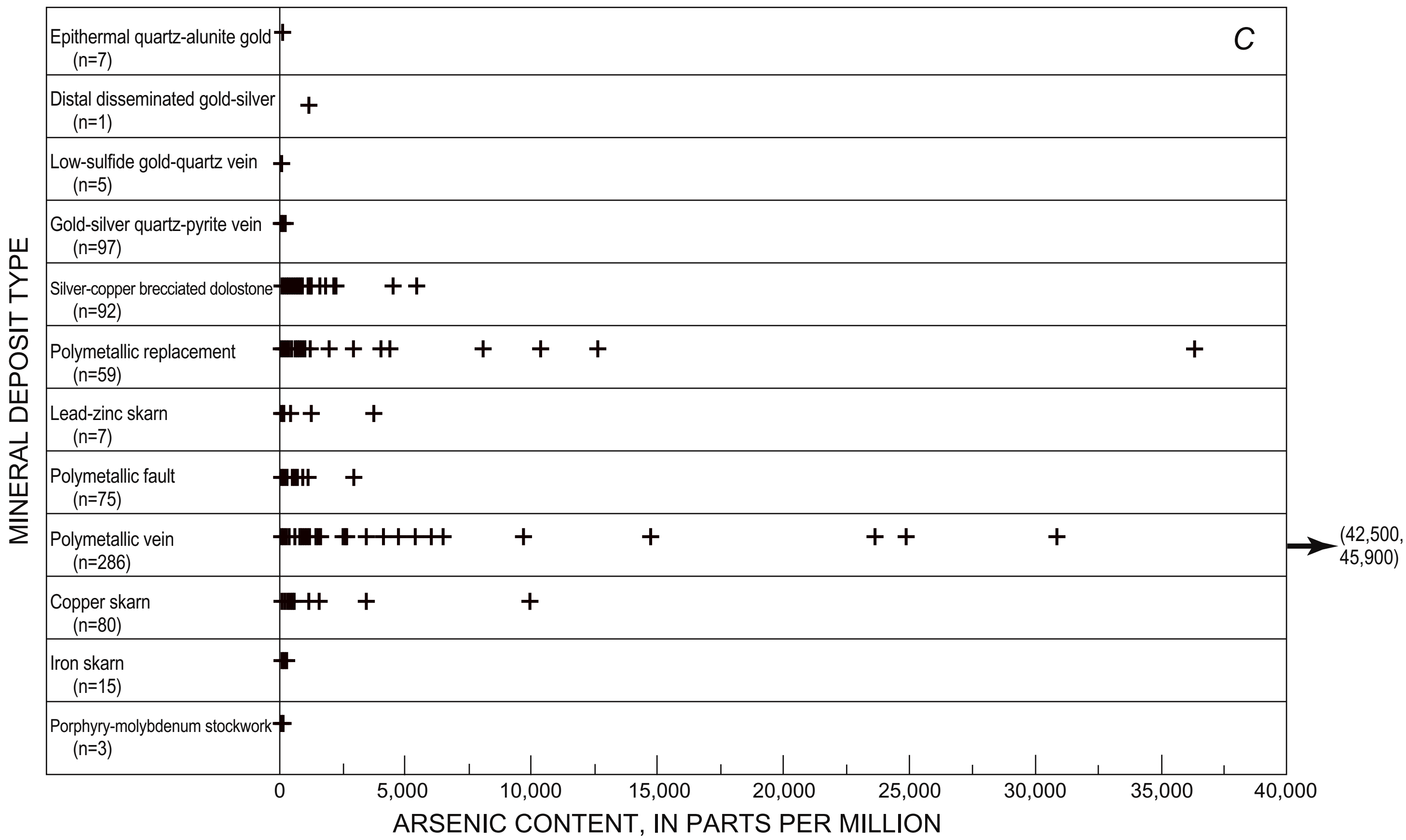

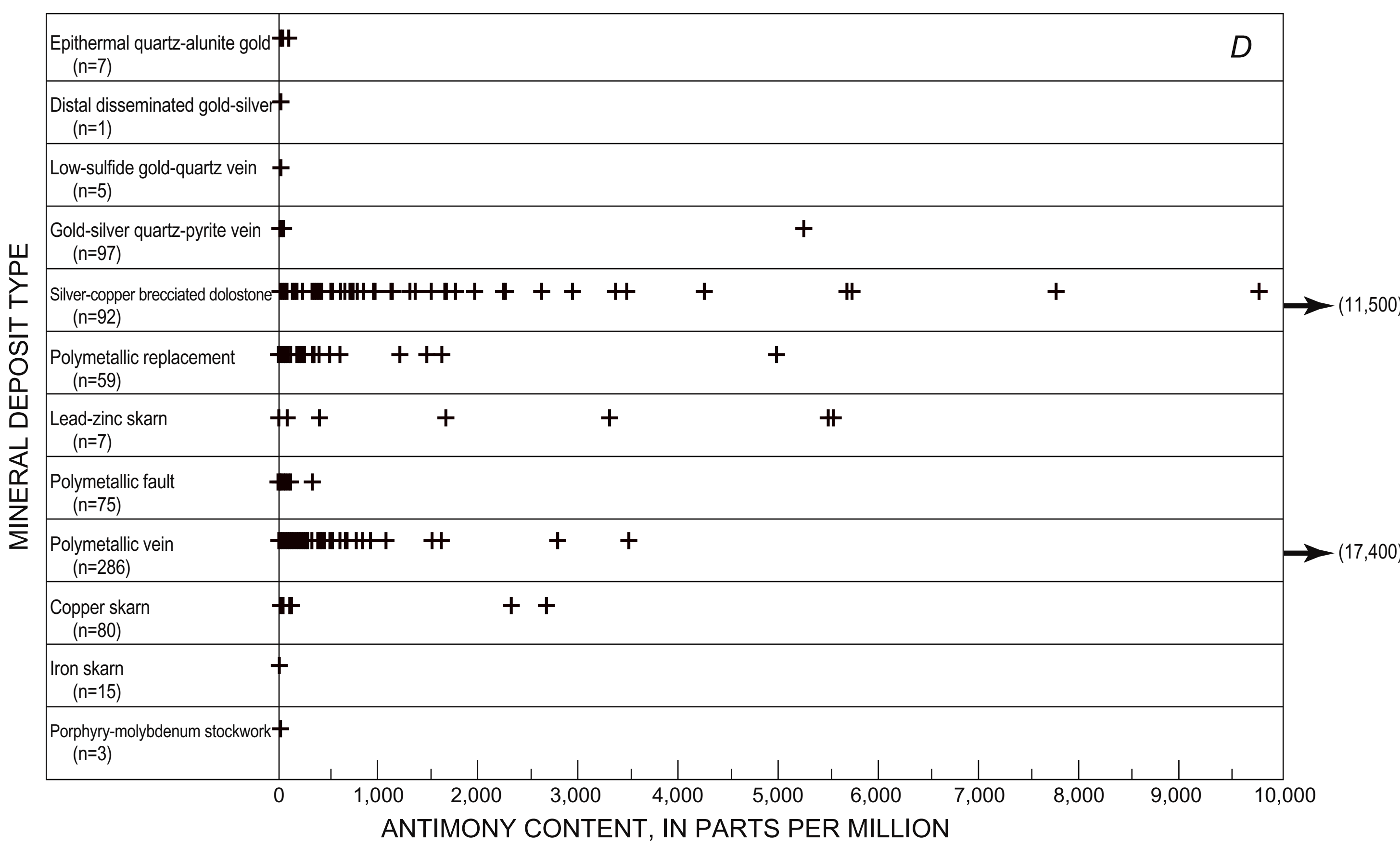

Figure 86. Plots showing detectable concentrations, grouped by deposit type, of four metals in mineralized rocks in East Mojave National Scenic Area, Calif. Analyses by U.S. Bureau of Mines (1990a); n, number of samples analyzed. *A*, Gold; *B*, Silver; *C*, Arsenic; *D*, Antimony—Continued.

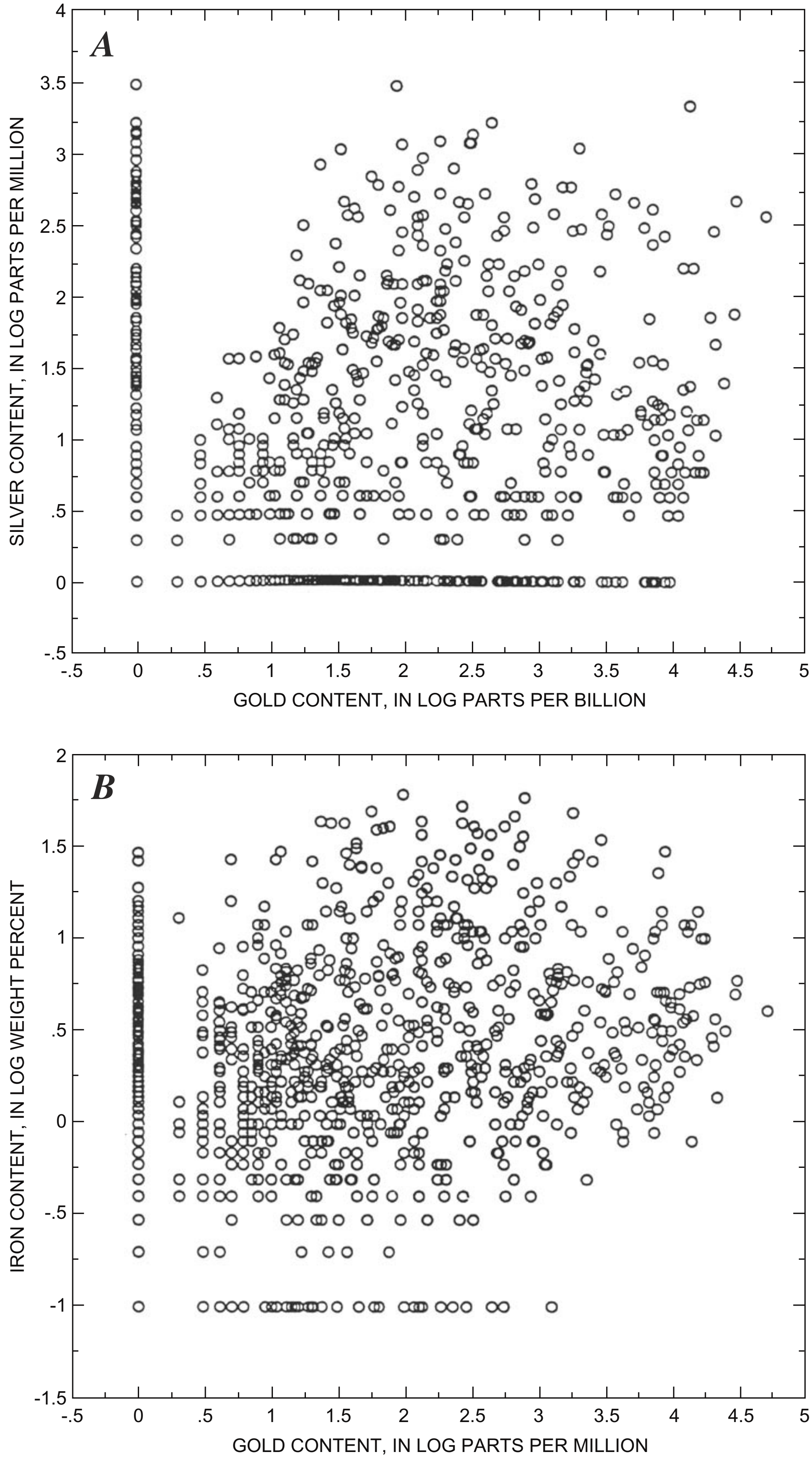

Figure 87. Chemical variation diagrams for 1,050 rocks from East Mojave National Scenic Area, Calif. Analyses by the U.S. Bureau of Mines (1990a). *A*, Silver versus gold content. *B*, Iron versus gold content. *C*, Samarium versus lanthanum content. *D*, Antimony versus silver content. *E*, Iron versus cobalt content. *F*, Barium versus uranium content.

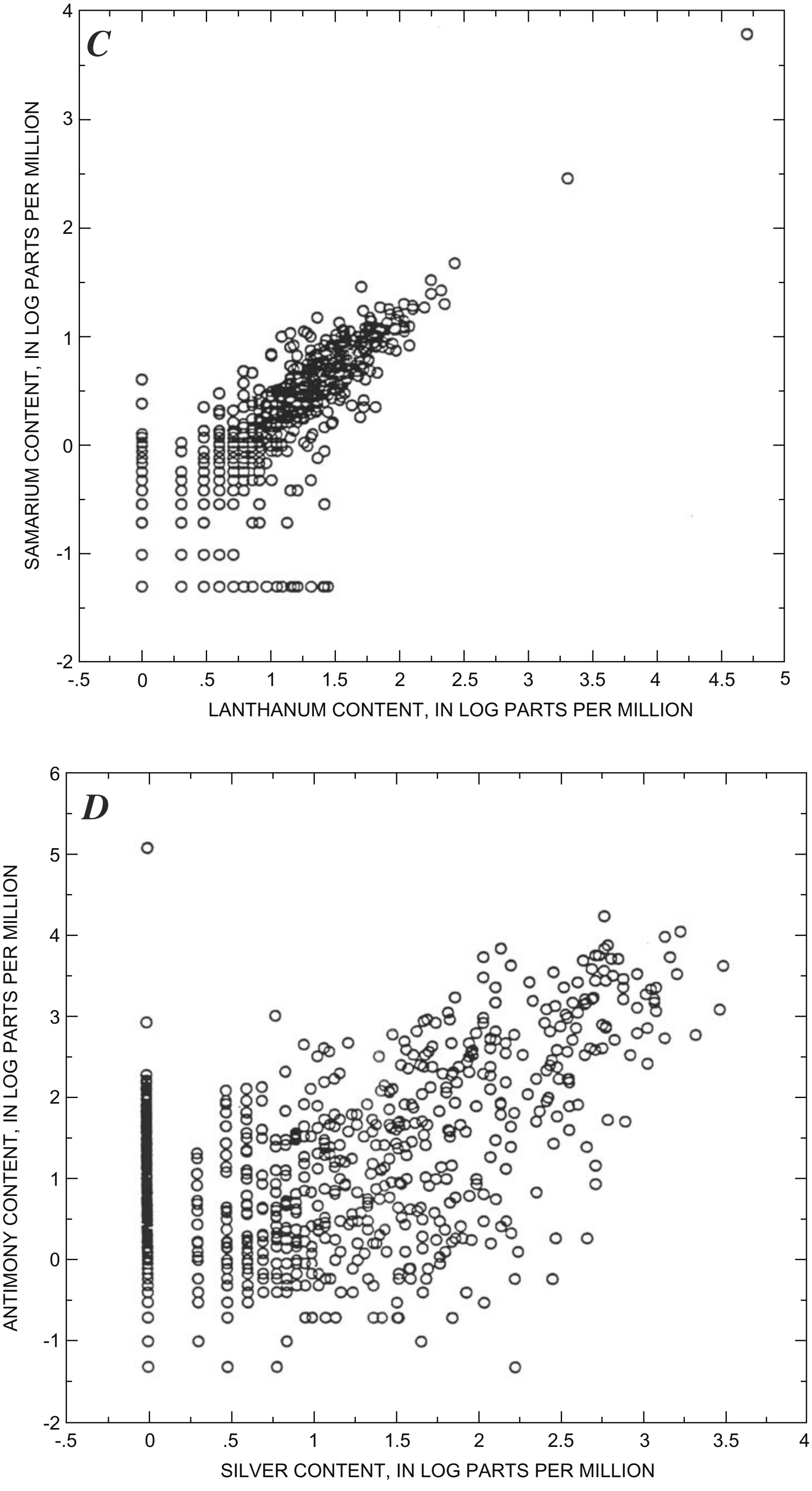

Figure 87. Chemical variation diagrams for 1,050 rocks from East Mojave National Scenic Area, Calif. Analyses by the U.S. Bureau of Mines (1990a). *A*, Silver versus gold content. *B*, Iron versus gold content. *C*, Samarium versus lanthanum content. *D*, Antimony versus silver content. *E*, Iron versus cobalt content. *F*, Barium versus uranium content—Continued.

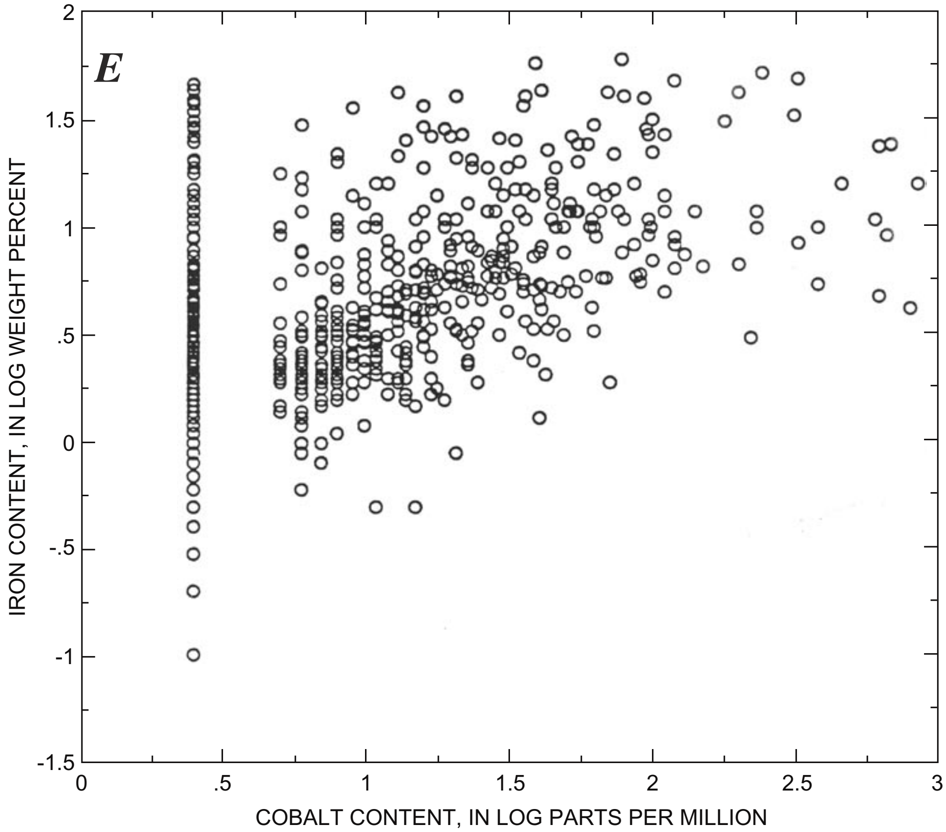

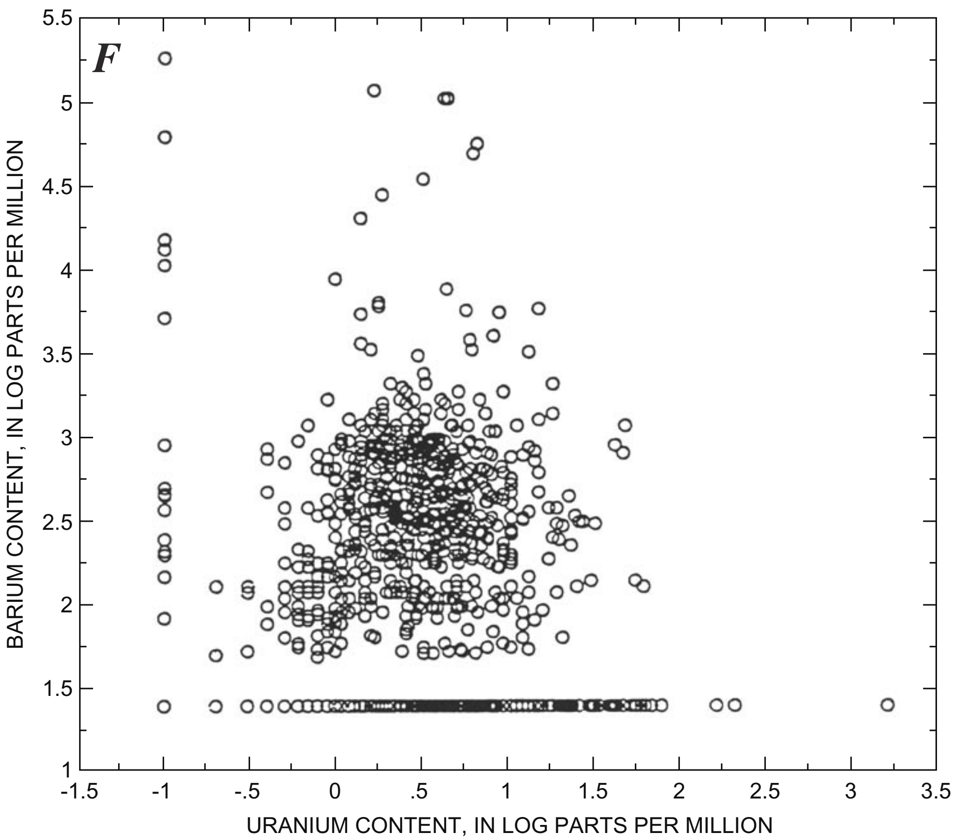

Figure 87. Chemical variation diagrams for 1,050 rocks from East Mojave National Scenic Area, Calif. Analyses by the U.S. Bureau of Mines (1990a). *A*, Silver versus gold content. *B*, Iron versus gold content. *C*, Samarium versus lanthanum content. *D*, Antimony versus silver content. *E*, Iron versus cobalt content. *F*, Barium versus uranium content—Continued.

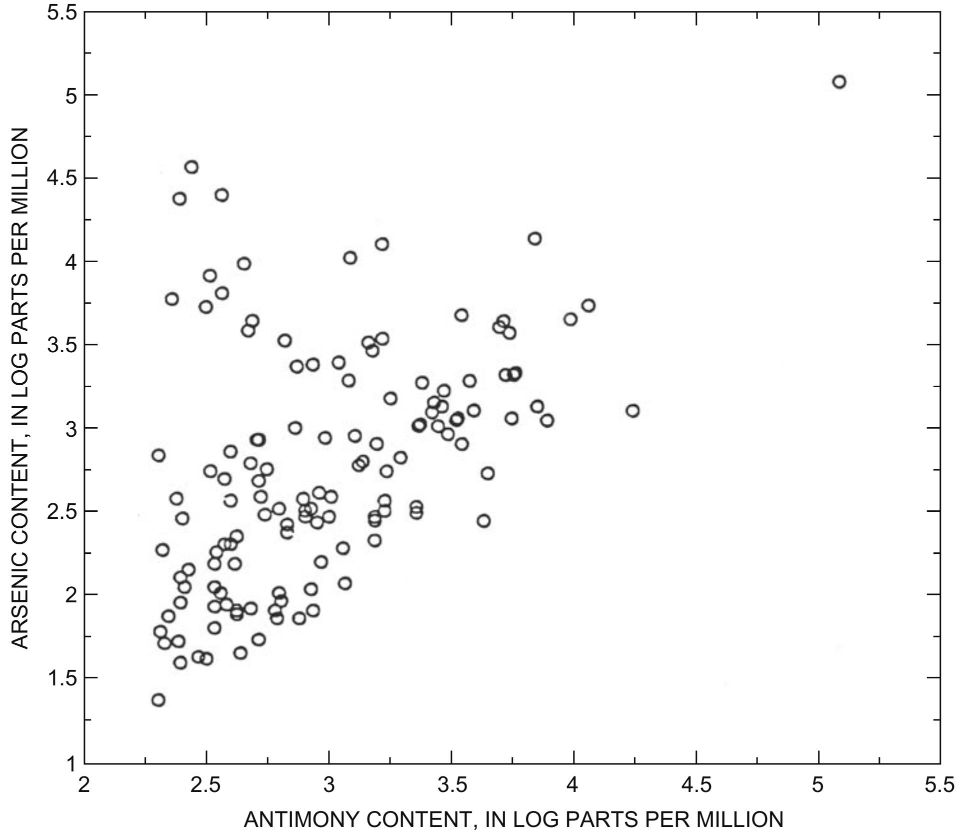

Figure 88. Plot showing arsenic versus antimony content in 131 samples that contain greater than 200 parts per million antimony, which have been selected from 1,050–rock data base from East Mojave National Scenic Area, Calif. Analyses by U.S. Bureau of Mines (1990a).

Table 10. Areas in the East Mojave National Scenic Area, Calif., and their references to interpretive geochemical reports and (or) releases of raw geochemical data.

[--, no published report]

Area on figure 49	Interpretive report	Raw geochemical data
Soda Mountains	--	--
Little Cowhole Mountain	--	--
Cowhole Mountain	--	--
Cinder Cone	Wilshire and others, 1987	Adrian and others, 1986b
Marl Mountains	--	--
Old Dad Mountain	--	--
Kelso Mountains	--	--
Bristol Mountains	--	--
Clark Mountain Range	--	--
Mescal Range	--	--
Ivanpah Mountains	--	--
Cima Dome	--	--
New York Mountains	Miller and others, 1986	Adrian and others, 1986c
Mid Hills	--	--
Providence Mountains	Goldfarb and others, 1988	Folger and others, 1986
Do.	Miller and others, 1985	Detra and others, 1984
Granite Mountains	Howard and others, 1987	Detra and Kilburn, 1985
Do.	Yeend and others, 1984	--
Van Winkle Mountain	--	--
Groto Hills	--	--
Pinto Mountain	--	--
Table Mountain	--	--
Woods Mountains	--	--
Hackberry Mountain	--	--
Von trigger Hills	--	--
Piute Range	Nielson and others, 1987	Adrian and others, 1986a
Castle Mountains	--	--
Homer Mountain	--	--

Table 11. Analyses of select rock samples from some mineralized occurrences in the East Mojave National Scenic Area, Calif.

[Semiquantitative and quantitative optical spectroscopic analyses by inductively coupled plasma methods (Lichte and others, 1987; Motooka, 1988); analysts, D.L. Fey and J.M. Motooka; partial extraction of reported elements by selectively dissolving sulfides present in samples and analyzing contents of resulting solution. Looked for but not found, at detection levels shown in parentheses: Ho (4), Ta (40), and U (100). Precision for concentrations higher than 10 times detection limit is better than ±10 percent relative standard deviation; precision of scanning instrument is ±2 percent relative standard deviation. Chemical analyses are in parts per million except Au, which are in parts per billion: Au determined by combined graphite furnace and atomic-absorption spectroscopy; W determined colorimetrically; Hg determined by cold-vapor atomic-absorption; and As determined by hydride-generation atomic-absorption spectrometry (Wilson and others, 1987; Aruscavage and Crock, 1987); analysts, A.H. Love, E.P. Welsch, P.L. Hageman, and B.H. Roushey. --, not detected. See table 12 for sample locations and descriptions]

		Inductively coupled plasma atomic-emission spectroscopy (total)												
Analysis No.	Field No. 90TT	Ag	Ba	Be	Bi	Cd	Ce	Co	Cr	Cu	Eu	Ga	La	Li
1	015	99	28	<1	440	<2	8	7	12	30,100	<2	5	12	5
2	016	147	188	<1	1,140	<2	10	7	5	57,700	<2	<4	13	4
3	019	15	8	<1	70	7	<4	12	5	10,660	<2	6	4	11
4	020	3	13	1	50	3	<4	5	5	2,330	<2	9	7	11
5	027	9	7	2	20	3	6	58	118	13,500	<2	20	5	11
6	030	<2	4	<1	<10	4	4	227	1	151	<2	26	5	5
7	031	<2	3	<1	<10	<2	<4	2	<1	40	<2	<4	3	3
8	032	<2	347	3	<10	<2	117	1	<1	30	<2	15	56	3
9	035	<2	44	<1	<10	3	<4	126	5	224	<2	18	3	41
10	038	17	234	<1	220	<2	11	40	10	10,800	<2	4	7	6
11	040	<2	1,270	1	<10	<2	33	3	<1	16	<2	8	23	3
12	041	8	453	2	10	<2	13	4	4	637	<2	6	6	75
13	042	6	505	2	10	<2	34	5	3	1,510	<2	5	21	6
14	043	20	66	<1	70	<2	<4	1	<1	5,690	<2	<4	<2	5
15	045	6	356	<1	70	<2	34	9	10	464	<2	5	28	12
16	046	<2	673	2	<10	<2	88	3	<1	55	<2	14	58	2
17	047	<2	185	<1	<10	<2	<4	12	5	130	<2	<4	3	304
18	049	<2	338	3	<10	<2	120	1	<1	22	<2	14	57	3
19	050	<2	34	1	<10	<2	61	<1	<1	6	<2	14	33	<2
20	051	<2	262	1	40	<2	26	<1	<1	5	<2	9	16	3
21	052	<2	30	1	<10	<2	56	<1	<1	3	<2	14	33	2
22	053	<2	20	2	<10	<2	86	<1	<1	7	<2	15	50	2
23	054	<2	11	<1	<10	<2	24	<1	<1	2	<2	11	18	2
24	055	<2	494	1	10	<2	115	4	1	218	<2	13	66	3
25	056	6	220	1	30	<2	167	2	25	520	<2	17	78	6
26	058	<2	23	2	<10	2	99	<1	<1	15	<2	16	65	2
27	059	<2	371	3	<10	<2	152	<1	<1	6	<2	13	100	2
28	060	<2	27	2	<10	<2	115	<1	<1	23	<2	15	61	2
29	061	178	125	<1	<10	<2	11	<1	<1	411	<2	4	7	6
30	062	13	29	<1	<10	<2	<4	1	<1	2,120	<2	<4	<2	4
31	063	<2	485	2	<10	<2	137	2	<1	7	<2	14	76	4
32	065	<2	293	2	<10	<2	47	13	44	3	<2	12	28	18
33	066	150	101	<1	250	8	24	9	9	1,830	<2	6	14	12
34	067	<2	114	2	<10	<2	137	30	67	192	3	21	80	38
35	068	<2	690	2	<10	<2	101	13	28	62	2	19	55	27
36	069	25	54	<1	20	14	7	6	2	969	<2	<4	4	11
37	070	178	33	<1	140	3	6	<1	1	464	<2	5	4	22
38	071	103	29	<1	210	4	6	1	1	1,070	<2	6	4	19
39	072	4	86	1	<10	<2	44	12	20	65	<2	15	24	9
40	073	<2	757	2	<10	<2	132	<1	13	9	29	70	8	77
41	074	198	91	3	520	<2	13	23	73	96	2	<4	28	8
42	075	2	87	<1	<10	<2	42	4	<1	15	2	<4	18	34
43	076	<2	706	2	<10	<2	46	1	13	5	<2	37	28	13
44	077	<2	606	2	<10	<2	61	<1	13	6	<2	37	35	11
45	078	<2	445	1	<10	<2	49	<1	22	3	<2	24	26	5
46	079	<2	269	3	<10	<2	66	7	11	30	<2	14	57	39
47	080	9	46	1	<10	<2	<4	<1	<1	41	<2	<4	<2	88
48	081	4	65	2	<10	<2	14	1	2	101	<2	7	8	62
49	082	57	59	2	30	13	8	<1	<1	175	<2	7	5	68
50	083	385	282	<1	60	18	<4	<1	<1	2,560	<2	<4	<2	19
51	084	15	91	<1	<10	<2	<4	<1	<1	162	<2	<4	2	41
52	085	37	120	2	30	9	7	<1	1	289	<2	7	4	21
53	086	13	149	<1	<10	5	<4	<1	<1	99	<2	<4	<2	16
54	088	7	143	<1	20	4	5	1	1	632	<2	<4	3	9
55	089	7	115	2	140	<2	19	1	1	44	<2	16	10	8
56	090	<2	1,070	1	<10	2	8	2	<1	7	<2	5	9	3
57	091	<2	557	2	<10	<2	32	2	<1	5	<2	6	21	18
58	092	407	459	3	<10	85	<4	1	<1	4,690	<2	<4	3	112
59	093	7	393	6	200	<2	7	3	<1	20	<2	6	4	51
60	094	30	46	1	<10	<2	<4	<1	<1	98	<2	<4	<2	89

Table 11. Analyses of select rock samples from some mineralized occurrences in the East Mojave National Scenic Area, Calif.—Continued.

Inductively coupled plasma atomic-emission spectroscopy (total)

Analysis No.	Field No. 90TT	Ag	Ba	Be	Bi	Cd	Ce	Co	Cr	Cu	Eu	Ga	La	Li
61	096	593	63	<1	490	13	<4	3	1	12,800	<2	<4	<2	12
62	100	<2	320	1	<10	<2	61	15	49	45	<2	9	30	16
63	101	<2	617	2	<10	<2	38	12	55	10	<2	16	24	18
64	102	7	1,010	1	10	<2	44	19	63	6,990	<2	12	21	18
65	103	3	746	1	<10	<2	30	20	44	851	<2	11	17	17
66	104	23	69	<1	<10	<2	<4	2	6	30	<2	<4	2	2
67	105	<2	1,370	1	<10	4	52	3	3	17	<2	10	29	5
68	106	<2	945	2	<10	5	219	24	6	22	3	15	97	18
69	107	<2	312	<1	<10	<2	74	<1	4	6	<2	7	41	9
70	108	14	409	2	170	<2	96	17	9	11	<2	14	48	29
71	109	<2	896	<1	<10	<2	46	1	6	3	<2	14	24	8
72	110	189	50	<1	20	75	<4	5	1	3,840	<2	<4	2	3
73	113	109	42	<1	<10	182	4	3	1	4,570	<2	<4	4	4
74	115	<2	104	1	<10	<2	23	5	15	124	<2	25	18	17
75	118	424	1,620	<1	190	46	<4	140	9	1,640	<2	<4	<2	2
76	128	2	76	<1	<10	<2	14	10	13	31	<2	6	8	13
77	130	20	246	<1	<10	297	7	3	6	305	<2	6	7	5
78	131	55	388	<1	<10	1,790	5	<1	7	360	<2	13	5	5

Inductively coupled plasma atomic-emission spectroscopy (total)

Analysis No.	Field No. 90TT	Mn	Mo	Nb	Nd	Ni	Pb	Sc	Sn	Sr	Th	V	Y	Yb	Zn
1	015	2,220	<2	7	18	<2	49	<2	130	24	<4	47	20	1	141
2	016	1,490	2	11	13	<2	86	<2	40	20	<4	39	14	<1	117
3	019	2,970	<2	<4	11	<2	15	<2	10	32	<4	13	10	<1	1,540
4	020	4,890	6	<4	13	3	10	<2	430	32	<4	15	15	<1	792
5	027	5,130	<2	5	4	18	18	<2	40	16	8	42	7	<1	378
6	030	465	<2	<4	<4	165	13	<2	<10	54	5	168	<2	<1	82
7	031	506	<2	<4	9	<2	5	<2	<10	61	<4	<2	<2	<1	6
8	032	99	<2	39	47	<2	8	3	<10	119	20	5	51	6	14
9	035	327	<2	<4	<4	36	7	<2	<10	64	<4	41	<2	<1	44
10	038	802	4	<4	7	15	58	2	<10	62	<4	22	4	<1	54
11	040	57	<2	10	11	<2	10	<2	<10	135	37	3	8	2	3
12	041	28	12	<4	6	4	18,600	2	<10	94	<4	32	3	<1	13
13	042	46	<2	<4	17	<2	66	2	<10	15	9	23	6	<1	16
14	043	7	2	<4	<4	<2	28	<2	<10	<10	<4	<2	<2	<1	9
15	045	553	4	<4	16	4	425	4	<10	<10	<4	50	5	<1	14
16	046	54	<2	20	37	2	10	2	<10	<10	31	5	25	3	8
17	047	21	17	<4	<4	10	5	<2	<10	<10	<4	115	<2	<1	24
18	049	98	<2	42	48	<2	10	3	<10	<10	29	5	55	6	12
19	050	19	<2	20	22	<2	<4	<2	<10	<10	24	3	9	2	3
20	051	31	5	6	10	<2	13	<2	<10	<10	4	12	<2	<1	9
21	052	15	3	13	19	<2	<4	<2	<10	<10	6	3	3	<1	<2
22	053	12	<2	11	29	<2	<4	2	<10	<10	39	3	13	2	<2
23	054	7	<2	5	13	<2	<4	<2	<10	<10	20	3	5	1	2
24	055	9	16	<4	44	<2	21	4	<10	<10	17	23	<2	<1	7
25	056	55	<2	7	72	<2	15	13	<10	<10	6	138	4	<1	5
26	058	11	2	<4	36	<2	6	<2	<10	<10	14	6	8	1	4
27	059	23	16	8	56	<2	10	2	<10	<10	25	4	27	3	5
28	060	21	4	13	42	<2	<4	3	<10	<10	19	7	15	2	9
29	061	44	17	<4	5	<2	6,060	<2	<10	<10	<4	5	<2	<1	51
30	062	64	66	<4	<4	<2	2,670	<2	<10	<10	<4	<2	<2	<1	9
31	063	80	<2	10	49	2	11	4	<10	<10	24	19	19	3	9
32	065	385	<2	<4	17	19	21	4	<10	<10	22	21	6	<1	45
33	066	55	<2	<4	11	<2	3,070	5	<10	<10	<4	16	3	<1	1,180
34	067	2,460	<2	11	61	37	55	16	<10	<10	13	105	26	2	385
35	068	1,040	<2	12	48	11	32	16	<10	<10	15	52	33	3	175
36	069	14	<2	<4	<4	<2	6,100	<2	<10	<10	<4	<2	<2	<1	1,910
37	070	48	26	<4	4	<2	3,010	<2	<10	<10	<4	9	<2	<1	495
38	071	49	4	<4	<4	<2	1,960	<2	<10	<10	<4	9	<2	<1	1,220
39	072	72	<2	4	19	7	177	10	<10	<10	9	39	5	<1	70
40	073	77	22	<4	64	<2	19	10	<10	28	29	47	16	<1	13
41	074	1,080	14	<4	36	36	5,810	7	<10	125	<4	44	29	2	328
42	075	132	2	<4	31	2	29	<2	<10	33	<4	3	121	9	13
43	076	104	69	4	21	3	8	10	<10	41	8	94	4	<1	8
44	077	72	24	4	25	<2	4	11	<10	64	7	104	5	<1	7
45	078	65	49	<4	23	<2	<4	9	<10	24	9	60	4	<1	6
46	079	102	664	<4	14	18	56	7	<10	849	9	155	8	1	64
47	080	16	15	<4	<4	4	65	<2	<10	10	<4	9	<2	<1	55
48	081	48	27	<4	7	<2	136	2	<10	24	5	26	<2	<1	162
49	082	260	126	<4	5	<2	3,730	<2	<10	17	<4	280	<2	<1	136
50	083	14	11	<4	<4	<2	4,800	<2	<10	15	<4	119	<2	<1	428

Table 11. Analyses of select rock samples from some mineralized occurrences in the East Mojave National Scenic Area, Calif.—Continued.

		Inductively coupled plasma atomic-emission spectroscopy (total)													
Analysis No.	Field No. 90TT	Mn	Mo	Nb	Nd	Ni	Pb	Sc	Sn	Sr	Th	V	Y	Yb	Zn
51	084	18	5	<4	<4	<2	138	<2	<10	7	<4	11	<2	<1	15
52	085	455	7	<4	<4	<2	1,130	<2	<10	49	<4	52	<2	<1	232
53	086	4,820	<2	<4	<4	<2	324	<2	<10	14	<4	5	2	<1	232
54	088	2,620	<2	<4	<4	<2	60	<2	<10	19	<4	6	3	<1	284
55	089	23	12	<4	7	<2	178	<2	<10	39	<4	41	<2	<1	68
56	090	5,640	4	<4	20	<2	224	<2	<10	422	<4	20	36	3	26
57	091	3,480	2	<4	24	6	123	<2	<10	240	<4	16	24	2	18
58	092	57	112	<4	<4	<2	20,100	<2	<10	76	<4	760	4	<1	663
59	093	1,570	70	<4	<4	5	221	<2	<10	30	<4	11	5	<1	91
60	094	36	56	<4	<4	<2	539	<2	<10	9	<4	54	<2	<1	3,640
61	096	10	39	<4	<4	<2	12,500	<2	<10	196	<4	115	<2	<1	1,840
62	100	606	<2	<4	31	30	425	16	<10	303	<4	56	19	2	77
63	101	455	<2	<4	17	33	18	7	<10	660	<4	54	8	<1	48
64	102	471	<2	<4	19	34	119	7	<10	468	<4	65	10	1	60
65	103	721	<2	<4	13	26	215	4	<10	333	<4	58	6	<1	51
66	104	28	<2	<4	<4	4	271	<2	<10	<10	<4	17	<2	<1	9
67	105	144	<2	<4	24	3	130	4	<10	<10	11	13	17	2	73
68	106	2,650	6	<4	27	3	24	2	<10	<10	33	38	30	3	258
69	107	39	69	<4	27	3	24	2	<10	<10	21	8	5	<1	23
70	108	713	53	<4	51	10	120	6	<10	<10	9	44	26	2	116
71	109	29	8	<4	17	<2	29	3	<10	<10	45	11	3	<1	14
72	110	47	15	<4	<4	3	243,000	<2	20	<10	<4	4	<2	<1	9,940
73	113	878	<2	4	<4	<2	50,300	<2	<10	<10	<4	2	<2	<1	64,700
74	115	1,400	<2	<4	26	3	26	16	350	<10	9	109	22	3	85
75	118	46	33	<4	<4	<2	110	<2	<10	<10	5	4	<2	<1	6,840
76	128	153	<2	<4	7	23	76	2	<10	<10	<4	17	<2	<1	164
77	130	1,660	5	<4	9	2	19,400	<2	<10	<10	<4	7	4	<1	68,500
78	131	1,530	117	<4	6	3	39,000	<2	<10	<10	<4	9	<2	<1	257,000

		Inductively coupled plasma atomic-emission spectroscopy (partial)									Chemical Analyses			
Analysis No.	Field No. 90TT	Ag	As	Au	Bi	Cd	Cu	Mo	Pb	Sb	Zn	As	Hg	W	Au
1	015	87	--	--	360	--	25,000	--	72	--	28	16	0.38	--	450
2	016	130	--	--	920	--	45,000	--	88	46	15	7.8	0.14	--	400
3	019	14	46	--	73	7.7	10,000	--	14	7.9	1,300	37	0.04	2	50
4	020	2	52	--	51	3.1	2,400	1.3	--	--	720	39	--	--	26
5	027	0.86	--	--	--	0.8	7,300	--	--	--	--	31	0.04	2	24
6	030	--	22	--	--	--	170	--	1.1	--	1.6	26	--	--	<2
7	031	--	--	--	--	--	44.	--	--	--	1.6	2.1	--	--	150
8	032	--	--	--	--	--	28.	--	7.8	--	2.9	0.5	--	--	--
9	035	--	13	--	--	--	230	--	--	--	8.8	30	--	--	--
10	038	16	--	--	270	1.2	12,000	2.6	79	11	44	1.2	8.6	--	450
11	040	--	--	--	--	--	9.1	--	6.8	--	--	0.6	--	--	2
12	041	5.8	--	--	--	--	680	13	25,000	8.3	--	2.4	0.04	--	100
13	042	6.5	15	--	9.7	--	1,800	--	42	--	94	13	0.18	2	1,700
14	043	18	9.3	--	76	--	6,300	1.5	35	16	6.4	15	0.78	--	2,800
15	045	5.8	--	22	74	--	510	4.1	490	--	7.5	8	0.1	2	25,000
16	046	--	--	--	--	--	51	2	6	--	1.4	0.3	--	--	--
17	047	--	--	--	--	--	140	18	6.6	--	22	1.6	0.02	15	4
18	049	--	--	--	--	--	21	--	--	--	3.4	0.5	--	--	--
19	050	--	--	--	--	--	0.74	--	--	--	--	0.2	--	--	--
20	051	--	--	--	41	--	--	4.2	--	--	--	0.4	--	2	28
21	052	--	--	--	--	--	--	2.2	--	--	--	0.2	--	1	2
22	053	--	--	--	--	--	5.3	--	--	--	--	0.5	--	--	2
23	054	--	--	--	--	--	--	--	--	--	--	<0..2	--	--	--
24	055	--	--	--	6.4	--	210	15	7.8	--	--	1.8	0.04	--	4
25	056	6.7	--	--	--	--	510	1.2	--	--	--	0.8	0.16	7	6
26	058	--	--	--	--	--	8.8	1.6	--	--	--	<0.2	--	--	--
27	059	--	--	--	--	--	2.5	18	--	--	--	0.2	--	--	--
28	060	--	--	--	--	--	18.	3.4	--	--	--	0.3	--	--	--
29	061	200	--	1.7	--	1.9	490	18	8,100	--	40	1.5	0.28	--	3,600
30	062	10	--	--	--	0.81	2,300	58	3,300	--	4	<0.2	0.02	--	500

Table 11. Analyses of select rock samples from some mineralized occurrences in the East Mojave National Scenic Area, Calif.—Continued.

		Inductively coupled plasma atomic-emission spectroscopy (partial)										Chemical Analyses			
Analysis No.	Field No. 90TT	Ag	As	Au	Bi	Cd	Cu	Mo	Pb	Sb	Zn	As	Hg	W	Au
31	063	--	--	--	--	--	0.92	--	11	--	5.6	0.7	--	--	--
32	065	--	--	--	--	--	--	1.7	22	--	41	1.1	--	--	2
33	066	190	--	5.6	290	9.7	2,100	--	4,400	--	1,000	14	0.34	--	7,600
34	067	--	--	--	--	1.6	210	--	41	--	390	2.5	--	1	6
35	068	--	--	--	--	--	73	--	20	--	180	0.6	--	2	--
36	069	26	--	--	18	17	1,100	--	8,100	--	1,800	3.2	0.08	--	450
37	070	210	--	7.1	160	3	540	29	4,100	--	370	5.2	0.28	--	5,100
38	071	110	11	2.3	240	5.2	1,200	3.7	2,600	--	1,200	13	0.32	--	3,150
39	072	4.4	--	--	--	--	72	1.4	240	--	31	4.1	0.02	--	100
40	073	--	--	--	--	--	0.38	24	12	--	6.3	4	0.02	4	2
41	074	250	68	--	620	0.78	110	16	9,600	--	300	50	0.06	3	45
42	075	0.55	6.7	--	--	--	13	2.7	21	--	6.8	6.6	0.02	--	800
43	076	--	--	--	--	--	2.8	66	--	--	--	0.4	--	4	--
44	077	--	--	--	--	--	1.4	19	--	--	--	0.5	--	4	--
45	078	--	--	--	--	--	--	53	--	--	--	0.5	--	3	--
46	079	--	22	--	--	--	32	730	63	--	70	23	0.02	4	6
47	080	2.4	96	--	--	--	37	13	83	--	52	78	0.36	--	300
48	081	2.4	140	--	--	--	110	30	180	14	160	100	0.32	4	150
49	082	71	260	--	42	11	190	160	5,500	760	120	260	9	38	50
50	083	520	360	--	260	23	3,000	11	7,100	1,800	440	270	17.1	12	1,450
51	084	12	--	--	--	1	160	4.5	160	160	8.9	13	1.2	3	4
52	085	42	150	--	22	5.1	340	8.7	1,500	790	240	190	10.5	56	100
53	086	12	77	--	--	1.1	110	2.7	430	220	46	86	1	1,700	30
54	088	5.7	68		13	3.4	710	2	90	190	310	66	3.9	1,080	4
55	089	2.1	27	--	130	--	44	8.8	220	110	65	26	1.2	13	12
56	090	--	--	--	--	2.7	4.7	3.6	310	--	23	9.9	0.12	67	2
57	091	--	--	--	--	1.5	3.8	2.5	170	--	14	8.7	0.02	85	4
58	092	500	760	1.9	41	96	5,400	180	29,000	4,700	530	490	>34	9	4,150
59	093	12	--	--	210	0.32	18	75	380	14	81	6.4	0.28	28	54
60	094	28	--	--	--	--	110	51	670	20	3,600	7.1	0.26	8	50
61	096	620	--	--	500	14	12,000	28	16,000	320	1,200	51	19.2	8	800
62	100	0.62	150	--	--	--	33	--	660	--	87	110	0.04	--	2
63	101	--	--	--	--	--	5.4	--	10	--	51	2	0.04	--	--
64	102	2.1	--	--	8.8	0.35	8,500	--	190	--	64	5.4	0.08	1	4,050
65	103	--	9.2	--	--	--	1,000	--	330	--	54	18	--	--	300
66	104	12	--	13	--	--	29	1	240	--	4.7	9.2	0.08	2	7,300
67	105	--	--	--	--	5.1	16	--	140	--	66	2.1	0.08	--	10
68	106	--	23	--	--	7.4	23	7.5	72	--	180	23	0.1	1	--
69	107	--	--	--	--	--	3.4	75	6.5	--	16	2	0.02	1	--
70	108	15	25	2.8	200	0.35	9.3	53	170	--	110	28	0.12	3	5,800
71	109	--	--	--	--	--	--	8.9	--	--	5.1	2.7	0.14	1	--
72	110	130	430	--	--	75	1,800	--	9,300	30	--	35,000	0.58	2	42
73	113	4.9	5,000	--	--	230	480	--	290	240	56	57,000	0.34	2	8
74	115	--	140	--	--	--	130	2.6	150	--	140	31	--	6	--
75	118	540	18	--	230	65	2,000	33	270	--	6,500	570	0.2	3	150
76	128	--	--	--	--	--	36	--	120	--	180	14	--	2	--
77	130	20	10	--	--	430	350	5.6	32,000	67	15,000	43	>34	1	20
78	131	57	10	--	--	2,400	390	110	53,000	240	110,000	61	>34	1	22

Table 12. Descriptions and locations of select rock samples collected from some mineralized occurrences in the East Mojave National Scenic Area, Calif.

[Mineral abbreviations: Gar, garnet; diop, diopside; trem, tremolite; mal, malachite; py, pyrite; px, pyroxene; hfs, hornfels; sph, sphalerite; qtz, quartz; cp, chalcopyrite; mag, magnetite; gn, galena; hb, hornblende; hm, hematite; cc, calcite; bx, breccia; cov, covellite; chrys, chrysocolla; bio, biotite; chl, chlorite; wm, white mica; pg, plagioclase; stib, stibiconite; wolf, wolframite; fl, fluorite; epi, epidote; fs, feldspar; kfs, K–feldspar; asp, arsenopyrite; zois, zoisite. See table 11 for analyses]

Analysis No.	Field No. (90TT...)	Location	Latitude	Longitude	Description
1	015	Evening Star Mine	35 21'39"	115 32'32"	Massive diop skarn retrograded to trem; two generations diop; mal and iron oxides after py.
2	016	do.	do.	do.	Do.
3	019	do.	do.	do.	Px hfs developed in sulfidized marble.
4	020	do.	do.	do.	Calc-silicate hfs, trem, and sph; replacement of marble.
5	027	Copper King Mine	35 21'06"	115 32'38"	Cp–mag skarn; includes retrograde chl and zois.
6	030	Vulcan Mine	34 55'23.91"	115 33'54.75"	Py–bearing, mag skarn.
7	031	do.	do.	do.	Marble; less than 0.5 m from skarn front.
8	032	do.	do.	do.	Py–bearing mag skarn.
9	035	do.	do.	do.	Mag skarn.
10	038	Big Horn Mine	34 50'28.7"	115 32'24.76"	Qtz–cp–py vein; late stage cc fills fractures.
11	040	do.	34 50'32.10"	115 32'23.47"	Rhyolite bx.
12	041	do.	do.	do.	Qtz–gn–cp veins; multiple qtz generations.
13	042	do.	34 48'28.66"	115 32'42.36"	Qtz–cp±hm veins; comb qtz, open-cavity fillings.
14	043	do.	34 48'32.5"	115 32'55.21"	Qtz–cp–base metal veins.
15	045	do.	34 48'41.71"	115 32'50.74"	Qtz–py (trace)–cc along fault; sparse wm.
16	046	Vic. Quail Spring Wash	34 49'46.92"	115 33'40.97"	
17	047	do.	34 49'55.33"	115 33'40.44"	Qtz–py veins associated with syenogranite of Quail Spring (Jqs, plate 1) (Miller and others, 1985).
18	049	do.	34 50'2.77"	115 33'31.91"	Syenogranite of Quail Spring (Jqs, plate 1).
19	050	do.	34 49'59.83"	115 33'24.36"	Do.
20	051	do.	34 49'50.09"	115 33'17.02"	Qtz–py vein; brick-red associated iron oxide(s).
21	052	do.	34 49'40.45"	115 33'19.18"	Py along east-west fractures in syenogranite of Quail Spring (Jqs, plate 1).
22	053	do.	54 49'38.12"	115 33'26.16"	Clay-altered syenogranite of Quail Spring (Jqs, plate 1).
23	054	do.	34 49'38.71"	115 33'30.97"	Syenogranite of Quail Spring (Jqs, plate 1).
24	055	do.	34 48'59.95"	115 33'11.59"	Fault bx; abundant gossan.
25	056	do.	do.	do.	Iron-oxide-stained metavolcanic rock.
26	058	do.	34 49'40.48"	115 33'54.7"	Porphyritic felsite dike.
27	059	do.	do.	do.	Hb–bio monzodiorite.
28	060	do.	do.	do.	Do.
29	061	Okaw Mine	35 2'45.22"	115 33'12.74"	Qtz–gn–cp–py vein; secondary cov.
30	062	do.	35 2'41.61"	115 33'5.21"	Qtz–gn–cp vein; secondary chrys.
31	063	do.	35 2'42.48"	115 33'1.13"	Porphyritic leucogranite dike; primary bio altered to chl; sparse wm alteration of pg.
32	065	Globe Canyon	35 3'6.75"	115 31'00"	Fault bx and gossan.
33	066	South Star Mine	35 3'5.42"	115 29'33.69"	Qtz–py vein; includes some wm.
34	067	do.	do.	do.	Qtz–cc veined and chl-altered dacite(?) dike.
35	068	do.	do.	do.	Qtz–py vein.
36	069	do.	35 3'6.65"	115 29'31.44"	Qtz–py–sph veins; brecciated, multiple generations of qtz.
37	070	S.S. nos. 17–19 , north	35 3'6.78"	115 29'46.97"	Fault bx; silicified.
38	071	do.	do.	do.	Gossan; along fault bx.
39	072	South Star Mine	35 3'12.89"	115 29'33.7"	Qtz vein; py-impregnated; abundant brick-red granitoid fragments.
40	073	SS. no.17	35 2'58.16"	115 29'55.04"	Qtz vein; massive outcrop; sericitically altered granitoid fragments.
41	074	Globe Mine	35 2'39.9"	115 29'8.23"	Gossan; reddish orange brown.
42	075	do.	do.	do.	Qtz–fl–py vein; abundant gossan.
43	076	S.S. no. 17	35 2'58.16"	115 29'55.04"	Qtz–wm–altered bio granite.
44	077	do.	do.	do.	Do.
45	078	do.	do.	do.	Ditto; heavily qtz veined and iron oxide stained.
46	079	do.	do.	do.	Gossan; brick red to brownish maroon.
47	080	Tungsten Flat	35 3'23.46"	115 2'50.74"	Qtz–py vein; moderate amounts fine-grained wm.
48	081	do.	do.	do.	Gossan; ochre.
49	082	do.	35 3'8.76"	115 2'50.41"	Qtz–py–stib (trace)-gn vein.
50	083	do.	35 3'8.76"	115 2'45.32"	Ditto; includes some secondary chrys.
51	084	do.	35 3'8.96"	115 2'37.23"	Qtz–py veins.
52	085	do.	35 2'53.85"	115 2'44.68"	Do.
53	086	do.	35 2'55.76"	115 2'49.63"	Qtz–wolf–gn (trace)–stib (trace)–py vein.
54	088	do.	35 2'47.19"	115 2'48.08"	Do.
55	089	do.	35 2'42.33"	115 2'31.1"	Qtz–py vein.
56	090	do.	35 2'30.43"	115 2'40.8"	Manganiferous cc vein; coarsely crystalline; streaked with iron oxide.
57	091	do.	do.	do.	Qtz–manganiferous cc vein.
58	092	do.	35 2'11.66"	115 2'47.39"	Qtz–chrys–gn–stib vein; coarsely
59	093	do.	35 2'7.33"	115 2'54.81"	Gossan; reddish brown.
60	094	do.	35 2'10.23"	115 2'55.87"	Qtz–sph vein; multiple generations qtz.
61	096	Leiser Ray Mine	35 1'33.22"	115 2'13.67"	Qtz–cp–gn–sph vein bx; multiple generations qtz.
62	100	True Blue Mine	35 5'2.04"	115 9'6.47"	Qtz vein; cuts chloritized gneissic granite; wm and epi alteration.
63	101	do.	do.	do.	Chloritized gneissic granite; relict bio; phyllonitic, strained fs porphyroclasts.
64	102	do.	35 4'54.14"	115 8'57.37"	Qtz–chrys veins; open-cavity fillings.
65	103	do.	do.	do.	Qtz–py–cp (trace) vein; some secondary Mn–bearing minerals.

Table 12. Descriptions and locations of select rock sample collected from some mineralized occurrences in the East Mojave National Scenic Area, Calif.—Continued.

Analysis No.	Field No. (90TT...)	Location	Latitude	Longitude	Description
66	104	American Flag	35 4'35.89"	115 7'27.84"	Qtz–py–gn (trace) vein.
67	105	Rattlesnake Mine	35 6'7.72"	115 4'48.12"	Qtz–kfs±iron oxide (trace) vein; locally mylonitic fabric.
68	106	do.	35 5'50.12"	115 4'51.82"	Gossan; ochre to maroon; narrow seams in granite.
69	107	do.	35 5'40.93"	115 5'0.37"	Silicified fault zone.
70	108	do.	35 5'43.83"	115 5'7.71"	Qtz–py vein.
71	109	do.	35 5'39.74"	115 4'55.97"	Silicified granite; clay altered.
72	110	Mohawk Mine	35 28'43"	115 37'01"	Sulfidized (gn, asp, sph) shear zone; oxidized; some vein qtz.
73	113	do.	do.	do.	Oxidized gn, asp, and sph in vein qtz; some cp and py.
74	115	do.	do.	do.	Gar–px skarn; late stage wm and qtz.
75	118	Copper World Mine	35 30'20.49"	115 36'9.78"	Gossan.
76	128	Conquistador No. 2	35 31'23.8"	115 38'34.02"	Qtz–py (altered to buff-colored vein oxide) vein; chl- and wm-altered fragments
77	130	Emperor Mine	35 31'26.25"	115 37'51.45"	Gn–sph–cc along fault zone.
78	131	do.	do.	do.	Do.

Table 13. Geochemical statistics for analyses of selected elements in stream-sediment, heavy-mineral concentrate, rock, and soil samples from the East Mojave National Scenic Area and surrounding area, Calif. and Nev.

[Minimum, maximum, 50th (equal to 50th percentile; at least one-half of samples have concentrations equal to or less than value shown), 90th (equal to 90th percentile; at least 90 percent of samples have concentrations equal to or less than value shown), and threshold concentrations, as well as lower and upper limits of determination, are in parts per million (ppm). Concentrations in Rock Analysis Storage System (RASS) and PLUTO samples determined by emission-spectrographic methods; in National Uranium Resource Evaluation (NURE) samples, by neutron activation. Threshold (defined as highest background) concentrations for this study determined by visual and statistical examination of data, by observation of elemental concentrations near known mineralized areas, and by references to Goldfarb and others (1988) and Miller and others (1985); for PM (Providence Mountains Wilderness Study Area), determined by Goldfarb and others (1988, table 3); for SPM (South Providence Mountains Wilderness Study Area), determined by Miller and others (1985, tables 1, 2). Abbreviations: G, greater than upper limit of determination; L, detected below lower limit of determination; N, not detected at lower limit of determination; <, less than value shown; <<, threshold concentration is less than lower limit of determination (any concentration is anomalous); >, greater than value shown; --, unknown for lower or upper limits of determination, no data for PM and SPM. See table 14 for summary of geochemical anomalies]

	Limits of determination		Concentrations				Threshold concentrations			Number of analyzed samples	Number of anomalous samples
	Lower	Upper	Minimum	Maximum	50th	90th	This study	PM	SPM		
				RASS and PLUTO stream-sediment samples[1, 2] (locations plotted in figure 50, data plotted in figures 54, 59, 62)							
Ag	0.5-1	5,000	N	>20	<0.5	0.5	0.7	--	<0.5	368	22
B	5-10	2,000	N	>100	10	50	50	--	--	368	16
Ba	20	5,000	70	5,000	700	1,000	1,500	--	--	368	11
Be	1-5	1,000	N	15	2	5	5	--	--	368	7
Co	1-5	2,000	L	100	10	30	30	--	--	368	30
Cu	2-5	20,000	<5	1,200	20	70	70	--	100	368	18
Mn	50	5,000	<50	7,000	700	2,000	2,000	--	--	368	17
Mo	1-5	2,000	N	100	3	15	10	--	--	368	54
Pb	5-10	20,000	N	5,000	20	70	70	--	--	368	22
Sn	2-10	1,000	N	30	<5	<5	<10	--	--	368	15
W	20-100	10,000	N	70	<50	<50	<50	--	--	368	5
Zn	5-200	10,000	N	7,000	50	150	N(200) or 100[5]	--	--	367	78
				RASS nonmagnetic heavy-mineral-concentrate samples[1] (locations plotted in figure 51; data plotted in figures 55, 57, 60, 63, 65)							
Ag	1	10,000	N	1,000	N	3	3	L	3	498	69
As	500	20,000	N	3,000	N	N	N	N	--	498	3
Au	20	1,000	N	G	N	N	N	N	N	498	11
B	20	5,000	N	700	20	50	70	--	--	498	23
Ba	50	10,000	N	G	1,000	G	5,000	7,000	3,000	498	102
Be	2	2,000	N	200	L	3	3	--	--	498	28
Bi	20	2,000	N	G	N	N	N	N	30	498	34
Co	10-20	5,000	N	300	N	10	15	--	--	498	39
Cu	10	50,000	N	10,000	N	70	70	30	70	498	39
La	50-100	2,000	N	G	300	1,000	1,500	--	--	498	15
Mn	20	10,000	N	10,000	500	1,000	1,000	--	--	498	45
Mo	10	5,000	N	5,000	N	30	10	150	N	498	77
Nb	50	5,000	N	700	L	100	150	--	--	498	19
Pb	20	50,000	N	G	70	3,000	700	1,500	100	498	92
Sb	200	20,000	N	3,000	N	N	N	N	--	498	9
Sn	20	2,000	N	2,000	N	100	30	--	--	498	87
Th	200	5,000	N	G	L	1,500	2,000	--	--	480	26
W	50-100	20,000	N	10,000	N	500	300	--	--	498	83
Zn	500	20,000	N	G	N	N	N	N	--	498	19
				PLUTO heavy-mineral-concentrate samples[3] (locations plotted in figure 51; data plotted in figures 55, 57, 60, 63, 65)							
Ag	1	--	<1	70	<1	2	1.5	--	--	262	58
Au	20	--	<10	20	<10	<10	10	--	--	262	3
B	20	--	<10	>200	50	100	100	--	--	262	18
Ba	2	--	100	>10,000	700	1,500	1,500	--	--	262	25
Be	1	--	<2	70	3	7	7	--	--	262	15
Bi	10	--	<20	200	<20	<20	<<	--	--	262	22
Co	5	--	3	200	50	100	70	--	--	262	33
Cu	1	--	3	7,000	70	200	100	--	--	262	51
La	20	--	20	>2,000	500	>2,000	1,500	--	--	262	39
Mn	2	--	200	>20,000	3,000	10,000	10,000	--	--	262	21
Mo	5	--	<2	300	15	50	20	--	--	262	63
Nb	10	--	5	3,000	150	500	700	--	--	262	9
Pb	10	--	<5	2,000	70	300	300	--	--	262	17
Sn	10	--	<5	>10,000	10	30	20	--	--	262	39
Th	200	--	<500	3,000	<500	500	500	--	--	262	19
W	100	--	<100	2,000	<100	<100	<<	--	--	262	9
Zn	200	--	30	5,000	200	700	300	--	--	262	53

Table 13. Geochemical statistics for analyses of selected elements in stream-sediment, heavy-mineral-concentrate, rock, and soil samples from the East Mojave National Scenic Area and surrounding area, Calif. and Nev.—Continued.

	Limits of determination		Concentrations				Threshold concentrations			Number of analyzed samples	Number of anomalous samples
	Lower	Upper	Minimum	Maximum	50th	90th	This study	PM	SPM		
				PLUTO heavy-mineral-concentrate samples[1] (locations plotted in figure 51; data plotted in figures 68, 71)							
Ce	200[3]	--	<200	10,000	700	3,000	3,000	--	--	262	29
Dy	50[3]	--	<20	1,000	<20	<20	<<	--	--	262	20
Eu	2-15[4]	--	<2	100	10	30	30	--	--	262	10
Nd	100[3]	--	<100	>2,000	300	1,000	1,000	--	--	262	26
Sm	100[3]	--	<100	1,000	100	200	200	--	--	262	21
Tb	50[4]	--	<50	300	<50	50	<50	--	--	262	35
Yb	5[3]	--	1.5	700	30	100	100	--	--	262	21
				RASS and PLUTO rock samples[1, 2] (locations plotted in figure 52, data plotted in figures 56, 58, 61, 64, 66)							
Ag	0.5-1	5,000	N	1,000	<0.5	15	<0.5	--	--	943	249
As	100-500	10,000	N	G	<700	<200	<<	--	--	943	249
Au	5-10	500	N	150	<15	<5	<<	--	--	943	21
B	2-10	2,000	N	500	<10	30	20	--	--	937	111
Ba	2-30	5,000	N	G	300	1,500	1,500	--	--	943	80
Be	1-5	1,000	N	150	1	3	5	--	--	944	30
Bi	10-20	1,000	N	300	<10	<10	<<	--	--	944	107
Co	0.5-10	2,000	N	1,000	5	30	30	--	--	944	85
Cu	0.2-5	20,000	N	G	15	700	100	--	--	944	203
La	5-30	1,000	N	1,000	30	100	150	--	--	944	29
Mn	10	5,000	N	G	300	1,500	2,000	--	--	943	53
Mo	1-10	2,000	N	2,000	<5	10	7	--	--	942	125
Nb	5-20	2,000	N	100	<20	20	30	--	--	944	11
Pb	3-10	20,000	N	G	20	300	50	--	--	944	233
Sb	20-100	10,000	N	7,000	<100	<20	<<	--	--	944	27
Sn	5-10	1,000	N	G	<10	<5	<<	--	--	933	34
Th	100-500	2,000	N	300	<200	<300	<<	--	--	944	3
W	20-100	10,000	N	5,000	<50	<50	<<	--	--	944	46
Zn	5-200	10,000	N	G	500	500	N(200) or 100[5]	--	--	944	176
				PLUTO rock samples[1] (locations plotted in figure 52; data plotted in figures 69, 72)							
Ce	200[3]	--	<20	300	70	100	150	--	--	155	8
Dy	50[3]	--	<10	20	<10	<20	<<	--	--	155	11
Eu	1-2[4]	--	<1	5	2	3	3	--	--	155	9
Nd	100[3]	--	<50	150	<100	70	70	--	--	155	14
Tb	20-50[4]	--	<20	30	<20	<50	<<	--	--	155	10
Yb	53	--	<0.5	10	1	3	3	--	--	155	6
				NURE stream-sediment and soil samples[1, 4] (locations plotted in figure 53; data plotted in figures 67, 70, 73)							
Ce	10-20	--	<10	930	70	140	169	--	--	1,136	61
Dy	0.1-3.8	--	<1	45	2.7	7.7	7.9	--	--	911	85
Eu	0.1-3	--	<0.1	7.6	0.6	2.1	1.6	--	--	1,009	169
La	1-20	--	<1	1,900	36	77	169	--	--	1,157	108
Lu	0.1-0.6	--	<0.1	7.8	0.4	0.86	1.1	--	--	804	34
Sm	1-2	--	<1	130	6	12	16	--	--	963	48
Tb	--	--	0.13	2.3	0.9	1.8	1.6	--	--	28	3
Th	2	--	<2	320	13	24	39	--	--	1,153	67
U	--	--	0.10	30	2.4	3.9	5.9	--	--	1,259	42
Yb	1-2	--	<1	55	1.8	4.6	5.9	--	--	942	52

[1]Lower limits of determination are variable.
[2]Upper limits of determination for RASS samples are customary values.
[3]Lower limits of determination are from Myers and others (1961, table 2).
[4]Lower limits of determination are from the data.
[5]Lower limits of determination for Zn: RASS, 200 ppm; PLUTO, 5 ppm. Any detectable concentration in RASS samples and concentrations greater than 100 ppm in PLUTO samples are anomalous.

Table 14. Summary of geochemical anomalies in the East Mojave National Scenic Area, Calif.

[Geochemical anomalies are shown using the following notation: for each element, values indicate number of samples analyzed/number of samples having high concentrations/number of samples having anomalous concentrations; na, no samples have high concentrations because any detectable concentration is considered anomalous; NS, no samples analyzed; NAH, concentrations of considered elements (see table 13) are neither anomalous nor high (the number of samples are in parentheses). Determination of whether or not area is geochemically anomalous with respect to a given element is based on (1) presence and proportion of samples having anomalous concentrations, (2) presence and proportion of samples having high but not necessarily anomalous concentrations, and (3) comparison of area with entire East Mojave National Scenic Area and its surrounding areas; see figure 49 for location of geographic areas. The absence of any notation for a specific sample type from an area means that samples of that type exist for the area but that none of the considered elements is present in either high or anomalous concentrations in those samples. Analyses of Rock Analyses Storage System (RASS) and and PLUTO samples determined by emission-spectrographic methods; of National Uranium Resource Evaluation (NURE) samples, by neutron activation; see table 13 for complete listing of geochemical statistics]

RASS and PLUTO Stream-sediment samples	RASS Heavy-mineral-concentrate samples	PLUTO Heavy-mineral-concentrate samples	RASS and PLUTO Rock samples	NURE Stream-sediment and soil samples
		Soda Mountains		
B 8/0/1	NS	Ag 8/4/4	NS	Eu 4/0/2
Mo 8/0/1		Au 8/na/1		
Sn 8/01/1		B 8/01/1		
Zn 8/1/1		Ba 8/0/1		
		Be 8/0/2		
		Bi 8/na/1		
		Co 8/0/1		
		Cu 8/1/2		
		Mn 8/2/1		
		Mo 8/1/2		
		Nb 8/0/1		
		Pb 8/3/1		
		Sn 8/3/2		
		Th 8/1/1		
		Zn 8/0/3		
		Ce 8/0/1		
		Dy 8/na/2		
		La 8/0/1		
		Tb 8/0/2		
		Yb 8/2/1		
		Little Cowhole Mountain		
NAH (2)	NS	Be 2/1/1	NS	NAH (0-4)
		Bi 2/na/1		
		Cu 2/1/1		
		Mo 2/0/1		
		Sn 2/0/1		
		Th 2/0/1		
		Tb 2/0/1		
		Cowhole Mountain		
NAH (1)	NS	NS	NS	NAH (0-1)
		Cinder Cone Area		
Co 17/0/1	Be 28/1/1	Ag 17/4/4	Ag 18/1/9	Th 26/0/1
Mo 17/3/6	Co 28/2/6	Be 17/6/1	As 18/na/1	Ce 25/0/1
Zn 17/3/2	Mn 28/4/2	Bi 17/na/4	B 18/1/2	Eu 15/1/1
	Nb 28/4/2	Cu 17/3/1	Bi 18/na/4	
	Sn 28/0/4	Mn 17/1/1	Cu 18/2/7	
	Th 28/4/9	Mo 17/3/4	Mn 18/0/2	
		Sn 17/5/3	Mo 17/2/2	
		Tb 17/10/4	Pb 18/3/9	
		Th 17/2/2	Sb 18/na/1	
		Yb 17/3/1	W 18/na/3	
		Zn 17/2/1	Zn 18/0/5	

RASS and PLUTO Stream-sediment samples	RASS Heavy-mineral-concentrate samples	PLUTO Heavy-mineral-concentrate samples	RASS and PLUTO Rock samples	NURE Stream-sediment and soil samples
		Marl Mountains		
Ag 5/0/1 Mo 5/0/1 Pb 5/0/1 Zn 5/0/1	NS	Ag 5/1/1 Au 5/na/1 Bi 5/na/1 Ce 5/1/1 Cu 5/0/1 Dy 5/na/1 La 5/0/2 Mo 5/0/1 Nd 5/0/1 Sm 5/0/1 Tb 5/0/1 Th 5/0/1 Yb 5/0/1 Zn 5/0/1	NS	Dy 10/1/1 Th 10/0/1
		Old Dad Mountain		
NAH (6)	Ag 3/0/2 Bi 3/na/1 Cu 3/0/1 Nb 3/0/1 Pb 3/0/2 Sn 3/1/2	Tb 6/0/1 Th 6/0/1	Ag 6/0/1 Au 6/na/1 B 6/0/1 Be 6/0/1 Bi 6/na/1 Co 6/0/1 Cu 6/0/1 Mo 6/1/1 Pb 6/1/1 Zn 6/0/1	NAH (0-22)
		Kelso Mountains		
NAH (4)	NS	Ag 4/2/1 Au 4/na/1 Ce 4/0/1 Cu 4/0/1 Dy 4/na/1 La 4/0/1 Sn 4/3/0 Nd 4/1/1 Sm 4/0/1 Tb 4/0/1 W 4/na/1	NS	Dy 9/1/1 Eu 7/0/1
		Bristol Mountains		
B 9/0/1 Mn 9/0/2 Mo 9/1/3 Pb 9/2/1 Sn 9/0/2 Zn 9/1/2	NS	Ag 8/3/1 Be 8/4/0 Cu 8/2/3 Dy 8/na/1 Eu 8/2/3 La 8/4/0 Mn 8/4/2 Mo 8/2/4 Nb 8/1/1 Nd 8/3/1 Sm 8/4/2 Sn 8/3/4 Yb 8/4/2 Zn 8/2/4	NS	Eu 6/0/1
		Clark Mountain Range		
Ag 25/8/8 Be 25/1/1 Pb 25/3/3 Zn 25/4/1	Ag 15/0/8 As 15/na/2 B 15/0/14 Ba 15/5/2 Be 15/6/9 Bi 15/na/2 Cu 15/0/7 La 15/4/5 Mo 15/3/5 Nb 15/0/1 Pb 15/0/6 Sb 15/na/5 Sn 15/4/4 W 15/3/9 Zn 15/na/3	Ag 10/1/3 Ba 10/0/2 Be 10/1/2 Ce 10/1/2 Co 10/0/1 Cu 10/4/2 Eu 10/0/1 La 10/0/2 Nd 10/1/2 Pb 10/1/1 Tb 10/0/1 Th 10/0/1 W 10/na/1	Ag 3/0/2 Sn 3/0/1	Ce 19/2/2 Dy 20/1/4 Eu 11/1/2 La 24/0/2 Lu 14/2/2 Sm 13/1/2 Th 21/1/2 Yb 14/3/1

Table 14. Summary of geochemical anomalies in the East Mojave National Scenic Area, Calif.—Continued.

RASS and PLUTO Stream-sediment samples	RASS Heavy-mineral-concentrate samples	PLUTO Heavy-mineral-concentrate samples	RASS and PLUTO Rock samples	NURE Stream-sediment and soil samples
		Mescal Range		
NAH (3)	NS	Pb 3/0/1	NS	NAH (0-10)
		Tb 3/0/1		
		Zn 3/0/1		
		Ivanpah Mountains		
Ag 26/2/1	Ag 15/0/1	Ag 8/3/1	Ag 26/1/12	Ce 19/1/1
Cu 26/5/5	Au 15/na/1	Be 8/2/1	As 26/na/4	Dy 20/3/5
Mo 26/2/1	Bi 15/na/5	Bi 8/na/1	B 26/2/8	Eu 12/3/2
Sn 26/0/7	Co 15/0/11	Ce 8/3/2	Be 26/2/4	La 20/0/1
W 26/na/3	Cu 15/12/3	Co 8/2/1	Bi 26/na/10	Lu 13/4/3
Zn 26/4/19	Mn 15/6/8	Cu 8/2/2	Co 26/3/7	Sm 15/0/1
	Mo 15/0/12	Dy 8/na/2	Cu 26/3/12	Tb 1/0/1
	Pb 15/2/7	La 8/2/2	Mn 26/3/13	Yb 15/3/1
	Sb 15/na/1	Mn 8/1/1	Mo 26/0/4	
	Sn 15/0/14	Mo 8/1/1	Pb 26/4/3	
	Th 15/1/10	Nd 8/3/1	Sn 26/1/16	
	W 15/2/10	Pb 8/3/1	W 26/na/16	
		Sm 8/4/1	Zn 26/0/23	
		Tb 8/0/1		
		Th 8/0/1		
		W 8/na/1		
		Cima Dome		
NS	NS	NS	Tb 1/0/1	NS
		New York Mountains		
Ag 18/1/1	Ba 59/4/4	Ag 18/6/4	Ag 35/1/8	Ce 25/6/3
B 18/0/1	La 59/0/4	B 18/2/4	As 35/na/3	Dy 24/7/4
Be 18/1/3	Pb 59/1/1	Ba 18/0/3	Au 35/na/3	Eu 19/1/1
Co 18/3/1	W 59/6/4	Be 18/3/3	B 35/0/2	Lu 14/1/2
Cu 18/1/2		Bi 18/na/5	Ba 35/5/1	Th 26/2/2
Mn 18/2/1		Ce 18/2/4	Bi 35/na/4	Yb 15/1/2
Mo 18/3/1		Co 18/2/2	Co 35/1/1	
Pb 18/1/1		Cu 18/9/6	Cu 35/3/10	
W 18/na/1		Dy 18/na/2	La 35/4/2	
Zn 18/3/7		Eu 18/3/2	Mo 35/2/3	
		La 18/0/7	Pb 35/6/9	
		Mn 18/6/1	Sb 35/na/2	
		Mo 18/1/6	Zn 35/0/8	
		Nd 18/3/5		
		Pb 18/7/2		
		Sm 18/3/5		
		Sn 18/7/3		
		Tb 18/0/1		
		Th 18/2/4		
		Yb 18/5/1		
		W 18/na/3		
		Zn 18/2/8		
		Mid Hills		
B 8/0/1	Ba 6/1/2	Ag 7/3/1	Ag 10/0/3	Ce 12/4/1
Mo 8/1/2	Bi 6/na/2	Ba 7/0/1	Bi 10/na/1	
Zn 8/3/1	Mn 6/0/5	Bi 7/na/3	Mn 10/0/1	
	Mo 6/0/1	Ce 7/1/1	Pb 10/2/2	
	Nb 6/0/1	Eu 7/4/0	Zn 10/0/1	
	W 6/1/2	La 7/2/1		
		Nd 7/3/1		

Table 14. Summary of geochemical anomalies in the East Mojave National Scenic Area, Calif.—Continued.

RASS and PLUTO Stream-sediment samples	RASS Heavy-mineral- concentrate samples	PLUTO Heavy-mineral- concentrate samples	RASS and PLUTO Rock samples	NURE Stream-sediment and soil samples
		Providence Mountains		
Ag 82/3/5 Ba 85/6/3 Co 82/24/20 Cu 82/7/8 Mn 82/5/5 Mo 82/4/4 Pb 82/3/5 Sn 82/0/2 W 82/na/1 Zn 82/4/12	Ag 225/20/49 As 225/na/1 Au 225/na/8 B 225/7/7 Ba 225/73/81 Be 225/21/11 Bi 225/na/18 Co 225/6/17 Cu 225/53/17 La 225/0/5 Mn 225/59/23 Mo 225/2/50 Nb 225/10/14 Pb 225/22/66 Sb 225/na/2 Sn 225/8/55 Th 225/9/4 W 225/17/46 Zn 225/na/10	Ag 12/2/3 Bi 12/na/1 Ce 12/5/1 Co 12/4/2 Cu 12/6/1 Eu 12/2/1 La 12/2/3 Mo 12/1/3 Nd 12/4/1 Pb 12/4/2 Sm 12/4/1 Sn 12/6/2 Tb 12/0/3 Th 12/1/1 Zn 12/5/2	Ag 554/63/163 As 554/na/5 Au 554/na/13 B 554/40/57 Ba 554/24/52 Be 554/8/16 Bi 554/na/64 Co 554/19/55 Cu 554/49/124 Eu 14/3/3 La 554/16/22 Mn 554/12/22 Mo 554/34/82 Nb 554/18/2 Nd 14/3/1 Pb 554/80/146 Sb 554/na/11 Sn 554/5/6 Th 554/na/1 W 554/na/8 Zn 554/0/93	Dy 20/2/2 Eu 21/4/1 La 25/0/1 Lu 20/1/1 Th 25/0/1 Yb 24/4/1
		Granite Mountains		
NAH (7)	Ag 28/1/1 Ba 28/8/2 Bi 28/na/2 Co 28/0/2 Cu 28/2/3 La 28/1/1 Mn 28/11/2 Mo 28/0/4 Pb 28/1/2 Sn 28/0/4 Th 28/0/1 W 28/5/4 Zn 28/na/3	Ag 11/1/2 Ba 11/0/2 Be 11/1/1 Ce 11/1/1 Co 11/0/3 La 11/0/1 Mn 11/1/1 Mo 11/1/2 Nb 11/0/1 Nd 11/0/1 Pb 11/2/1 Sn 11/5/2 Tb 11/0/1 Yb 11/0/1 Zn 11/0/1	Ag 88/2/3 As 88/na/1 B 88/0/3 Ba 88/32/8 Bi 88/na/4 Ce 77/3/2 Co 88/1/4 Cu 88/4/5 Dy 77/na/4 La 88/0/1 Mo 88/1/2 Nd 77/15/16 Pb 88/11/3 Sn 88/1/1 Tb 77/0/6 Yb 77/5/1 Zn 88/7/10	Eu 19/2/4 La 19/0/1
		Van Winkle Mountain		
NS	NS	NS	Nd 3/0/1	La 1/0/1
		Grotto Hills		
Ag 1/0/1 Mo 1/0/1 Zn 1/0/1	NS	Co 1/0/1 Cu 1/0/1 Mn 1/0/1 Mo 1/0/1 Zn 1/0/1	NS	NAH (0-2)
		Pinto Mountain		
NS	NS	NS	NS	NAH (0-3)
		Table Mountain		
Co 2/0/1 Mo 2/0/1 Zn 2/0/1	NS	Ag 2/1/1	Ag 2/0/1 Cu 2/0/1 Eu 2/0/1 Mo 2/1/1 Pb 2/0/1 Sb 2/0/1 Sn 2/0/1	Ce 2/0/1 Dy 2/1/1 La 2/0/1 Th 2/0/1

Table 14. Summary of geochemical anomalies in the East Mojave National Scenic Area, Calif.—Continued.

RASS and PLUTO Stream-sediment samples	RASS Heavy-mineral-concentrate samples	PLUTO Heavy-mineral-concentrate samples	RASS and PLUTO Rock samples	NURE Stream-sediment and soil samples
		Homer Mountain		
Ag 1/0/1 Mo 1/0/1	NS	Mn 1/0/1	NAH (1)	Dy 4/1/1 Eu 4/1/1
		Woods Mountains		
NAH (2)	NAH (1)	Ag 2/0/1 La 2/0/1	NS	Dy 2/0/2
		Hackberry Mountain		
Ba 3/0/1	NS	Ag 3/0/1 Ba 3/0/1 Mn 3/0/1 Mo 3/0/1 Zn 3/0/1	NS	Ce 7/3/1 Dy 8/2/4 Eu 7/2/3 Yb 7/2/1
		Vontrigger Hills		
NAH (1)	NS	Ag 1/0/1 Ba 1/0/1	Ag 15/0/4 As 15/na/1 B 15/1/8 Be 15/3/2 Bi 15/na/4 Cu 15/1/4 Mn 15/1/4 Mo 15/0/1 Nb 15/0/1 Pb 15/5/2 Zn 15/0/1	NAH (0-2)
		Piute Range		
Be 6/0/1 Mo 6/0/1 Zn 6/0/1	Ag 29/0/1 B 29/3/1 Be 29/2/2 Bi 29/na/1 Cu 29/1/1 Mo 29/0/1 Pb 29/1/3 Sn 29/0/2 W 29/0/1 Zn 29/na/1	Ag 6/2/1 Ba 6/0/1 La 6/0/1 Sm 6/0/1 Tb 6/0/1 Zn 6/0/1	Ag 25/2/8 Au 25/na/1 B 25/0/1 Be 25/1/1 Bi 25/na/16 Cu 25/0/7 Mo 25/0/4 Pb 25/3/8 Sb 25/na/4 W 25/na/3 Zn 25/0/6	Ce 18/3/4 Dy 17/4/5 Eu 18/4/5 Lu 15/2/2 Sm 10/1/2 Yb 17/0/3
		Castle Mountain		
B 4/0/1 Co 4/0/2 Mn 4/1/1 Mo 4/1/1	B 7/0/2	Ba 4/0/2 Bi 4/na/2 Ce 4/0/2 Co 4/0/1 Cu 4/0/2 Dy 4/na/2 Eu 4/1/1 La 4/0/2 Mn 4/1/1 Mo 4/1/1 Nd 4/0/2 Sm 4/0/2 Th 4/0/2 Yb 4/0/2 Zn 4/0/1	Ag 15/2/4 B 15/1/1 Ba 15/0/1 Eu 5/2/1 Mn 15/0/2 Mo 15/1/4 Nb 15/0/3 Pb 15/2/1 Sb 15/na/4 Tb 5/0/1	Dy 8/2/1 Eu 5/2/1

Table 15. Types of mineral deposits known in the East Mojave National Scenic Area, Calif., as of 1993.

[Abbreviations: C, amount of contained metal or ore before onset of mining; M, amount of metal or ore mined; --, not available]

Mineral-deposit model[1, 2]	Number identified in EMNSA[3]	Typical example of mineral deposit in EMNSA Name	Principal commodities Amount	Type	Additional metals present
Carbonatite, rare-earth element (10)	5	Esperanza Group	--	Ce, La, Sm	U, Th
Polymetallic vein (22c)	206	Morningstar	480,000 oz Au (M)	Au	Ag, Pb, Zn, Cu
Low sulfide, Au-quartz vein (36a)	5	Conquistador No. 2	--	Au	--
Polymetallic replacement (19a)	23	Iron Horse	400 tons ore (M)	Pb, Zn	Fe, Cu, Au, Ag
Distal disseminated Au-Ag (--)	1	Unamed prospect	--	Au, Ag	Zn
Au breccia pipe (--)	2	Coloseum	10,500,000 tons ore (C)	Au, Ag	Cu, Pb, Zn
Ag-Cu brecciated dolostone (--)	25	Beatrice Mine	--	Ag, Cu	Au, V
Fluorite vein (--)	16	Pacific Fluorite	--	F	Sb, Ag, Pb, Zn
Tungsten vein (15a)	18	Mojave Tungsten	38,400 lb (M)	WO_3	Ba, F
Au-Ag, quartz-pyrite vein[5] (--)	80	Little Dove	--	Au, Ag	--
Polymetallic fault (--)	79	Billy Boy	--	Au	Zn, Cu, Ag
Polymetallic skarn (--)	18	Copper Commander	--	Cu, Pb, Zn	Au, Sb, As, Ag
Zn-Pb skarn (18c)	6	Mohawk Mine area	1,793,422 lb (M)	Zn	Cu, Pb, Ag, As
W skarn (14a)	3	Silverado-Tungsite	Small tonnage (M)	W	Au, Ag, Cu, Pb, Zn
Fe skarn (18d)	10	Vulcan	2,643,000 tons ore (M)	Fe	--
Sn (W) skarn (14b)	1	Evening Star Tin	3,200 lb (M)	Sn	W, Au, Ag, Zn, Cu
Cu Skarn (18b)	26	Copper World	5,321,184 lb (M)	Cu	Pb, Ag, Au, Zn
Vein barite (--)	6	Susan's Peak	--	Ba	--
Vein magnesite (--)	1	New Trail Magnesite	~300 tons ore (M)	Mg	--
Porphyry Mo, low F (21b)	3	Big Hunch	800,000,000 lbs MoS_2	Mo	Ag
Epithermal qtz-adularia (alunite) (Au) (25e)	11	Castle Mountains (Hart)	2,020,000 oz Au (C)	Au	Ag
Placer Au-PGE[6] (39a)	34	Terry	--	Au	--
Placer Fe±Ti (--)	2	Kelso Dunes	1,000 tons Fe_3O_4 (M)	Fe	Ti, Au

[1] Numbers in parentheses indicate model numbers as described by Cox and Singer (1986); other listed models from various sources in literature.

[2] Additional types of mineral deposits in EMNSA (and their number of occurrences) include sand and gravel (4), cinder (3), sandstone (1), marble (3), slate (1), limestone (6), dolomite (4), graphite (1), talc (1), mica (2), gemstone (1), decorative and dimension stone (5), pyrophyllite (1), clay (9), perlite (3), and pumice (2).

[3] Mineral-deposit models have been assigned provisionally in this report to 587 of 701 occurrences in EMNSA that were reported by U.S. Bureau of Mines (1990a, table 2). Small number of localities have been assigned to more than one deposit type.

[4] From U.S. Bureau of Mines (1990a, map no. 161).

[5] Deposits are mostly Mesozoic in age but also include some Tertiary gold-silver vein occurrences that are epithermal and apparently related to wrench-style tectonics, as exemplified by Telegraph Mine (Lange, 1988).

[6] Presence of PGE (platinum-group elements) has not been established in placers in EMNSA (U.S. Bureau of Mines, 1990a); however, model name has been retained to preserve terminology used by Cox and Singer (1986).

[7] Field examinations (U.S. Bureau of Mines, 1990a) indicate presence of visible gold at only nine placer localities in EMNSA, and nowhere in EMNSA is placer-gold production occurring.

Table 16. Summary statistics for 20 elements in 1,050 samples of rock analyzed from the East Mojave National Scenic Area, Calif.

[All concentrations in parts per million except where noted; --, not applicable. Data from U.S. Bureau of Mines, 1990a, tables 2*A*, *B*]

	Number of undetermined concentrations	"Less than" concentrations		"Greater than" concentrations		Data matrix (including substituted values)							Log-transformed data	
		Number	Value substituted[1]	Number	Value substituted[2]	Minimum	Maximum	Mean	Geometric mean	50th percentile	Mode	Standard deviation	Kurtosis	Skewness
Ag	481	481	1	0	--	1	3,080	70.6	6.1	3	1	238	–0.0387	0.883
As	24	23	0.5	1	10,000	0.5	120,000	664	22.5	16	2	4,790	0.453	0.811
Au[3]	253	253	1.	0	--	1.0	51,700	973	30.7	20.5	1.0	3,380	–0.778	0.456
Ba	369	369	25	0	--	25	184,000	1,150	151	170	25	8,900	0.478	0.598
Ce	402	402	2.5	0	--	2.5	7,200	51.3	14.4	17	2.5	268	–1.13	0.2
Co	642	642	2.5	0	--	2.5	859	20	6	2.5	2.5	66.8	1.28	1.36
Cr	209	209	10	0	--	10	3,990	181	99.5	160	10	2.8	–0.661	–0.74
Cs	549	549	0.5	0	--	0.5	138	2.6	1.2	0.5	0.5	6.2	0.113	1.01
Fe[4]	83	83	0.1	0	--	0.1	62	4.9	2	2	0.1	8	–0.185	–0.209
La	181	181	1	0	--	1	52,600	71.1	8.8	10	1	1,620	0.444	0.081
Mo	376	376	0.5	0	--	0.5	2,080	34.3	4	3	0.5	135	–0.618	0.589
Ni	801	801	5	0	--	5	560	15.7	7.8	5	5	39	3.63	2.04
Sb	18	18	0.05	0	--	0.05	122,000	346	5.9	3.2	0.2	3,890	–0.249	0.647
Sc	185	185	0.1	0	--	0.1	123	4.2	1.4	1.8	0.1	7.4	–0.875	–0.232
Sm	91	91	0.05	0	--	0.05	6,360	9.5	1.3	1.7	0.05	196	0.161	–0.355
Ta	687	687	0.25	0	--	0.25	10	0.6	0.42	0.25	0.25	0.9	0.887	1.34
Th	154	154	0.1	0	--	0.1	26,300	40.3	2.6	3.3	0.1	22	–0.054	–0.139
U	69	69	0.1	0	--	0.1	1,590	9.3	2.7	3.1	0.1	70	1.06	–0.286
W	256	256	0.5	0	--	0.5	165,000	93	5.2	4	0.5	6,050	1.74	1.16
Zn	477	477	50	0	--	50	325,000	4,080	254	130	50	17,400	0.608	1.22

[1]Substituted values are 50 percent of the minimum detection limit.
[2]Substituted value is concentration of maximum determination limit.
[3]Concentration values in parts per billion.
[4]Concentration values in weight percent

Table 17. Array of Spearman correlation coefficients for 20 elements in 1,050 rock samples from the East Mojave National Scenic Area, Calif.

[See text. Calculated using data from U.S. Bureau of Mines (1990a); --, not applicable.]

	Log (Au)	Log (Ag)	Log (As)	Log (Ba)	Log (Ce)	Log (Co)	Log (Cr)	Log (Cs)	Log (Fe)	Log (La)	Log (Mo)	Log (Ni)	Log (Sb)	Log (Se)	Log (Sm)	Log (Ta)	Log (Th)	Log (U)	Log (W)	Log (Zn)
Log (Au)	1.0	--	--	--	--	--	--	--	--	--	--	--	--	--	--	--	--	--	--	--
Log (Ag)	.323	1.0	--	--	--	--	--	--	--	--	--	--	--	--	--	--	--	--	--	--
Log (As)	.136	.485	1.0	--	--	--	--	--	--	--	--	--	--	--	--	--	--	--	--	--
Log (Ba)	–.139	–.349	–.285	1.0	--	--	--	--	--	--	--	--	--	--	--	--	--	--	--	--
Log (Ce)	–.152	–.473	–.341	.614	1.0	--	--	--	--	--	--	--	--	--	--	--	--	--	--	--
Log (Co)	.241	.01	.046	.089	.108	1.0	--	--	--	--	--	--	--	--	--	--	--	--	--	--
Log (Cr)	.177	–.218	–.343	.222	.15	–.016	1.0	--	--	--	--	--	--	--	--	--	--	--	--	--
Log (Cs)	–.181	–.305	–.092	.519	.54	.156	–.012	1.0	--	--	--	--	--	--	--	--	--	--	--	--
Log (Fe)	.319	.013	.167	.133	.149	.691	.019	.14	1.0	--	--	--	--	--	--	--	--	--	--	--
Log (La)	–.101	–.345	–.221	.627	.883	.147	.085	.525	.22	1.0	--	--	--	--	--	--	--	--	--	--
Log (Mo)	.292	.367	.294	–.185	–.328	.053	.142	–.22	.166	–.271	1.0	--	--	--	--	--	--	--	--	--
Log (Ni)	.082	–.041	.077	.087	.089	.356	.042	.12	.313	.111	–.004	1.0	--	--	--	--	--	--	--	--
Log (Sb)	–.009	.552	.751	–.258	–.363	–.129	–.358	–.09	–.08	–.244	.248	.029	1.0	--	--	--	--	--	--	--
Log (Sc)	–.097	–.449	–.271	.579	.724	.417	.11	.555	.454	.714	–.279	.244	–.346	1.0	--	--	--	--	--	--
Log (Sm)	–.17	–.429	–.278	.621	.879	.177	.113	.554	.2	.896	–.341	.11	–.312	.777	1.0	--	--	--	--	--
Log (Ta)	–.184	–.349	–.3	.448	.649	.02	.054	.452	.07	.621	–.259	.034	–.278	–.535	.65	1.0	--	--	--	--
Log (Th)	–.091	–.459	–.334	.593	.838	.089	.206	.523	.182	.804	–.274	.053	–.387	.705	.813	.674	1.0	--	--	--
Log (U)	.24	.108	.205	.001	.166	.261	–.007	.149	.435	.216	.242	.102	.067	.177	.109	.184	.252	1.0	--	--
Log (W)	.165	.146	.163	.02	–.071	.19	.017	.147	.278	–.024	.316	.07	.141	.057	–.022	–.029	–.023	.204	1.0	--
Log (Zn)	.226	.559	.47	–.216	–.241	.217	–.322	–.049	.297	–.129	.289	.08	.442	–.13	–.199	–.17	–.233	.26	.196	1.0